博士論文

Development of *N*-Hydroxy Activators and Oxidation State-Selective C(sp^3)–H Oxidation

（*N*-ヒドロキシル活性化剤と酸化度選択的C(sp^3)-H酸化反応の開発）

Graduate School of Pharmaceutical Sciences
The University of Tokyo

Jizhi Ni
倪　積智

Contents

Abbreviation

Ac	acetyl
ABNO	9-azabicyclo[3.3.1]nonane *N*-oxyl
Boc	*t*-butoxycarbonyl
BDE	bond dissociation energy
Bn	benzyl
Bu	butyl
Bz	benzoyl
CAN	cerium (IV) ammonium nitrate
DA	directing activator
DBU	1,8-diazabicyclo[5.4.0]undec-7-ene
DCM	dichloromethane
DDQ	2,3-dichloro-5,6-dicyano-1,4-benzoquinone
DG	directing group
DMF	*N*,*N*-dimethylformamide
DMSO	dimethylsulfoxide
ESI	electrospray ionization
Et	ethyl
eq./equiv	equivalent
h	hour
HFIP	1,1,1,3,3,3-hexafluoro-2-propanol
HPLC	high performance liquid chromatography
IPA	isopropyl alcohol
IR	infrared
ketoABNO	9-azabicyclo[3.3.1]nonan-3-one *N*-oxyl
LHMDS	lithium *bis*(trimethylsilyl)amide
M	molar
Me	methyl
*m*CPBA	*meta*-Chloroperoxybenzoic acid
Min	minite(s)
Ms	methanesulfonyl
MS	mass spectrometry
NBS	*N*-bromosuccinimide
NCS	*N*-chlorosuccinimide
NHPI	*N*-hydroxyphthalimide
NIS	*N*-iodosuccinimide
NMR	nuclear magnetic resonance
PG	protecting group
Ph	phenyl
Phth	phthaloyl

PINO	phthalimide *N*-oxyl
PMB	*p*-methoxybenzyl
ppm	parts per million
PTSA	*p*-toluenesulfonic acid
rsm	recovered starting material
rt	room temperature
t-	tertiary
TBAF	tetra-*n*-butylammonium fluoride
Tf	trifluoromethanesulfonyl
TFA	trifluoroacetic acid
TFE	2,2,2-trifluoroethanol
THF	tetrahydrofuran
TLC	thin layer chromatography
TMS	trimethylsilyl

Chapter 1.

Background

Traditional synthetic methods for installing functional groups usually rely on acid–base reactions which require extensive functional-group manipulations including low atom economic protection–deprotection sequences. In recent years, there has been a growing demand for the development of fundamentally new and environmentally benign catalytic systems for hydrocarbons which are operative on an industrial scale under mild conditions in a liquid-phase with a high degree of selectivity. Saturated hydrocarbons are inert because their carbon–hydrogen (C–H) bonds have high bond dissociation energy (~95–110 kcal/mol) and very low acidity and basicity. Functionalization of unactivated C–H bonds is currently under intensive investigation. Specifically, C(sp^3)–H functionalization can be a powerful tool for a streamlined synthesis of C(sp^3)-rich, drug lead complex molecules. Requiring no preactivation and prefunctionalization of the substrates for bond formations, it will dramatically streamline the synthesis of complex natural products and biologically active compounds. Although exciting breakthroughs have been achieved in recent decades, important challenges in the field of C(sp^3)–H activation still remain. Frontier issues that must be addressed include (1) the development of chemoselective catalysts that can oxidize aliphatic C–H bonds in the presence of more electron-rich functional groups (i.e. olefins, aromatics, oxygens, nitrogens), (2) preparative catalysts for intermolecular reactions.[1]

Radical C–H activation is a promising strategy because of radicals' inherently high reactivity and functional group tolerance. As a representative of redox–active *N*-hydroxyimides, *N*-hydroxyphthalimide (NHPI) can generate radical species phthalimide *N*-oxyl (PINO) radical, which is active enough to abstract a hydrogen atom from C(sp^3)–H bond.[2] Among the frontier challenges of modern synthetic chemistry, the design of catalysts for synthesis of organic molecules with high levels of efficiency is extremely important. To achieve general functionalization of C(sp^3)–H bonds under mild conditions, a two-stage transformation by employing an *N*-oxyl organocatalyst is

---

[1] White, M. C. *Synlett* **2012**, *23*, 2746.

[2] For reviews of NHPI, see: (a) Ishii, Y,; Sakaguchi, S.; Iwahamab, T. *Adv*. *Synth*. *Catal*. **2001**, *343*, 393. (b) Recupero, F.; Punta, C. *Chem*. *Rev*. **2007**, *107*, 3800.

shown in **Scheme 1–1**: Generated from its *N*-oxyl radical precursor, *N*-oxyl radical abstracts a H atom to give an alkyl radical. Then the very reactive species is quickly captured by suitable trapping reagents, and hence installing diverse functional groups.

Scheme 1–1 *N*-Oxyl radical promoted C(sp^3)-H functionalization

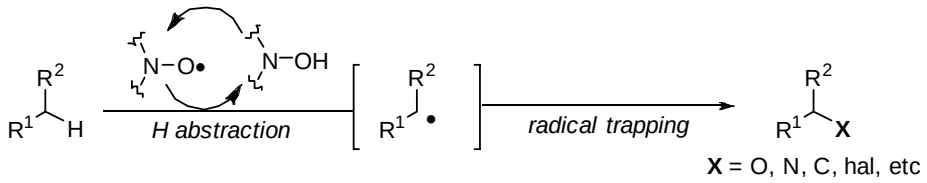

Methylene (secondary) C–H bonds are ubiquitous in organic compounds and are often viewed as the inert scaffold. Oxidation of non-activated methylene groups with oxygen usually produces carbonyl compounds or carboxylic acid (C–C bond cleavage) as the final product. Methylene oxygenation reactions sometimes involve the oxidation of C–H to single bond C–O units. One general difficulty in such cases is preventing overoxidation because the product H–CO bond is generally more reactive than the reactant C–H bond. Classical organic pathways often fail to overcome this problem.

To break through the above obstacles, in this thesis, I will present several novel *N*-hydroxy organocatalysts with hydrogen abstraction ability. Moreover, by employing a new *N*-oxyl radical directing activator, I will demonstrate the oxygenation of challenging acyclic methylene C(sp^3)–H bonds to C=O double bonds under Co(II)/O_2 condition, as well as preferential C–O single bonds forming in NO_x/O_2 system.

Chapter 2.

Catalytic Activation of C(sp^3)–H Bond by Novel *N*–Oxyl Radicals

2–1. Research background

The redox–active organocatalyst *N*-hydroxyphthalimide (NHPI) was first employed in 1977 by Grochowski and coworkers to catalyze the condensation of ethers with azodicarboxylate and the oxidation of isopropanol with *m*-chloroperbenzoic acid.[3] It can be converted to the phthalimide *N*-oxyl (PINO) radical species by heating or catalyzed by metal under oxygen atmosphere (**Scheme 2–1**). NHPI has been introduced as an effective system for hydrogen abstraction, even from the challenging tertiary (e.g. isobutene[4]) and secondary (e.g. cyclohexane and *n*–octane[5]) C–H bonds in alkanes. Under aerobic condition, the generated alkyl radical is trapped by oxygen to give oxygenated products like alcohols, ketones and carboxylic acids.[2]

Scheme 2–1. Aerobic C(sp^3)–H oxygenation catalyzed by NHPI

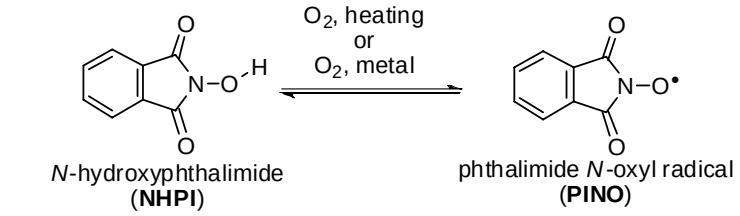

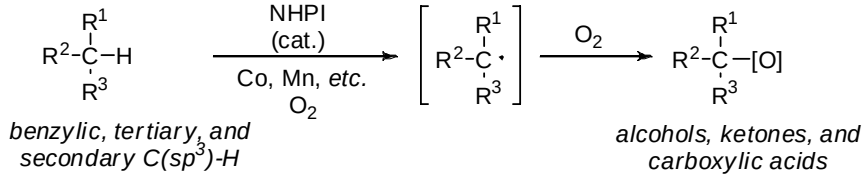

Ishii proposed the mechanism shown in **Scheme 2–2** to account for the hydrocarbons oxidation by NHPI/Co(acac)$_2$ catalysis.[2a] Initiation involves a two-step

[3] Grochowski, E.; Boleslawska, T.; Jurezak, J. *Synthesis* **1977**, 718.
[4] Sakaguchi, S.; Kato, S.; Iwahama, T.; Ishii, Y. *Bull. Chem. Soc. Jpn.* **1998**, *71*, 1237.
[5] Ishii, Y.; Iwahama, T.; Sakaguchi, S.; Nakayama, K.; Nishiyama, Y. *J. Org. Chem.* **1996**, *61*, 4520.

process in which cobalt(II) first reacts with oxygen followed by abstraction of a hydrogen atom from NHPI by the resulting superoxocobalt(III) species, giving the chain propagating PINO radical. The co-catalyst cobalt metal has dual functions: 1) it works as an initiator in generating PINO radical, and 2) it catalyzes the decomposition of intermediate hydroperoxides into products. In other words, the main role of the cobalt is an initiator while NHPI acts as a catalyst in the C–H oxidation.

Scheme 2–2. Plausible pathway for the aerobic oxidation of alkanes catalyzed by NHPI/Co(II)

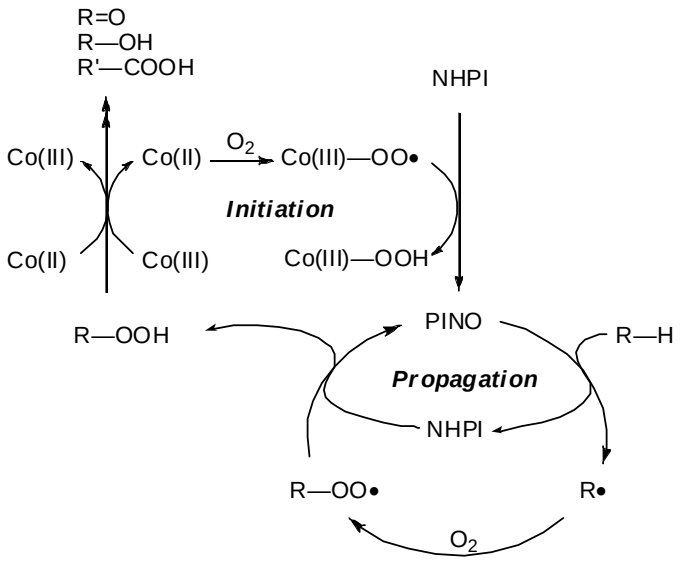

Despite that extensive researches were devoted to the development of NHPI catalyzed hydrocarbon transformations, the main drawbacks which may hinder its application are still remained untouched: 1) the instability of PINO under aerobic oxidation conditions, 2) the low solubility of polar NHPI in liquid hydrocarbon solvents, and 3) the structure and activity of NHPI which are not easy to tune. Considering about these, I aimed to overcome the limitations of NHPI by structural modification of *N*-hydroxyl activators.

2–2. *N*-oxyl radicals and their precursors

N-Oxyl radicals are *N*,*N*-disubstituted N–O radicals with a delocalized unpaired electron shared between the nitrogen and oxygen atoms (**Figure 2–1**).The first *N*-oxyl radical, Frémy's salt (**1**, $ON(SO_3K)_2$) was reported in 1845.[6] The organic *N*-oxyl radicals diphenylnitroxyl radical (**2**) was initially developed by Wieland and Offenbächer in 1914.[7] A very important contribution to *N*-oxyl radical chemistry was made by Lebedev and Kazarnovsky, who introduced the stable, non-conjugated 4-oxo-2,2,6,6-tertramethylpiperidine-*N*-oxyl radical (4-oxo-TEMPO, **3**) [8] and 2,2,6,6-tetramethylpiperidinyloxyl (TEMPO,**4**) as a readily prepared persistent radical in 1959.[9]

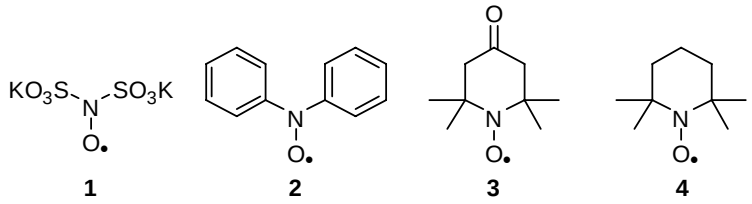

Figure 2–1. Structures of stable *N*-oxyl radicals

Delocalization of the unpaired electron, which contributes to the stabilization of *N*-oxyl radicals, is indicated by the three resonance structures **5a**, **5b** and **5c** as shown in **Figure 2–2:**

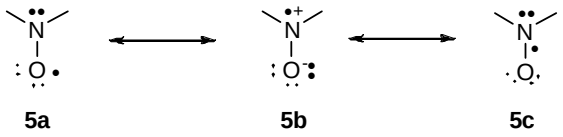

Figure 2–2. Resonance structures of *N*-oxyl radicals

---

[6] Frémy, E. *Ann. Chim. Phys*. **1845**, *15*, 408.

[7] Wieland, H. Offenbächer, M. *Ber. Dtsch. Chem. Ges*. **1914**, *47*, 2111.

[8] Lebedev, O. L. Kazarnovsky, S. N. *Tr. Khim. Khim. Tekhnol*. **1959**, *3*, 649; [Chem. Abstr. **1962**, *56*, 15479f].

[9] O. L. Lebeder, S. N. Kazarnovskii, *Zh. Obshch. Khim*. **1960**, 30, 1631; [Chem. Abstr. **1961**, *55*, 1473a].

N-oxyl radicals with α-hydrogen atoms are unstable, because the radical undergoes disproportionation to a hydroxylamine and a nitrone (**Figure 2–3**).[10]

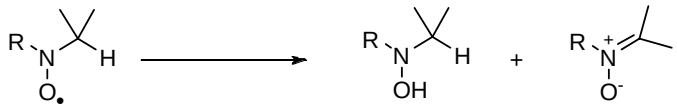

Figure 2–3. Unstable *N*-oxyl radicals

In contrast with the stable dialkyl *N*-oxyl radicals, which can inhibit free radical autoxidations, NHPI catalyzes autoxidations *via* the formation of the diacyl *N*-oxyl radical, PINO (see **Scheme 2–1**). A plausible explanation for this significant difference can be found by considering the stabilities of TEMPO and PINO, which are related to the bond dissociation energy (BDE) of the NO–H bond in the parent hydroxylamine. The strength of the NO-H bond in hydroxylamines is strongly dependent on the nature of the substituents linked to the nitrogen atom (**Table 2–1**). Actually, the O–H BDE value in dialkyl hydroxylamines is ca. 70 kcal/mol, while in alkyl acyl hydroxylamines it increases about 10 kcal/mol and in diacyl hydroxylamines even larger.

Table 2–1. O–H bond dissociation energies (BDE) in *N*-substituted hydroxylamines

	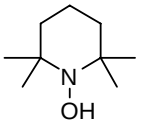	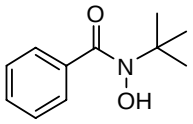	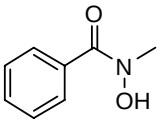	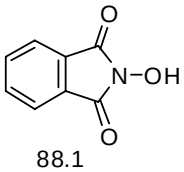
BDE (O–H) kJ/mol	69.8	77.2	79.6	88.1
	Ref.[11]	Ref.[12]	Ref.[13]	Ref.[12]

To explain this difference, it should be pointed out that the BDE value is a measure of the energy difference between the *N*–oxyl radical and the parent hydroxylamine; thus, any factor inducing a stabilization of the hydroxylamine or destabilization of the *N*–oxyl

[10] Bowman, D. F.; Gillan, T.; Ingold, K. U. *J. Am. Chem. Soc.* **1971**, *93*, 6555.

[11] Mahoney, L. R.; Mendenhall, G. D.; Ingold, K. U. *J. Am. Chem. Soc.* **1973**, *95*, 8610.

[12] Amorati, R.; Lucarini, M.; Mugnaini, M.; Pedulli, G. F.; Minisci, F.; Recupero, F.; Fontana, F.; Astolfi, P.; Greci, L. *J. Org. Chem.* **2003**, *68*, 1747.

[13] Jenkins, T. C.; Perkins, M. J. *J. Chem. Soc. Perkin Trans. 2* **1983**, 717.

radical increases the strength of the O–H bond (*higher BDE value*) (**Figure 2–3**).[14]

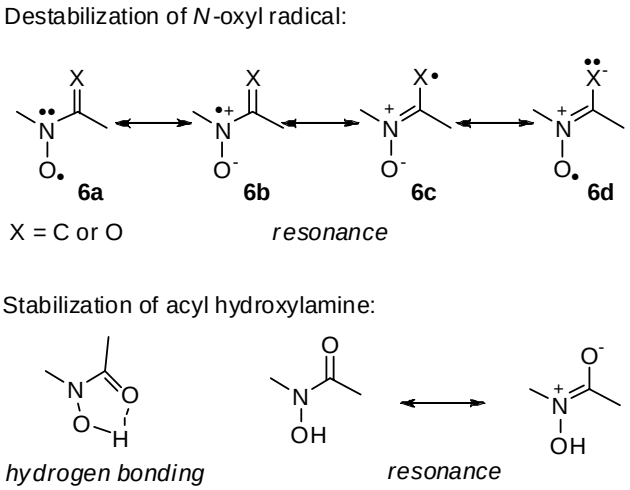

Figure 2–3. Factors affecting the strength of O–H bond

With conjugated C=X groups linking to the N atom, substitution of an alkyl with an aryl group (X = C atom) induces a decrease of spin density on both nitrogen and oxygen atoms due to delocalization, while substitution with an acyl group (X = O atom) produces a strong decrease of spin density on nitrogen and a small increase on oxygen. The later has a destabilizing effect by reducing the importance of the mesomeric structure **6b**. On the other hand, the carbonyl group increases the stability of the acylhydroxylamine *via* resonance stabilization and the formation of an intramolecular hydrogen bond. These effects are further amplified in the diacyl PINO radical and its precursor NHPI.

BDE is useful to represent the generation and stability of a radical. For NO–H bonds with low BDE, the radical generation is easier, but this *N*–oxyl radical is less reactive for C–H cleavage. In contrast, generated from high BDE precursor, the *N*-oxyl radical is more powerful for C–H abstraction. However, the NO–H activation requires more energy to produce the successor radical.

Based on the above-concerned factors, making *N*-hydroxy activator with suitable BDE is crucial for the efficient hydrogen abstraction.

[14] Amorati, R.; Lucarini, M.; Mugnaini, V.; Pedulli, G. F. *J. Org. Chem.* **2003**, *68*, 1747.

2–3.Design of novel *N*-hydroxy activators

Catalytic protocols play a central role in increasing the efficiency of chemical transformation. Based on previous elucidation (**2–1** background, and **2–2** knowledge of *N*-oxyl radical), I designed three types of *N*-hydroxy catalysts to overcome the limitations of NHPI: Type I (*N*-hydroxypyridone derivatives), Type II (3-hydroxy-4(3*H*)-quinazolinone derivatives) and Type III (*N*-hydroxyisoindolin-1-one derivatives) (**Figure 2–4**).

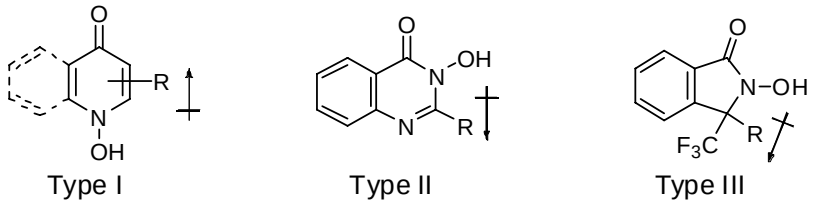

Figure 2–4. Novel *N*-hydroxy activators

Each type of catalyst contains a carbonyl moiety conjugating with or directly attached to the nitrogen atom (N). Specially, a functional group R can be installed to tune the electron density on N, which affects the strength of NO–H bond.

The synthetic procedures of Type I (**Scheme 2–3**), Type II (**Scheme 2–4**) and Type III (**Scheme 2–5**) are shown below:

Scheme 2–3. Synthesis of Type I activators

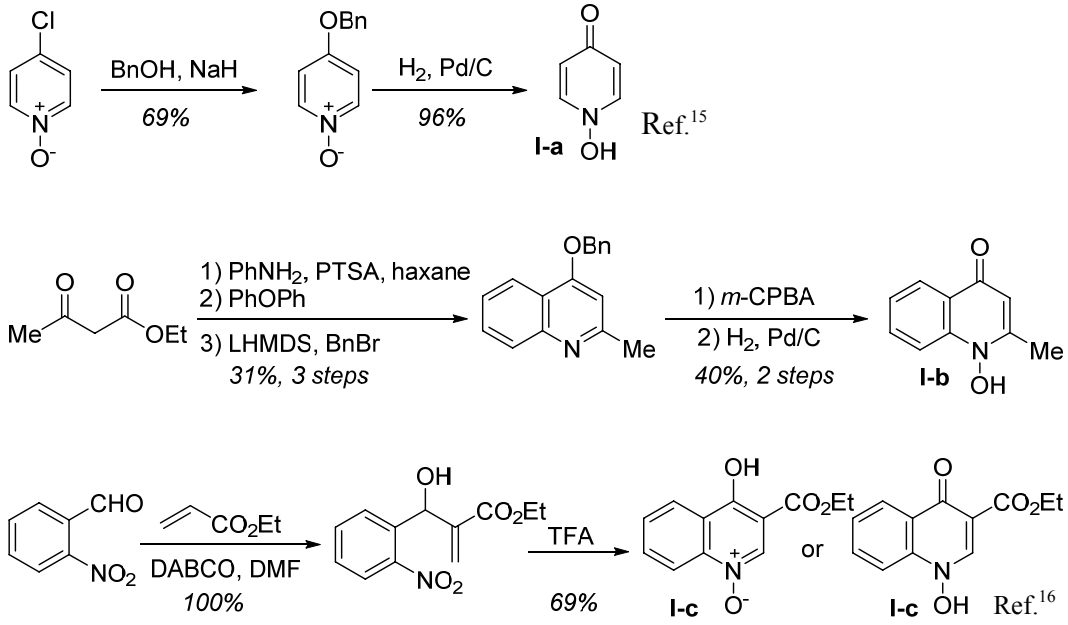

Scheme 2–4. Synthesis of Type II activators

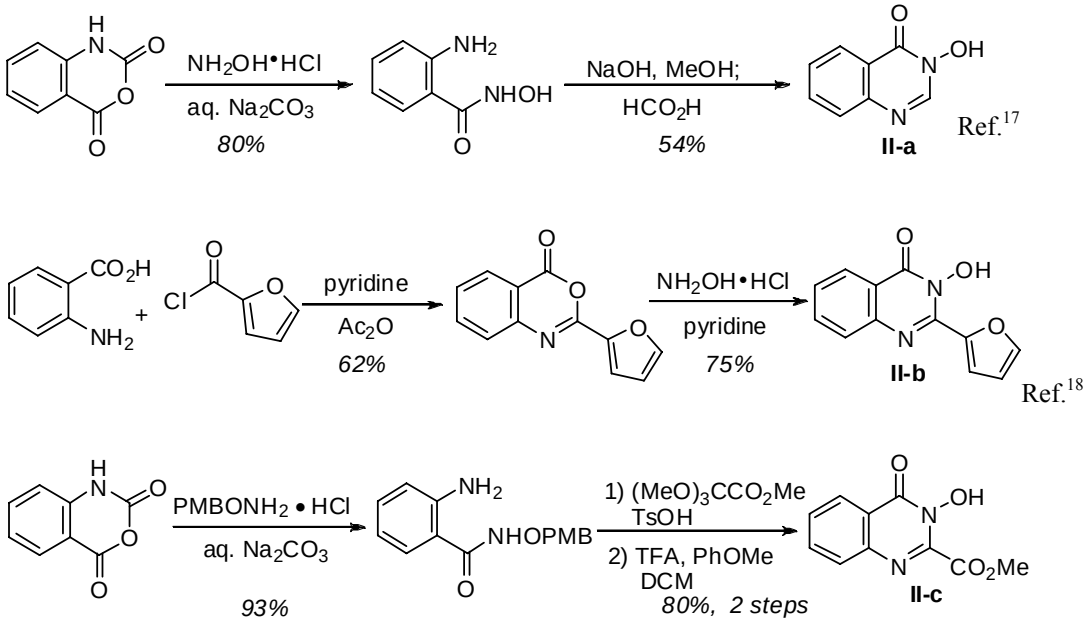

[15] Shaw, E. J. *Am. Chem. Soc*. **1949**, *71*, 67.
[16] Kim, J. N.; Lee, K. Y.; Kim, H. S.; Kim, T. Y. *Org. Lett*. **2000**, *2*, 343.
[17] Ayman, E.-F; Fernando, A. *Eur. J. Org. Chem*. ***2009***, 1499.
[18] Noolvi, M. N.; Patel, H. M.; Bhardwaj, V.; Chauhan, A. *Eur. J. Med. Chem*. **2011**, *46*, 2327.

Scheme 2–5. Synthesis of Type III activators

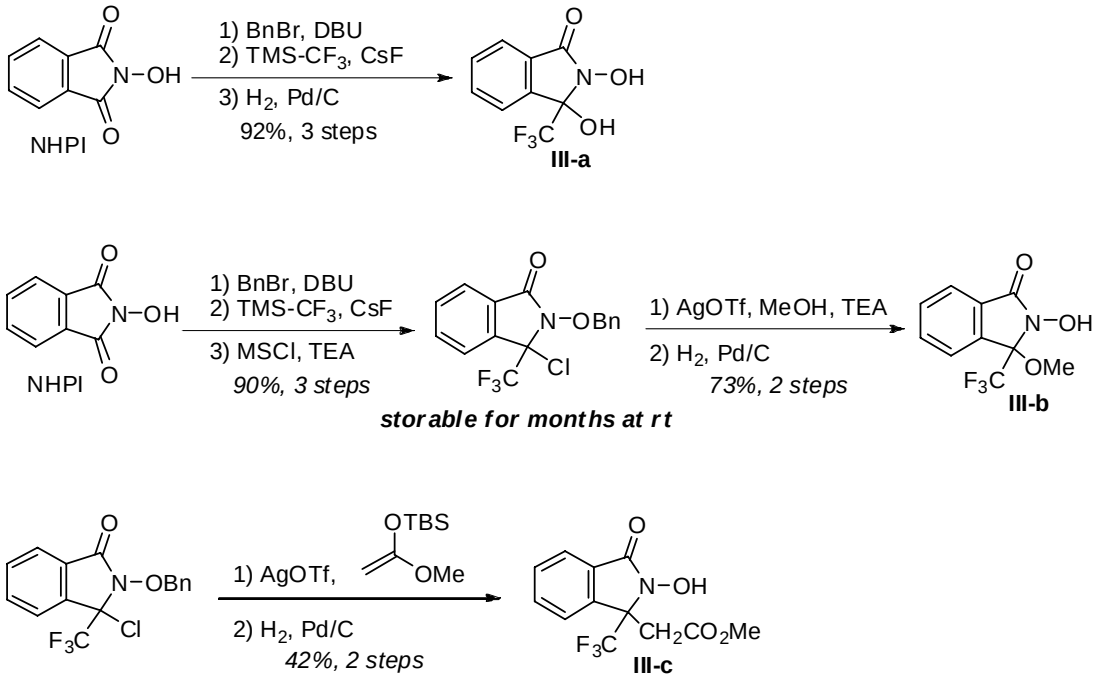

2–4. Performance of the *N*-hydroxy activators

Catalytic oxidative transformation of ubiquitously present C–H bonds to polar functional groups (e.g., C–O bonds) and molecular skeletons (e.g., C–C bonds) is a straightforward and versatile approach to constructing complex molecules. Molecular oxygen is the most ideal oxidant for such oxidative transformations. In order to examine the performance of the synthesized *N*-hydroxy activators in C–H activation process, I chose Ishii's reaction[19] as a model: conjugate addition of 2-methyl-1,3-dioxolane to *t*-butyl acrylate promoted by an organocatalyst in the presence of cobalt and oxygen. The result of Type I and Type II compounds are shown in **Table 2–2**.

Table 2–2. Performance of Type I and Type II catalysts

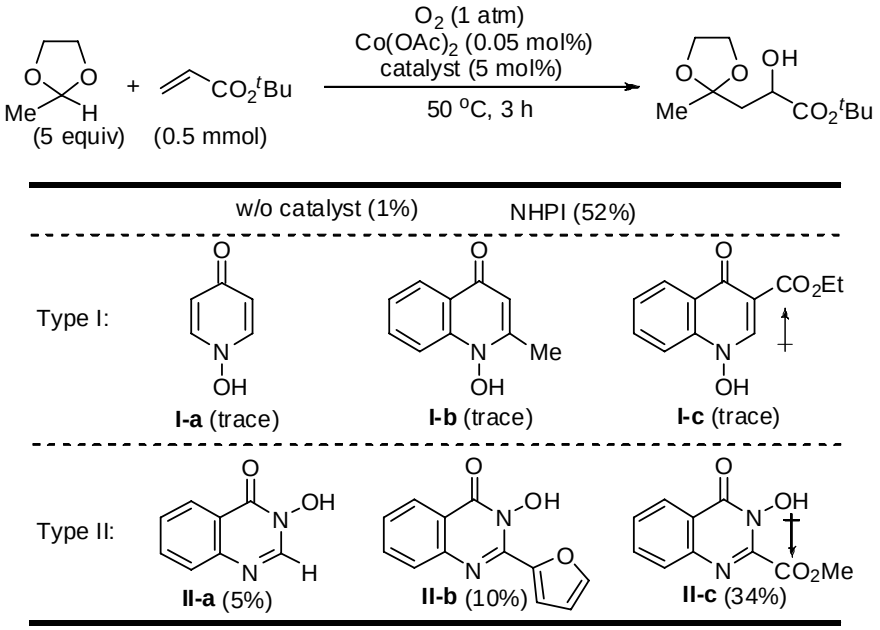

* NMR yields in parenthesis were given.

With poor solubility in the reaction mixture (neat condition), Type I catalysts did not show any reactivity in this process. The reaction mixtures turned clear after adding 1,1,1-trifluoroethanol, but still almost no products were obtained.

Type II showed some catalytic activity. Especially, when an ester group was introduced (**II-c**), the activity was much improved, although still lower than NHPI.

[19] Hirano, K.; Iwahama, T.; Sakaguchi, S.; Ishii, Y. *Chem. Commun*. **2000**, 2457.

Type III catalyst contains a trifluoromethyl moiety on the α-carbon of nitrogen atom. At the same position, **III-a**, **III-b** and **III-c** contain a methoxycarbonylmethylene group, a hydroxy group and a methoxy group, respectively. All of them exhibited much higher reactivity than the classic NHPI for this catalytic process and significantly improved solubility (**Table 2–3**).

Table 2–3. Performance of Type III catalyst

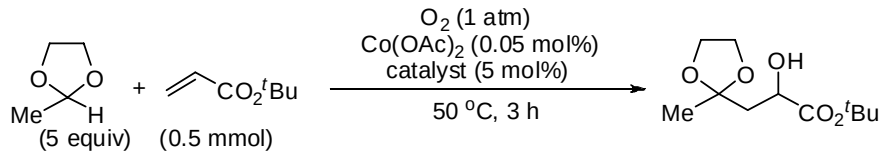

	w/o catalyst (1%)	NHPI (52%)	
Type III:	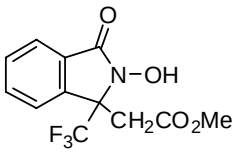	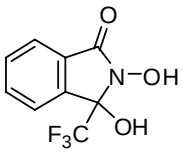	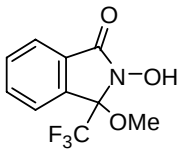
	III-a (71 %)	**III-b** (78 %)	**III-c** (82 %)

* NMR yields in parenthesis were given.

Bond dissociation energy (BDE) comparison

The BDE values of the NO–H bonds in the three types of organocatalysts were calculated. With EWG substituents (ester groups), the BDE values of **I-c** and **II-c** are much increased compared to their analogues. Type I catalysts have similar BDE values like ABNO precursor (ABNO–H). While Type II catalysts have higher BDE values than NHPI. The O–H bond in **II-c** has a BDE value around 100 kcal/mol, similar like that of alkane C–H bond. Modified from NHPI, the BDE values of Type III catalysts slightly decreased.

Table 2–4. Calculated BDE values of NO–H bonds (kcal/mol)

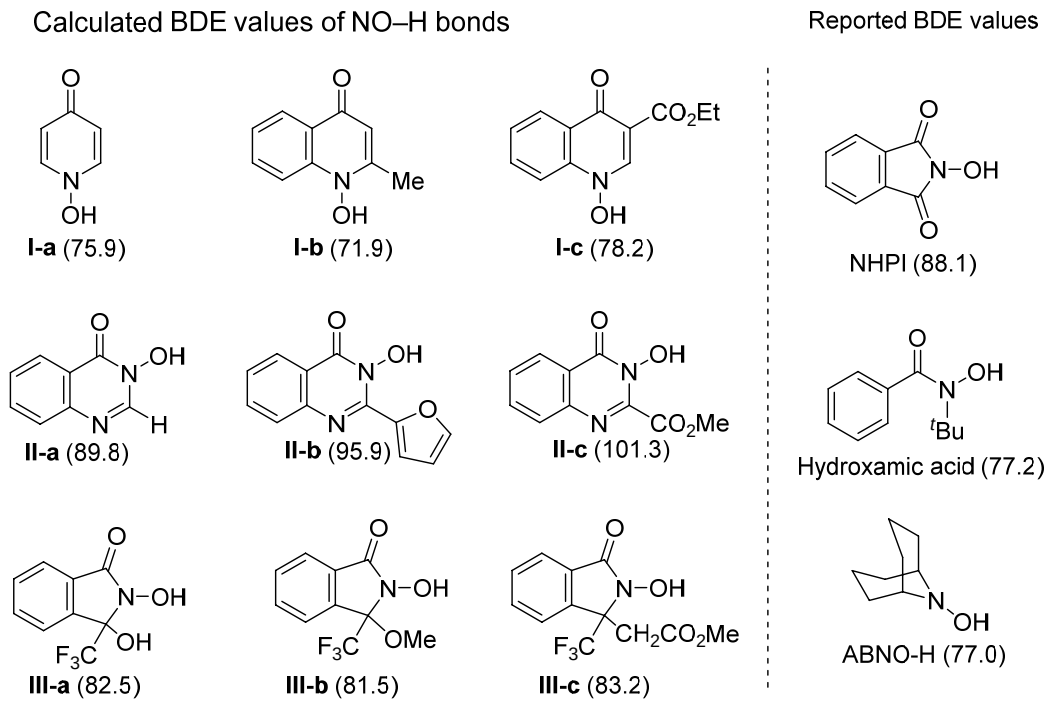

(1) BDE values in parentheses are in kcal/mol

(2) DFT calculations using Jaguar v7.9 at the B3LYP level with the 6-31G** basis set (Schroedinger)

The structure-performance relationships

As briefly summarized in **Figure 2–5**, Type I catalysts (*N*-hydroxypyridone) are very polar compounds and showed poor solubility and no reactivity. With EWGs attached to α-carbon of nitrogen atom, both the reactivity and solubility of Type II catalysts (3-hydroxy-4(3*H*)-quinazolinone) were much improved. For Type III catalysts (*N*-hydroxyisoindolin-1-one), besides a carbonyl moiety in the structures, trifluoromethyl groups were linked to α-carbon of nitrogen atom. Both the reactivity and solubility were significantly improved. This afforded a good direction for future modification of *N*-hydroxy catalysts. Development of Type III catalysts promoted organic transformation is ongoing in our group.

Figure 2–5. Summary of the structure-performance relationships

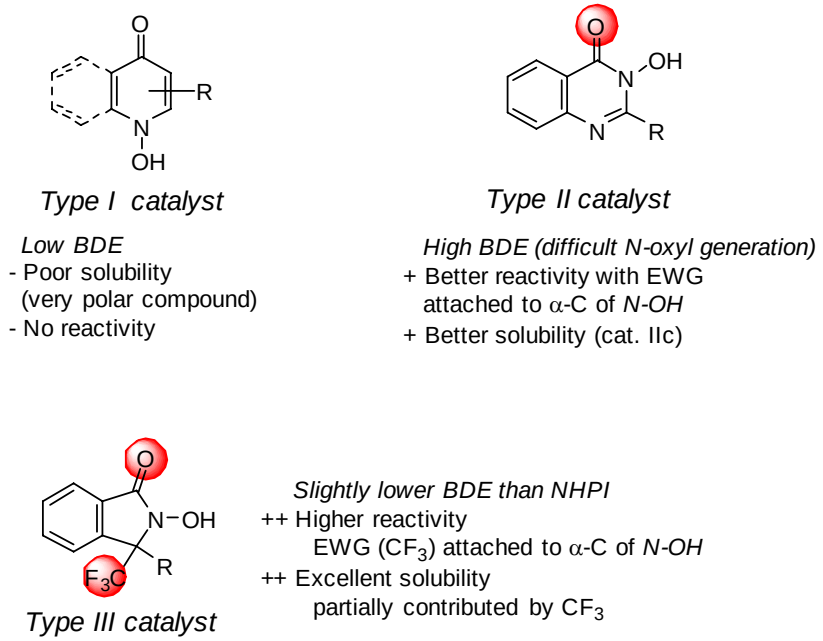

Chapter 3.

Site- and Oxidation State-Selective Methylene Oxidation

3–1. Background on strategies toward C(sp^3)–H activation

C–H bonds are the most abundant chemical bond in organic molecules. Inactive C–H bonds were typically ignored in the field of methodology development before early 2000s. It is quite challenging to develop synthetically useful C-H transformations because of the ubiquity (selectivity problem) and inertness (reactivity problem) of C–H bonds.

Catalytic functionalization of unactivated C–H bonds is currently under intensive investigation.[20] Specifically, C(sp^3)–H functionalization[21] can be a powerful tool for the streamlined synthesis of C(sp^3)-rich, drug lead complex molecules.[22]

To apply C(sp^3)–H functionalization to practical drug lead synthesis, two features are necessary: (1) mild reaction conditions to assure functional group tolerance,[23] and (2) site-selectivity to convert a specific C–H bond among omnipresent C–H bonds in one molecule.[24]

Two main approaches toward C(sp^3)–H functionalization were devised to assure predictable regioselectivity (**Figure 3–1**). One approach was based on innate reactivity as determined by steric and electronic biases in the molecule (i.e., a substrate control approach).[25] The observed selectivity, however, is often not perfect, and arbitrary

---

[20] (a) C–H Activation. In *Topics in Current Chemistry*; Yu, J.-Q.; Shi, Z.-J.; Eds.; Springer: Berlin, **2010**; Vol. 292. (b) Newhouse, T.; Baran, P. S.; Hoffmann, E. W. *Chem. Soc. Rev.* **2009**, *38*, 3010. (c) White, M. C. *Synlett* **2012**, *23*, 2764.

[21] (a) Christmann, M. *Angew. Chem. Int. Ed.* **2008**, *47*, 2740. (b) White, M. C. *Science* **2012**, *335*, 807. (c) *Alkane C–H Activation by Single-Site Metal Catalysis*; Pérez, P. J. Ed.; Springer: Dordrecht, 2012. (d) Jeffrey, J. L.; Sarpong, R. *Chem. Sci.* **2013**, *4*, 4092. (e) Girard, S. A.; Knauber, T.; Li, C.-J. *Angew. Chem. Int. Ed.* **2014**, *53*, 74.

[22] (a) Godula, K.; Sames, D. *Science* **2006**, *312*, 67. (b) Gutekunst, W. R.; Baran, P. S. *Chem. Soc. Rev.* **2011**, *40*, 1976. (c) Chen, D. Y.-K.; Youn, S. W. *Chem. Eur. J.* **2012**, *18*, 9452. (d) Yamaguchi, J.; Yamaguchi, A. D.; Itami, K. *Angew. Chem. Int. Ed.* **2012**, *51*, 8960. (e) Wenchel- Delord, J.; Glorius, F. *Nat. Chem.* **2013**, *5*, 369.

[23] Wencel-Delord, J.; Dörge, T.; Glorius, F. *Chem. Soc. Rev.* **2011**, *40*, 4740.

[24] (a)Giri, R.; Shi, B.-F.; Engle, K. M.; Maugel, N.; Yu, J.-Q. *Chem. Soc. Rev.* **2009**, *38*, 3242. (b) Newhouse, T.; Baran, P. S. *Angew. Chem. Int. Ed.* **2011**, *50*, 3362. (c) Mahatthananchai, J.; Dumas, A, M.; Bode, J. W. *Angew. Chem. Int. Ed.* **2012**, *51*, 10954. (d) Franzoni, I.; Mazet, C. *Org. Biomol. Chem.* **2014**, *12*, 233. (e) Robles, O.; Romo, D. *Nat. Prod. Rep.* **2014**, *31*, 318.

[25] Brückl, T.; Baxter, R. D.; Ishihara, Y.; Baran, P. S. *Acc. Chem. Res.* **2012**, *45*, 826.

control of the reaction site is not possible. The second approach is the use of a directing group.[6,26] This approach is currently the most general, reliable, and successful for regioselective C–H functionalization. The substrates must bear a specific functional group which can associate with the catalyst to achieve selectivity and reactivity. Abundant directing groups and functionalization reagents have been developed since the 2000s to enable palladium-catalyzed aryl C–H hydroxylations, aminations, arylations, alkylations and halogenations.[27] The reported directing group-guided C(sp^3)–H functionalizations, however, often require high temperature, which diminishes their practicality. This is partly due to the relatively high entropy cost in a bimolecular transition state of the C(sp^3)–H activation step involving a directing group-containing substrate and a reagent or catalyst (X).

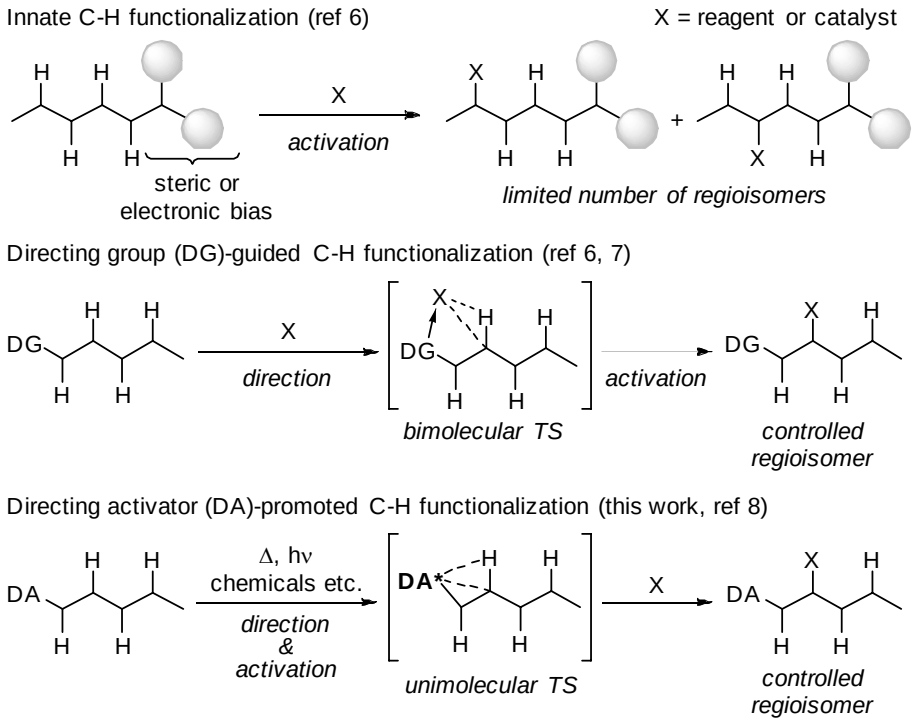

Figure 3–1. Three strategies to assure regioselectivity in C–H functionalization.

---

[26] Review for directed synthesis: (a) Snieckus, V. *Chem. Rev.* **1990**, *90*, 879. (b) Hoveyda, A. H.; Evans, D. A.; Fu, G. C. *Chem. Rev.* **1993**, *93*, 1307. Selected leading references for DG-guided C-H functionalizations: (c) Johnson, J. A.; Sames, D. *J. Am. Chem. Soc.* **2000**, *122*, 6321. (d) Lyons, T. W.; Sanford, M. S. *Chem. Rev.* **2010**, *110*, 1147–1169. (e) Rousseau, G.; Breit, B. *Angew. Chem. Int. Ed.* **2011**, *50*, 2450. (f) Engle, K. M.; Mei, T.-S.; Wasa, M.; Yu, J.-Q. *Acc. Chem. Res.* **2012**, *45*, 788. (g) Leow, D.; Li, G. Mei, T.-S.; Yu, J.-Q. *Nature* **2012**, *486*, 518. (h) Bigi, M. A.; Reed, S. A.; White, M. C. *J. Am. Chem. Soc.* **2012**, *134*, 9721. (i) Wang, Z.; Reinus, B. J.; Dong, G. *J. Am. Chem. Soc.* **2012**, *134*, 13954. (j) Rouquet, G.; Chatani, N. *Angew. Chem. Int. Ed.* **2013**, *52*, 11726.

[27] Lyons, T. W.; Sanford, M. S. *Chem. Rev*. **2010**, *110*, 1147.

Based on this consideration, I envisioned an alternative approach based on the directing activator (DA) strategy (**Figure 3–1**).[28] A DA is a reactive functional group covalently attached to the substrate, acting as both a reaction site determinant and a C(sp^3)–H bond activator.[29]

DA can be activated by external stimulus, such as heat, light or chemicals, and cleave a C–H bond of a specific site. In other word, this is a "reactive directing group". The activated DA requires no more external reagent to cleave C-H bond, and reaction goes through an entropically favorable unimolecular transition state, leading to site-selective C(sp^3)–H functionalization under mild conditions . In kinetic point of view, this design is advantageous, because in many cases, C-H activation is the most difficult chemical process.

Polyol unit synthesis

Polyol unit is omnipresent in many bioactive complex molecules (**Figure 3–2**). Polyketide natural products represent a broad class of secondary metabolites used extensively in human medicine.[30] Approximately 20% of the top–selling small molecule drugs are polyketides, and it is estimated that polyketides are five times more likely to possess drug activity compared to other natural product families. More efficient and flexible method to synthesize polyol unit is a longstanding research target among synthetic chemists.

---

[28] Representative examples: (a) Breslow, R.; Dale, J. A.; Kalicky, P.; Liu, S. Y.; Washburn, W. N. *J. Am. Chem. Soc.* **1972**, 94, 3276. (b) Breslow, R.; Corcoran, R. J.; Snider, B. B.; Doll, R. J.; Khanna, P. L.; Kaleya, R. *J. Am. Chem. Soc.* **1977**, *99*, 905. (c) Doyle, M. P.; Kalinin, A. V.; Ene, D. G. *J. Am. Chem. Soc.* **1996**, *118*, 8837. (d) Espino, C. G.; Wehn, P. M.; Chow, J.; Du Bois, J. *J. Am. Chem. Soc.* **2001**, *123*, 6935. (e) Chen, K.; Richter, J. M.; Baran, P. S. *J. Am. Chem. Soc.* **2008**, 130, 7247. (f) Kasuya, S.; Kamijo, S.; Inoue, M. *Org. Lett.* **2009**, *11*, 3630. (g) Yoshikai, N.; Mieczkowski, A.; Matsumoto, A.; Ilies, L.; Nakamura, E. *J. Am. Chem. Soc.* **2010**, *132*, 5568. (h) Voica, A.-F.; Mendoza, A.; Gutekunst, W. R.; Fraga, J. O.; Baran, P. S. *Nat. Chem.* **2012**, *4*, 629. (i) Jurberg, I. D.; Peng, B.; Wöstefeld, E.; Wasserloos, M.; Maulide, N. *Angew. Chem. Int. Ed.* **2012**, *51*, 1950. (j) Simmons, E. M.; Hartwig, J. F. *Nature* **2012**, *483*, 70. (k) Kuninobu, Y.; Nakahara, T.; Takeshima, H.; Takai, K. *Org. Lett.* **2013**, *15*, 426. (l) Chu, X.; Wang, Y.-F.; Ren, W.; Zhang, F.-L.; Chiba, S. *Org. Lett.* **2013**, *15*, 3214. (m) Ghavtadze, N.; Melkonyan, F. S.; Gulevich, A. V.; Huang, C.; Gevorgyan, V. *Nat. Chem.* **2014**, *6*, 122.

[29] For acceleration of reaction rate by intramolecularity, see: (a) Page, M. L.; Jencks, W. P. *Proc. Natl. Acad. Sci. U.S.A.* **1971**, *68*, 1678. (b) Pascal, R. *Eur. J. Org. Chem.* **2003**, *10*, 1813. (c) Tan, K. L. *ACS Catal.* **2011**, *1*, 877. (d) Tan, K. L. *Nat. Chem.* **2012**, *4*, 253.

[30] Koskinen, A. M. P.; Karisalmi, K. *Chem. Soc. Rev*. **2005**, *34*, 677.

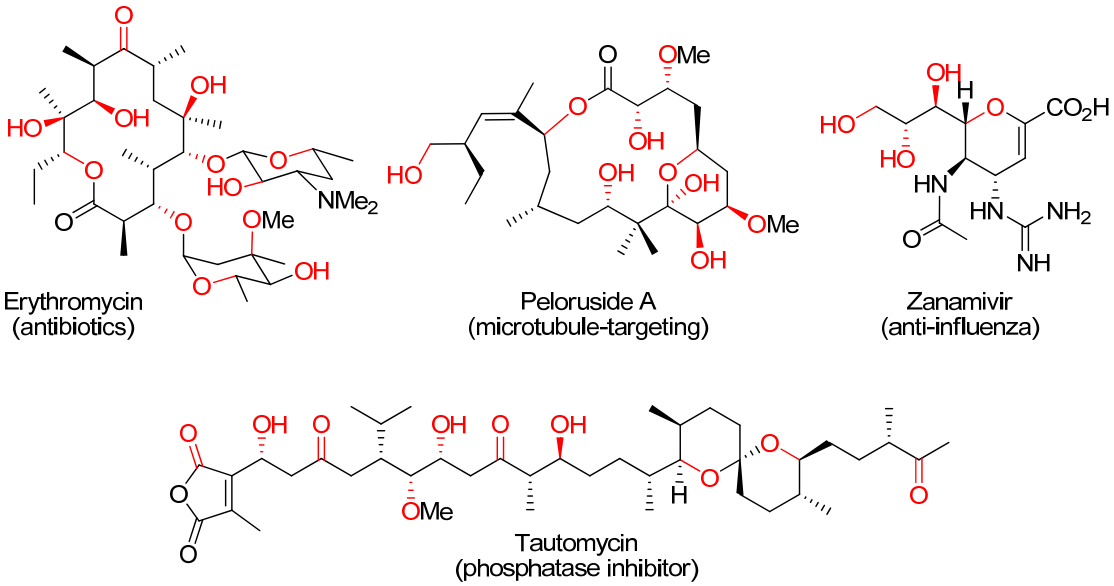

Figure 3–2. Omnipresent bioactive polyol chains

Many synthetic methods for polyol units have been developed and sophisticated. Representative methods, especially for 1,3-polyol synthesis, are shown in **Scheme 3–1**, such as aldol reaction, epoxide-opening, alkene oxidation or hydration and conjugate addition.

Scheme 3–1. Synthetic routes toward 1,3-polyol

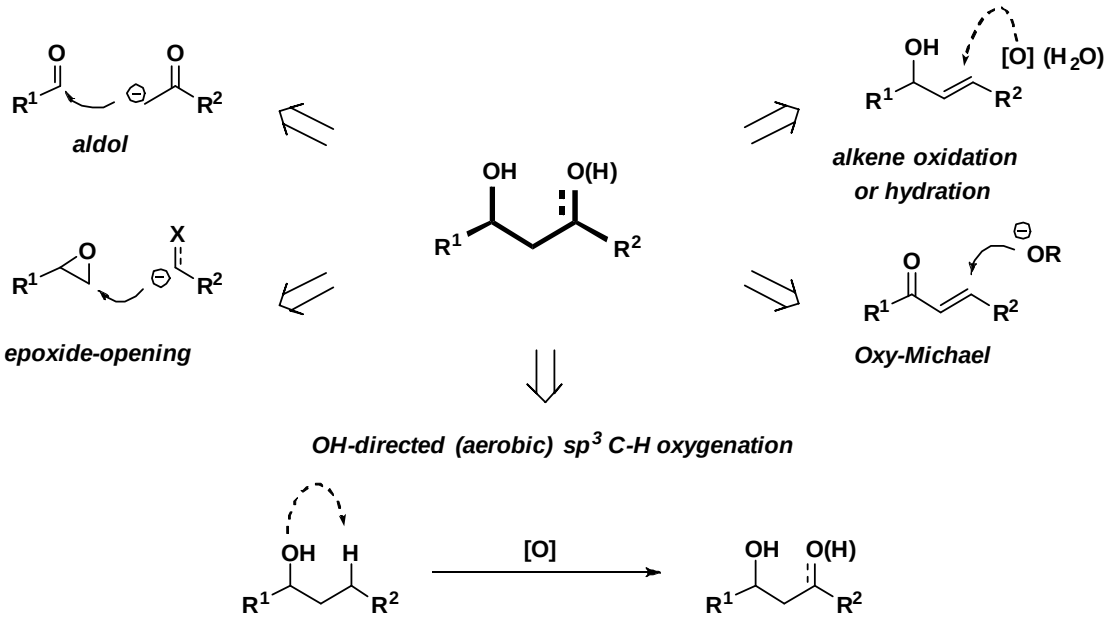

I became interested in a more straightforward method: hydroxy-group directed C(sp^3)–H bond oxygenation.[31] It is ideal to use abundant oxygen as the terminal oxidant, which produces water as the sole side product. The reaction should allow for conceptually altered synthetic routes of various biologically active drug leads with multiple oxygen functionalities.[32] Two main hurdles in developing such reactions are: (1) applicability to the most ubiquitous, but least reactive acyclic methylene C(sp^3)–H bonds,[33] and (2) low reactivity of O_2.[34]

Directing activator strategy in C(sp^3)–H oxygenation

Most methods for aliphatic C–H bond functionalization typically rely on the presence of one inherently reactive C–H bond,[35] or on installation and subsequent removal of directing groups that are not components of the desired molecule.[8] To overcome these limitations, some leading chemists sought activators that would facilitate aliphatic C–H bond functionalization at a single site directed by common functional groups contained in both the reactant and the products.

Up to now, seminal contributions were reported in the field of site-selective C(sp^3)–H oxygenation (**Scheme 3–2**, *vide infra*). Baran *et al*. reported modified

---

[31] Mo, F.; Tabor, J. R.; Dong, G. *Chem. Lett.* **2014**, *43*, 264.

[32] (a) Chen, K.; Baran, P. S. *Nature* **2009**, *459*, 824-828. (b) Ishihara, Y.; Baran, P. S. *Synlett* **2010**, *12*, 1733.

[33] Functionalization of acyclic methylene C(sp^3)–H bonds is still difficult. Recent examples of site-selective acyclic methylene C(sp^3)–H functionalization: (a) Chen, M. S.; White, M. C. *Science* **2010**, *327*, 566. (b) Zhao, Y.; Yim, W.-L.; Tan, C. K.; Yeung, Y.-Y. *Org. Lett.* **2011**, *13*, 4308. (c) Kochi, T.; Hamasaki, T.; Aoyama, Y.; Kawasaki, J.; Kakiuchi, F. *J. Am. Chem. Soc.* **2012**, *134*, 16544. (d) Kawamorita, S.; Murakami, R.; Iwai, T.; Sawamura, M. *J. Am. Chem. Soc.* **2013**, *135*, 2947. (e) Chen, F.-J.; Zhao, S.; Hu, F.; Chen, K.; Zhang, Q.; Zhang, S.-Q.; Shi, B.-F. *Chem. Sci.* **2013**, *4*, 4187. (f) Antonchick, A. P.; Burgmann, L. *Angew. Chem. Int. Ed.* **2013**, *52*, 3267. (g) Moteki, S. A.; Usui, A.; Zhang, T.; Alvarado, C. R. S.; Maruoka, K. *Angew. Chem. Int. Ed.* **2013**, *52*, 8657. (h) Shan, G.; Yang, X.; Zong, Y.; Rao, Y. *Angew. Chem. Int. Ed.* **2013**, *52*, 13606. (i) Li, Z.; Zhang, Y.; Zhang, L.; Liu, Z.-Q. *Org. Lett.* **2014**, *16*, 382.

[34] Selected examples of using molecular oxygen in unactivated C–H functionalization: (a) Schönecker, B.; Zheldakova, T.; Liu, Y.; Kötteritzsch, M.; Günther, W.; Görls, H. *Angew. Chem. Int. Ed.* **2003**, *42*, 3240. (b) Punniyamurthy, T.; Velusamy, S.; Iqbal, J. *Chem. Rev.* **2005**, *105*, 2329–2364. (c) Wang, D.-H.; Engle, K. M.; Shi, B. F.; Yu, J.-Q. *Science* **2009**, *327*, 315–319. (d) Wendlandt, A. E.; Suess, A. M.; Stahl, S. S. *Angew. Chem. Int. Ed.* **2011**, *50*, 11062. (e) Wang, Y.-F.; Chen, H.; Zhu, X.; Chiba, S. *J. Am. Chem. Soc.* **2012**, *134*, 11980. (f) Campbell, A. N.; Stahl, S. S. *Acc. Chem. Res.* **2012**, *45*, 851. (g) Oisaki, K.; Abe, J.; Kanai, M. *Org. Biomol. Chem.* **2013**, *11*, 4569. (h) Hashimoto, T.; Hirose, D.; Taniguchi, T. *Angew. Chem. Int. Ed.* **2014**, *53*, 2730.

[35] (a) Chen, M. S.; White, M. C. *Science* **2007**, *318*, 783. (b) Newhouse, T.; Baran, P. S. *Angew. Chem. Int. Ed.* **2011**, *50*, 3362.

Hofmann-Löffler-Freytag strategy to convert tertiary a C–H bond to a C–O bond with multistep operations.[36] By devising a detachable dioxirane precursor containing a trifluoromethyl ketone moiety, Inoue *et al*. reported an *in situ* generated dioxirane promoted site-selective tertiary C–H oxidation by at a proximal position.[37] These two reactions proceed under relatively mild conditions (room temperature). More recently, Hartwig group established iridium-catalyzed C–H silylation, converting primary and secondary C–H bonds to alcohol surrogate after Tamao oxidation of the silane intermediate.[38]

Scheme 3–2. Insight from seminal precedents

Baran, P. S. *et al*. *JACS* **2008**, *130*, 7247.

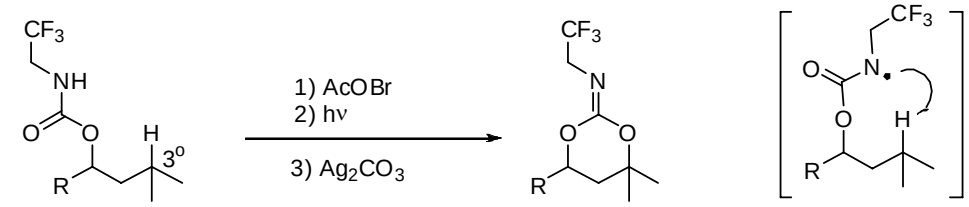

Inoue, M. *et al*. *OL* **2009**, *11*, 3630.

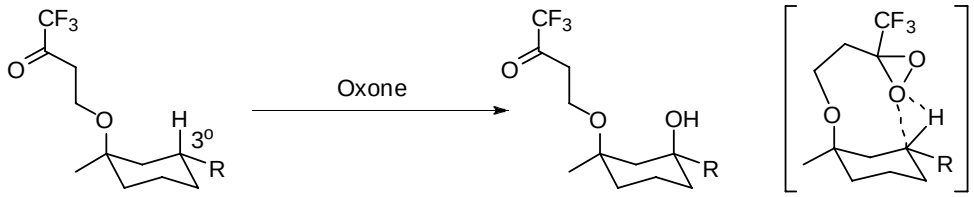

Hartwig. J. F. *et al*. *Nature* **2012**, *483*, 70.; *JACS* **2014**, *136*, 6586.

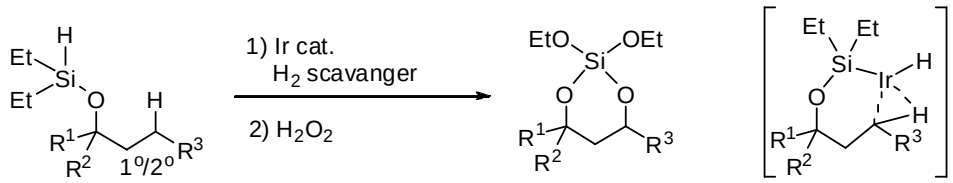

It can be deduced from these outstanding examples that all these challenging regioselective C(sp^3)–H oxygenations were promoted by well-designed directing activators. These precedents encouraged me to believe that directing activator strategy could be a great compass guiding for mild and selective C-H transformations.

[36] Chen, K.; Richter, J. M.; Baran, P. S. *J. Am. Chem. Soc*. **2008**, *130*, 7247.
[37] Kasuya, S.; Kamijo, S.; Inoue, M. *Org. Lett*. **2009**, *11*, 3630.
[38] (a) Simmons. E. M. Hartwig, J. F. *Nature* **2012**, *483*, 70. (b) Li, B.; Driess, M.; Hartwig, J. F. *J. Am. Chem. Soc*. **2014**, *136*, 6586

3–2. Novel directing activator for regioselective methylene oxygenation

Although NHPI can catalyze diverse C–H functionalizations, it shows no regioselectivity. For example, in heptane substrate, five positions were reactive towards NHPI catalyzed oxidation (**Scheme 3–3**).[39]

Scheme 3–3. NHPI catalyzed acetoxylation

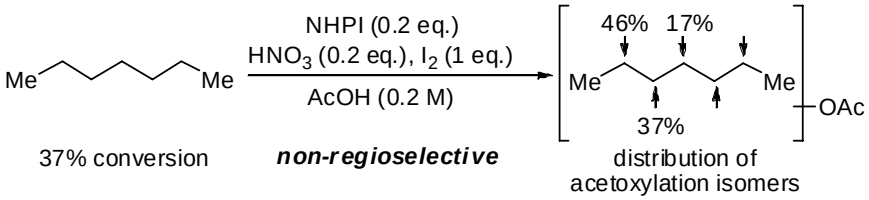

My target reaction is site-selective C(sp^3)–H oxygenation of methylene using aerobic oxygen (O_2) as the terminal oxidant. Toward this aim, a novel directing activator was devised (**Scheme 3–4**), inspired by NHPI chemistry,[40] as well as the study described in Chapter 2.

Scheme 3–4. Rational design of novel directing activator mediated regioselective C(sp^3)–H oxygenation

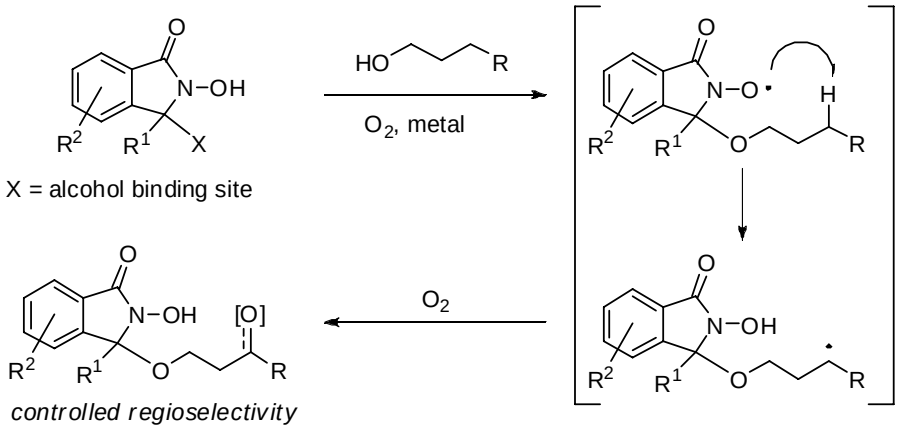

[39] Minisci, F.; Porta, O.; Recupero, F.; Gambarotti, C.; Paganelli, R.; Pedullib, G. F.; Fontana, F. *Tetrahedron Lett*. **2004**, *45*, 1607.
[40] Ishii, Y.; Sakaguchi, S.; Iwahama, T. *Adv. Synth. Catal.* **2001**, *343*, 393. (b) Recupero, F.; Punta, C. *Chem. Rev.* **2007**, *107*, 3800.

In the rational design, an *N*-hydroxy reactive site was essential for the reactivity, and an alcohol binding site is created. By covalently attaching the DA to the hydroxy group of substrate alcohols, the C(sp^3)–H activation step becomes an intramolecular process. A specific C(sp^3)–H bond proximal to the *in situ*-generated *N*-oxyl radical of the DA is selectively cleaved. The thus-generated carbon radical will be subsequently trapped by O_2 to produce oxygenated products (alcohols or ketones).[41]

Table 3–1. Screening for a suitable directing activator (DA)

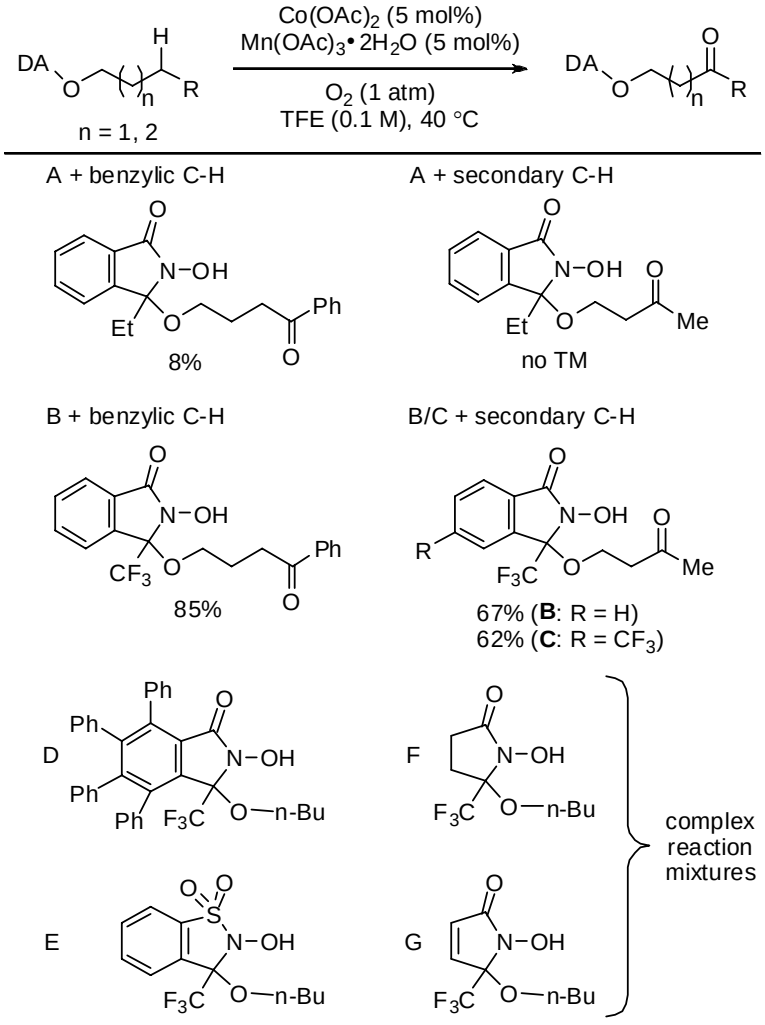

[41] Selective aerobic functionalization of alkenes using *N*-oxyl radical DA: (a) Schmidt, V. A.; Alexanian, E. J. *Angew. Chem. Int. Ed.* **2010**, *49*, 4491. (b) Schmidt, V. A.; Alexanian, E. J. *J. Am. Chem. Soc.* **2011**, *133*, 11402. (c) Schmidt, V. A.; Alexanian, E. J. *Chem. Sci.* **2012**, *3*, 1672. (d) Quinn, R. k.; Schmidt, V. A.; Alexanian, E. J. *Chem. Sci.* **2013**, *4*, 4030.

Based on this reaction design, investigation proceeded by modifying the DA structure and oxygenation conditions (**Table 3–1**). This work was mainly done by Mr. Ozawa in our group.[42] Several DA bound-alcohols (**A**-**G**) were synthesized and their reactivity was compared under condition A [$Co(OAc)_2$ (5 mol%), $Mn(OAc)_3 \cdot 2H_2O$ (5 mol%) in 2,2,2-trifluoroethanol (TFE, 0.1 M) under O_2 (1 atm) at 40 °C]. During the optimization, Mr. Ozawa found TFE solvent dramatically accelerated the reaction. Probably this was due to TFE's ability to stabilize radical cations, high solubility of molecular oxygen, and resistance to oxidation.[43]

With **A**, benzylic C–H oxygenation produced the corresponding phenyl ketone product in 8% yield. A more challenging methylene C(sp^3)–H oxygenation, however, did not proceed at all. In both cases, the efficiency of the C–H oxygenation was much lower than that of *N*-hydroxyphthalimide itself.[44] Because the reactivity of *N*-oxyl radicals is in accord with their electron-deficiency,[45] we next designed **B** bearing a CF_3 group at the α-carbon of the nitrogen atom to enhance the reactivity of the DA. As a result, **B** promoted simple methylene C(sp^3)–H oxygenation to produce γ-oxo product in 67% yield. Although the α-C(sp^3)–H bond adjacent to the ether oxygen atom is the innate reactive site,[46] the less reactive γ-C(sp^3)–H was predominantly oxygenated. Under the same conditions, benzylic C(sp^3)–H oxygenation also proceeded well (85% yield). Introducing an additional CF_3 substituent at the benzene ring (**C**), however, did not further improve the yield. Additional structural modifications (**D**,[47] **E**, **F**, or **G**) were not successful, resulting in complex mixtures and/or decomposition of the DA during the reaction. Thus, **B** proved to be the best DA.

I and Mr. Ozawa applied the optimized condition to the oxygenation of a variety of alcohols bound to the DA (**B**) (**Table 3–2**). Under condition A, simple methylene C(sp^3)–H bonds of aliphatic alcohols were regioselectively converted to the corresponding C=O double bonds. From **B**-bound butanol (entry 1) and substituted

---

[42] Ozawa, J. "The development of regioselective remote aerobic C(sp^3)–H oxygenation reaction of alkyl alcohols", MSc thesis, The University of Tokyo, **2014**.

[43] For beneficial effects of TFE in C-H functionalization, see: (a) Bégué, J.-P.;Delpon, D. B.; Crousse, B. *Synlett* **2004**, 18. (b) Shuklov, I. A.; Dubrovina, N. V.; Börner, A. *Synthesis* **2007**, 2925.

[44] Ishii, Y.; Iwahama, T.; Sakaguchi, S.; Nakayama, K.; Nishiyama, Y. *J. Org. Chem.* **1996**, *61*, 4520.

[45] (a) Sheldon, R. A.; Arends, I. W. C. E. *J. Mol. Catal. A: Chem.* **2006**, *251*, 200–214.(b) Sonobe, T.; Oisaki, K.; Kanai, M. *Chem. Sci.* **2012**, *3*, 3249.

[46] The bond dissociation energy of C–H bonds adjacent to heteroatoms are generally lower than those adjacent to alkyl groups. See: Blanksby, S. J.; Ellison, G. B. *Acc. Chem. Res.* **2003**, *36*, 255.

[47] Nechab, M.; Einhorn, C.; Einhorn, J. *Chem. Commun.* **2004**, *13*, 1500.

butanols (entries 2 and 3), γ-oxo products were selectively obtained. Substrate possessing a longer alkyl chain (entry 4) was converted to a 1.2:1 mixture of γ-oxo and δ-oxo products. Nevertheless, α-, β-, and ε-oxo products were either not detected at all or detected in only trace amounts. Oxygenation of substrates possessing an ester or a phthalimide functionality (entries 5–7) proceeded exclusively at the γ-position. The extremely high regioselectivity observed in these substrates is probably due to inactivation of the δ-position by the inductive effect of the electron-withdrawing groups at the ε-positions.

Table 3–2. Substrate scope

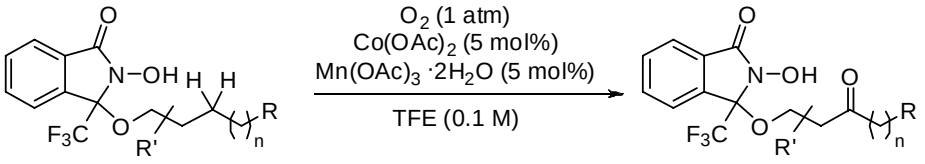

entry	SM	temp. time	product	yield NMR [isolated]
1	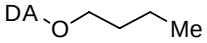	40 °C 18 h	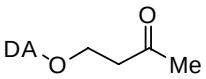	62%
2	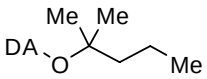	40 °C 24 h	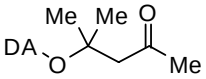	72%
3	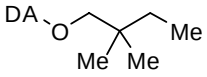	40 °C 22 h	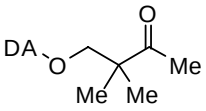	59%
4	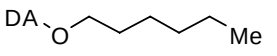	40 °C 6 h	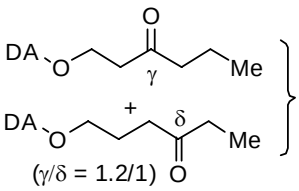	66%
5	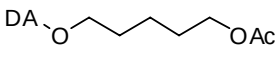	50 °C 26 h	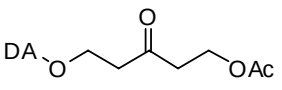	43%

Table 3–2. Substrate scope (continued)

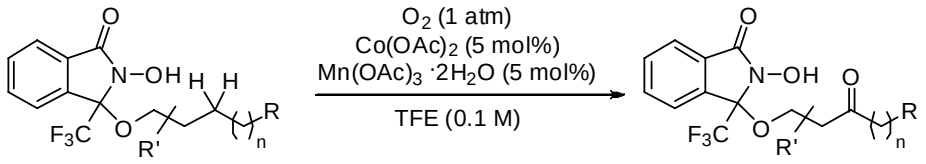

entry	SM	temp. time	product	yield NMR [isolated]
6	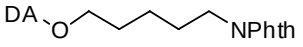	50 °C 18 h	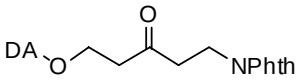	52%
7	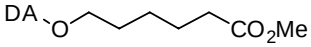	50 °C 18 h	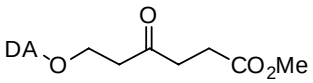	50%
8	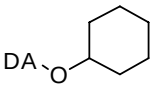	40 °C 24 h	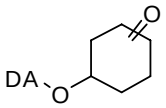	trace
9	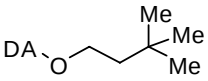	60 °C 12 h		NR
10	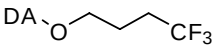	40 °C 22 h		NR
11	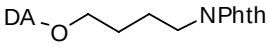	40 °C 24 h	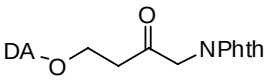	trace

For cyclohexanol substrate (entry 8), almost no oxidation products were isolated. Probably the C–H bonds on the ring oriented away from the reactive *N*-hydroxy group. No reaction occurred when the γ-H bonds were replaced by another two methyl groups (entry 9). Similar results were also observed for substrates with electron withdrawing group attached directly (entry 10) and close (entry 11) to the γ-position.

3–3. Background on oxidation state-selective oxidation

Applying the novel directing activator, methylenes were successfully converted to ketones as previously described. Compare to ketone stage, the partial C(sp^3)–H oxidation of methylene into the corresponding alcohols is even more challenging. Taking propane for example (**Figure 3–3**), the BDE value of methylene C–H bond is 98 kcal/mol. After the parent alkane is oxidized to a secondary alcohol, the α-oxy C–H bond (BDE ~ 91 kcal/mol) is inherently more reactive toward oxidation. Hence, direct methylene hydroxylation generally suffers from generation of side-products such as ketones and/or carboxylic acids.

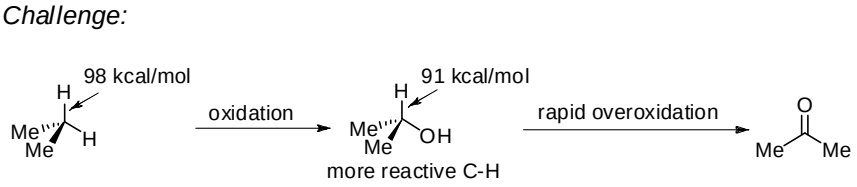

Figure 3–3. Energy difference

Oxidation of benzylic position could be controlled at C–O single bond stage. Attachment of an electron-withdrawing group to OH would suppress the possibility of the α-oxy C–H oxidation, thus preventing undesired over-oxidation reactions.[48]

[48] For representative examples on the preparation of benzyl alcohols and their derivatives through benzylic oxidation, see: (a) Rawlinson, D. J.; Sosnovsky, G. *Synthesis* **1973**, 567; (b) Belli, A.; Giordano, C.; Citterio, A. *Synthesis* **1980**, 477; (c) Bouquet, M.; Guy, A.; Lemaire, M.; Guetté, J. P. *Synth. Commun*. **1985**, *15*, 1153; (d) Goel, A. B. *Inorg. Chim. Acta* **1986**, *121*, L11; (e) Citterio, A.; Santi, R.; Pagani, A. *J. Org. Chem*. **1987**, *52*, 4925. (f) Ganin, E.; Amer, I. *J. Mol. Catal. A: Chem*. **1997**, *116*, 323. (g) Hamada, T.; Irie, R.; Mihara, J.; Hamachi, K.; Katsuki, T. *Tetrahedron* **1998**, *54*, 10017. (h) Dick, A. R.; Hull, K. L.; Sanford, M. S. *J. Am. Chem. Soc*. **2004**, *126*, 2300. (i) Shaikh, T. M.; Sudalai, A. *Tetrahedron Lett*. **2005**, 46, 5587. (j) Dohi, T.; Takenaga, N.; Goto, A.; Maruyama, A.; Kita, Y. *Org. Lett*. **2007**, *9*, 3129. (k) Kumar, V.; Sharma, A.; Sharma, M.; Sharma, U. K.; Sinha, A. K. *Tetrahedron* **2007**, *63*, 9718. (l) Feng, J.; Liang, S.; Chen, S-Y.; Zhang, J.; Fu, S-S.; Yu, X-Q. *Adv. Synth. Catal*. **2012**, *354*, 1287. (m) Akhlaghinia, B; Ebrahimabadi, H.; Goharshadi, E. K.; Samiee, S.; Rezazadeh, S. *J. Mol. Catal. A-Chem.* **2012**, *357*, 67. (n) Rout, S. K.; Guin, S.; Ghara, K. K.; Banerjee, A.; Patel, B. K. *Org. Lett*. **2012**, *14*, 3982. (o) Terent'ev, A. O.; Krylov, I. B.; Sharipov, M. Y. Kazanskaya, Z. M.; Nikishin, G. I. *Tetrahedron* **2012**, *68*, 10263. (p) Majji, G.; Guin, S.; Gogoi, A.; Rout, S. K.; Patel, B. K. *Chem. Commun*. **2013**, *49*, 3031. (q) Pandey, G.; Sujit Pal. S.; Laha, R. *Angew. Chem. Int. Ed*. **2013**, *52*, 5146.

NHPI is an efficient catalyst to promote benzylic C–O single bond formation. According to the mechanism, the products were formed through two types of process: (1) benzylic radical trap, and (2) nucleophilic trap of benzylic carbocation.

(1) Radical trap

Benzylic radical can be easily trapped by good radical trapping reagent, such as NO_2, O_2 and iodide (**Figure 3–4**).

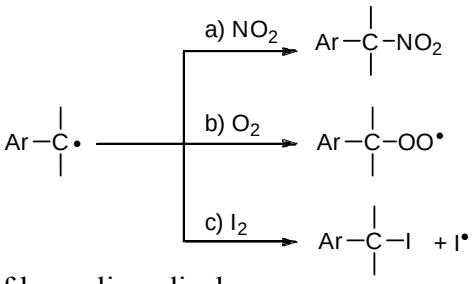

Figure 3–4. Trap of benzylic radical

Minisci *et al*. found that alkylbenzenes could be selectively functionalized to the corresponding acetates by aerobic oxidation catalyzed by NHPI/HNO_3 and iodine (**Scheme 3–5**).[49] Although the nitration of hydrocarbons by NO_2 and NHPI catalysis was reported (**Figure 3–4**, route a),[50] they proved that benzyl iodides were selectively formed if the concentration of I_2 was much higher than that of NO_2 and O_2. In the same reaction system, solvolysis of benzyl iodides leads to benzyl acetates.

Scheme 3–5. NHPI catalyzed benzylic acetoxylation

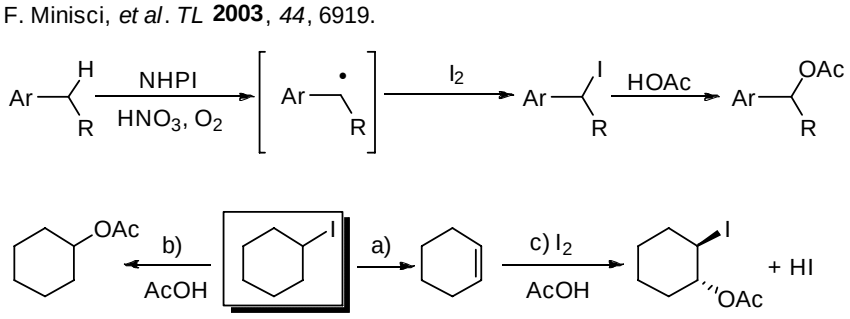

[49] Minisci, F.; Recupero, F.; Gambarotti, C.; Punta, C.; Paganelli, R. *Tetrahedron Lett*. **2003**, *44*, 6919.

[50] (a) Sakaguchi, S.; Nishiwaky, Y.; Kitamura, T.; Ishii, Y. *Angew. Chem., Int. Ed*. **2001**, 40, 222. (b) Isozaki, S.; Nishiwaky, Y.; Sakaguchi, S.; Ishii, Y. *Chem. Commun*. **2001**, 1352.

As an extension of benzylic oxygenation, Minisci *et al*. tried the same condition with cyclohexane. However, the cyclohexyl iodide mainly underwent elimination with formation of cyclohexene (**Scheme 3–5**, route a) and to a minor extent nucleophilic substitution (route b). I_2 was working as an electrophile to be added to cyclohexene, leading to the *trans*-2-iodocyclohexyl acetate (route c).

For a simple methylene oxygenation, to control the oxidation at C-O single bond stage is attractive, while it is much more challenging than benzylic CH_2. Like previous strategy, Minisci group reported NHPI catalyzed free-radical iodination of *n*-heptane at high temperature (100 ^oC). Followed by solvolysis, a mixture of acetoxylated regioisomers was provided with 37% starting material conversion (**Scheme 3–3**).[39]

Using stoichiometric amounts of NHPI and $PhI(OAc)_2$ in the presence of CuCl catalyst, Chang *et al*. developed a highly efficient protocol for the benzyl or allylic C-H functionalization of simple hydrocarbons (**Scheme 3–6**).[51]

Scheme 3–6. Cu-facilitated C-O bond formation using NHPI

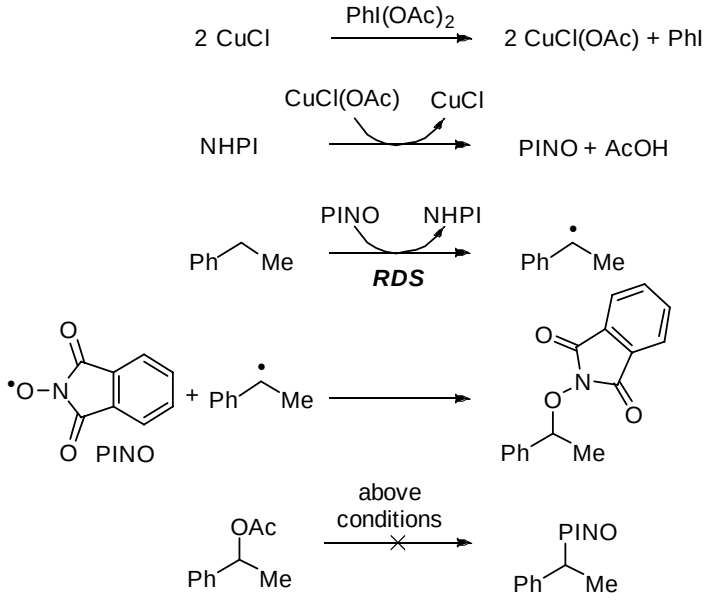

Condition: Substrate (5 equiv), NHPI (1.0 equiv), $PhI(OAc)_2$ (1.0 equiv), and CuCl (10 mol %) in CH_3CN (0.3 M) at 70 ^oC for 12 h under Ar.

The reaction was revealed to proceed *via* a radical pathway, in which PINO radical

[51] Lee, J. M.; Park, E. J.; Cho, S. H.; Chang, S. *J. Am. Chem. Soc*. **2008**, *130*, 7824

plays a dual role: a hydrogen abstractor from hydrocarbons as well as a stoichiometric reagent to couple with the resultant alkyl radicals. A benzylic or allylic position is selectively oxygenated, offering a new possibility of the selective C–O bond-forming methodology.

(2) Nucleophilic trap

C–H Nitrooxylation at benzylic positions has been achieved by Inoue group (**Scheme 3–7**).[52] They demonstrated that cerium (IV) ammonium nitrate (CAN) could further oxidize the generated benzylic radical to a carbocation. Delivery of the nitrate anion led to the formation of benzyl nitrate as the final product.

The nitrooxy group can be regarded as tentative hydroxy protecting groups, and the nitrooxy moiety worked as excellent leaving groups for *N*- and *C*-substitution reactions.

Scheme 3–7. NHPI catalyzed benzylic nitrooxylation

M. Inoue, *et al*. *TL* **2011**, *52*, 4654.

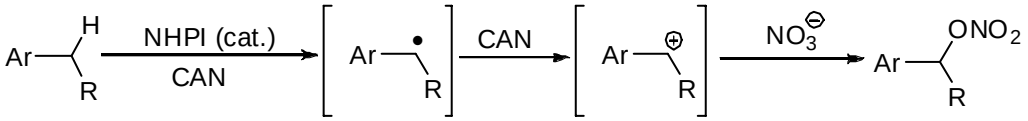

3–4. My strategy toward oxidation state-selective methylene oxidation

To the best of my knowledge, up to now, no promising strategy was exemplified in the direct oxidation-state controlled oxygenation of simple methylenes *via* a radical process. Based on the knowledge of the successful oxidation-state controlled benzylic oxygenation, I set my goal to realize oxidation state-controlled simple methylene oxidation.

Since the alkyl radical was an important intermediate, I anticipated that a protecting group (PG) could prevent the further oxidation of the C–O single bond. Typically the PG is an electron withdrawing group.

[52] Kamijo, S.; Amaoka, Y.; Inoue, M. *Tetrahedron Lett*. **2011**, *52*, 4654.

Initial screening of the trapping reagents

I tried several radical trapping reagents (**Table 3–3**), such as I_2, 1,2- diiodoethane, NCS, NBS, NIS, di-*tert*-butyl peroxide, *tert*-butyl hydroperoxide, benzoyl peroxide, DDQ, ketoABNO, TEMPO, boron reagent, Frémy's salt and in situ generated nitroso acceptor. Unluckily, no C–O single bond formation was observed.

Further radical oxidation to a carbocation followed by nucleophilic trap was also examined by using cerium (IV) ammonium nitrate (CAN) and hypervalent iodine. But also no desired products were obtained.

Table 3–3.

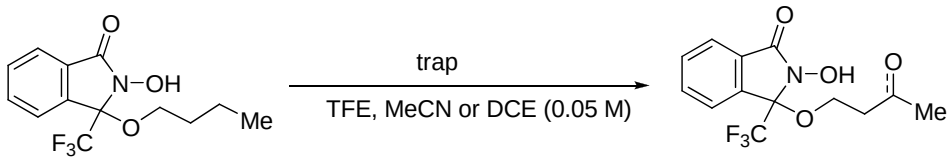

1) Radical trap

I_2, HNO_3, air, AcOH as solvent	SM decomposed	DDQ, $Co(NO_3)_2$, $Co(OAc)_2$, O_2	ketone product
I_2, $Co(OAc)_2$, O_2, AcOH as solvent	NR	KetoABNO, $Co(OAc)_2$, O_2	ketone product
I_2, $Co(OAc)_2$, O_2, TFIPA as solvent	NR	TEMPO, $Co(OAc)_2$, O_2	ketone product
ICH_2CH_2I, $Co(OAc)_2$, O_2	ketone product	Co(TPP)/$NaBH_4$, O_2	NR
NCS, $Co(OAc)_2$, O_2	ketone product	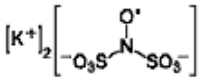 Frémy's salt	NR
NBS, $Co(OAc)_2$, O_2	ketone product		
NIS, $Co(OAc)_2$, O_2	ketone product		
$(PhCO_2)_2$	SM decomposed	in situ generated  , O_2	ketone product
^tBuOOH	NR		
$(^tBuO)_2$	SM decomposed		

2) Carbocation nucleophilic trap

CAN/NaOAc	almost NR
$PhI(OAc)_2$/CuOAc	SM decomposed

Alkoxyl radical trap

If molecular oxygen traps the alkyl radical, peroxyl radical will be first generated. Dimerization of the alkylperoxyl radical would produce tetraoxide ROOOOR, which, in

the case of R = tertiary alkyl, decomposes in solvent cage to molecular oxygen and two alkoxyl radicals with a relatively slow rate. On the other hand, according to the Russell mechanism, dissociation of primary or secondary peroxyl radicals by a nonradical 1,5-H-atom shift leads to the formation of equal yields of alcohol and ketone (**Figure 3–5**).[53]

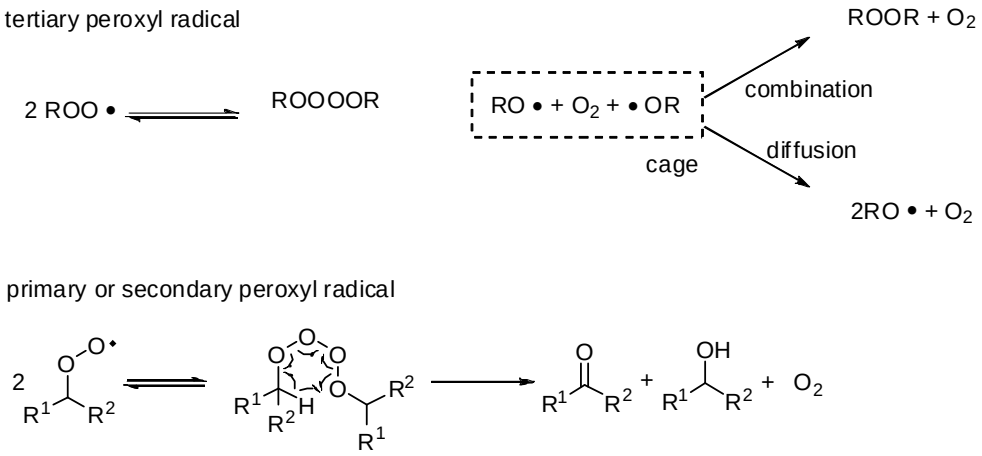

Figure 3–5. Termination of peroxyl radical

In the presence of *N*-hydroxy catalyst, two more steps are involved:

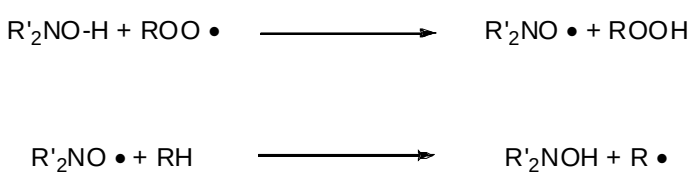

Figure 3–6. Termination of peroxyl radical in the presence of *N*-hydroxy catalyst

Under low concentration of R–H, dimerization of the peroxyl radical is less important. Therefore, in the case of the concerned substrate peroxyl radical, the following intramolecular hydrogen atom transfer seems to be possibly during the overoxidation (**Scheme 3–8**): the peroxyl radical **7** abstracts a H atom from the *N*-hydroxy group to give an *N*-oxyl radical species **8**, which is reactive enough to cleave the α-H of the peroxide oxygen atom. In this way, both H atoms of the methylene are

[53] Ingold, K. U. *Acc. Chem. Res.* **1969**, *2*, 1.

oxidized, giving ketone **10** as the final product.

Scheme 3–8. Possible hydrogen atom transfer process

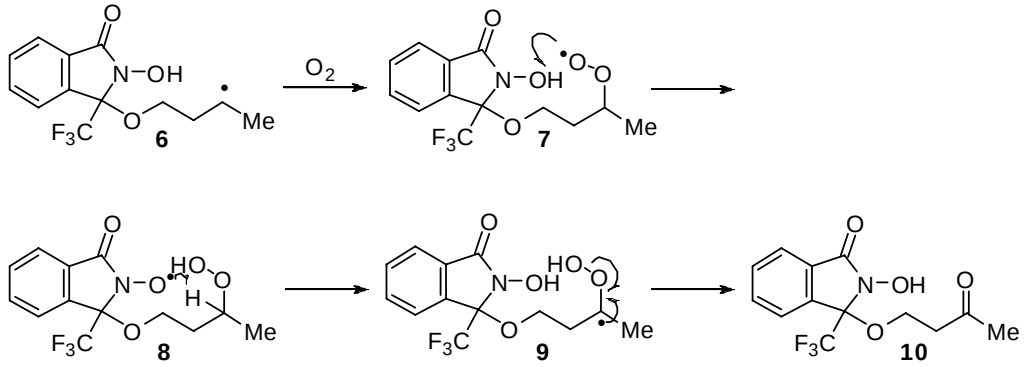

An efficient peroxyl radical trapping reagent is very important to prevent the overoxidation. Interestingly, when *tert*-butyl nitrite was used under aerobic condition, I obtained a nitrate ester product (**Scheme 3–9**).

Scheme 3–9. Successful trap by *in situ* generated NO/NO_2

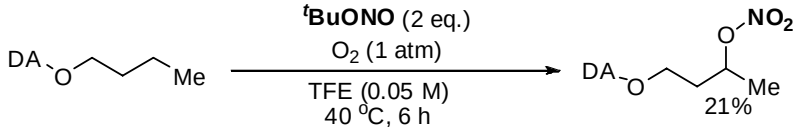

It is known that *tert*-butyl nitrite can homolytically split into *tert*-butoxy radical and nitric oxide (NO), which works as a good radical trapping reagent. Although the exact pathway is unclear, it is very likely that nitrogen dioxide (NO_2) is generated from NO.[54]

NO_2 gas is an economic nitrogen source in industrial chemistry, but its extreme reactivity and toxicity restrict its application. Moreover, the complicated handling of NO_2 has limited its laboratory use. Taniguchi *et al*. established oxidative nitration of alkenes with *tert*-butyl nitrite, providing various β- oxygenated nitro compounds. (**Scheme 3–10**).[55] All reagents were easily available and inexpensive. The reaction

[54] (a) A mechanistic study of the Barton reaction: Grossi, L. *Chem.–Eur. J*. **2005**, *11*, 5419. (b) Galliker, B.; Kissner, R.; Nauser T.; Koppenol, W. H. *Chem.–Eur. J.* **2009**, *15*, 6161. (c) A review on reactions using nitrogen dioxide (NO_2): Shiri, M.; Zolfigol, M. A.; Kruger, H. G.; Tanbakouchian, Z. *Tetrahedron* **2010**, *66*, 9077.

[55] (a) Taniguchi, T.; Yajima, A.; Ishibashi, H. *Adv. Synth. Catal*. **2011**, *353*, 2643. (b) Taniguchi, T.; Sugiura, Y.; Hatta, T.; Yajima, A.; Ishibashi, H. *Chem. Commun*. **2013**, *49*, 2198. (c) Hirose, D.; Taniguchi, T. *Beilstein J. Org. Chem*. **2013**, *9*, 1713.

conditions are mild and the experimental procedure is very simple and safe.

Scheme 3–10. Oxidative nitration of alkenes

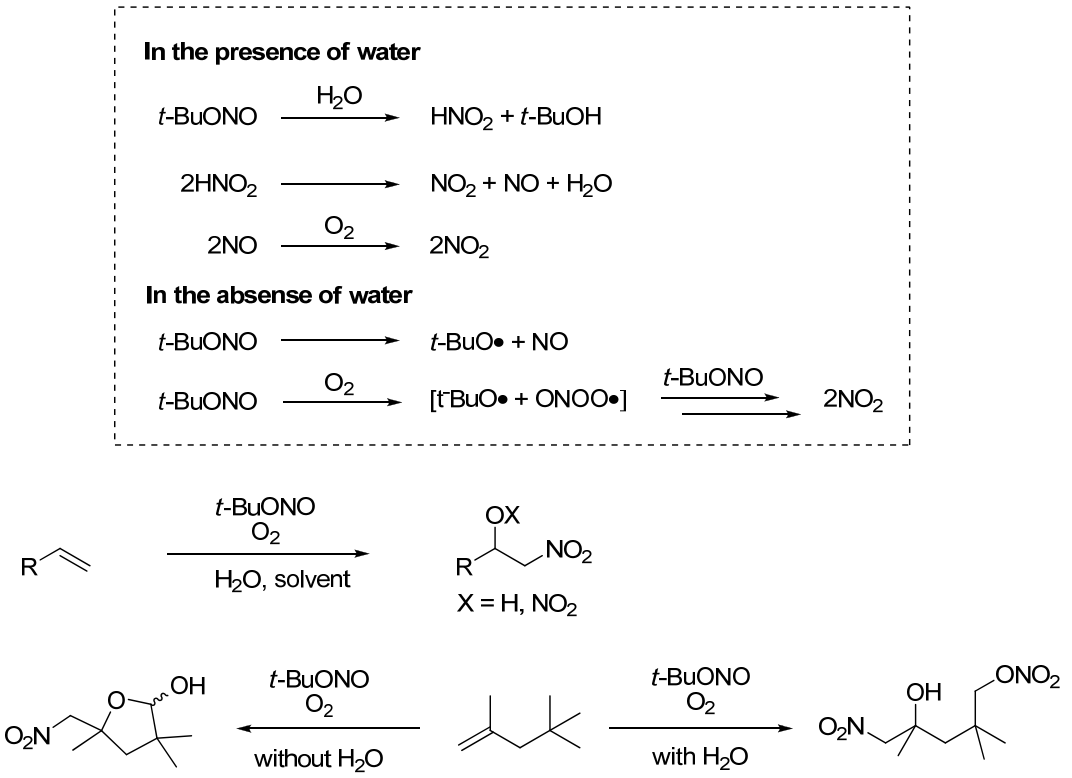

Based on these examples, I considered that any reagent which can release NO_x might capture the peroxyl radical. As an initial try, nitric oxide (NO) and nitrogen dioxide (NO_2) were applied in the reaction system (**Scheme 3–11**).

Scheme 3–11. Result with NO_x gas

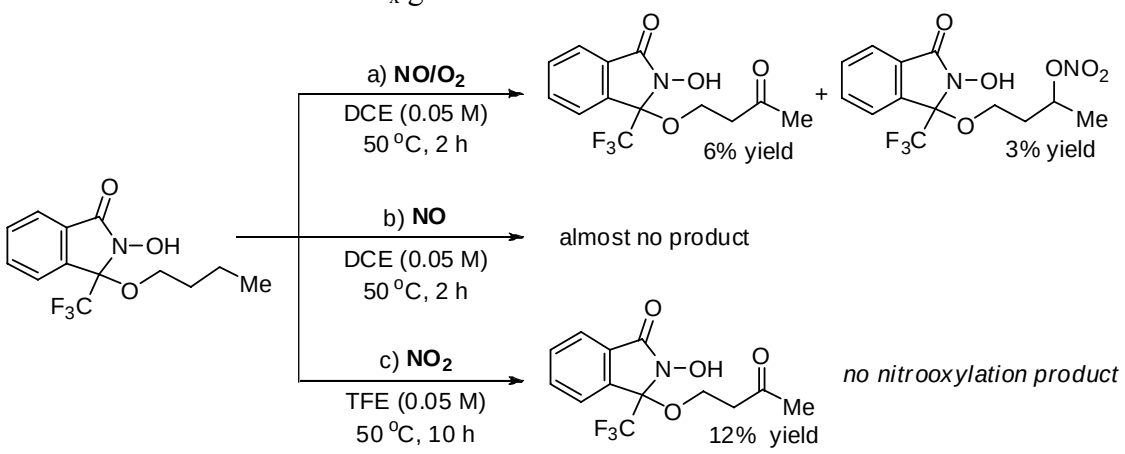

By analyzing the result, I found NO/O_2 system afforded the desired nitrate ester (C–O bond forming, **Scheme 3–11.** path a). However, when the reaction was run under anaerobic condition, no product was obtained when NO employed. On another hand, ketone product was obtained as almost the sole product when NO_2 was used to replace the NO (without O_2).

Scheme 3–12. Nitration/ nitrosation catalyzed by NHPI under argon

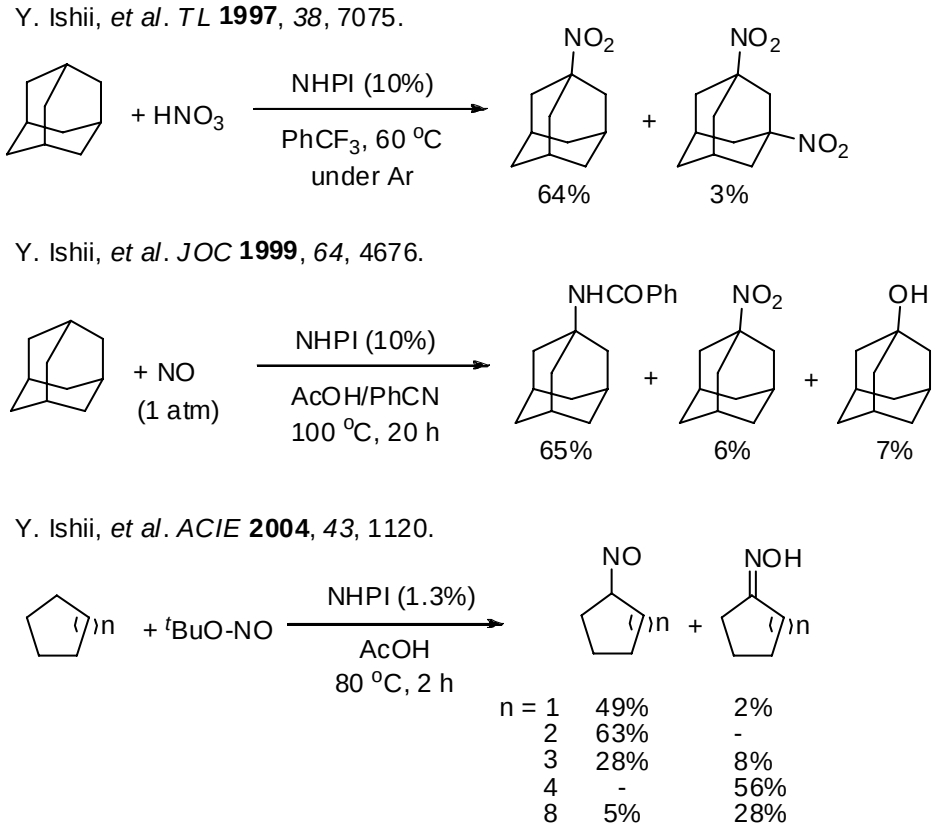

However, Ishii *et al*. demonstrated an NHPI catalyzed nitration of adamantine (**Scheme 3–12**) by using NO under argon.[56] Another reported approach involved NO gas. Adamantane in AcOH/PhCN was transformed to give Ritter-type products such as *N*-adamantylbenzamide, with small amounts of nitroadamantane and 1-adamantanol as byproducts.[57] They also established a new way involving *tert*-butyl nitrite with cycloalkanes in the presence of NHPI to form a mixture of nitrosocycloalkanes and

[56] Sakaguchi, S.; Eikawa, M.; Ishii, Y. *Tetrahedron Lett*. **1997**, *38*, 7075.
[57] Eikawa, M.; Sakaguchi, S.; Ishii, Y. *J. Org. Chem*. **1999**, *64*, 4676.

cycloalkanone oximes.[58] All of these C–N bond forming results were completely different from my observation in **Scheme 3–11** route b (no product) and route c (C–O bond forming).

Oxygen played an important role in the product-forming process (**Scheme 3–11** route a *vs.* route b). Following the initial study, I examined several other NO_x emitting reagents (HNO_3 and *t*-butyl nitrite) under oxygen atmosphere beside NO gas. The results are shown in **Table 3–4**.

Table 3–4.

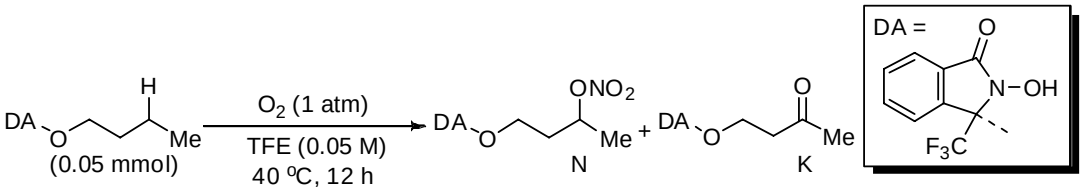

Entry	reactant (equiv)	combine yield (%)[a]	ratio (N/K)
1	NO gas (ca. 10)	15	0.4
2	HNO_3 (3)	23	1.3
3	^{t}BuONO (1)[b]	54	1.0
4	^{t}BuONO (2)[b]	51	1.4
5	^{t}BuONO (3)[b]	43	1.8

[a] NMR Yield. [b] Diluted by TFE (2,2,2-trifluoroethanol) and then slowly added in 8 h.

When NO gas was purged into the reaction tube, the oxidation products were observed with poor yield (15%, entry 1). Nitric acid afforded a poor yield, but with nitrate ester as the major product (entry 2). Good yield was observed by slow addition of *tert*-butyl nitrite (entries 3–4). By increasing the amount of *tert*-butyl nitrite, improved nitrate ester ratio was observed, though the combined yield slightly decreased. I assume that higher concentration of NO_x in the solution rendered the starting material more unstable. Although slow addition strategy can maintain the NO_x concentration at a low level, the convenient operation prompted me to pursuit other ways which generate NO_x *in situ* gradually.

[58] Hirabayashi, T.; Sakaguchi, S.; Ishii, Y. *Angew. Chem. Int. Ed*. **2004**, *43*, 1120.

NO_x generation by nitrite salt/Brønsted acid

The in situ slow generation of NO_x was important to guarantee a higher yield. Interestingly, after screening the nitrite salts (**Table 5**), I succeeded in obtaining both higher yield and C–O single bond forming ratio (N/K ratio) by combining sodium nitrite ($NaNO_2$) and trifluoroacetic acid (TFA) (entry 6), compared to previous *tert*-butyl nitrite conditions. $AgNO_2$ gave similar result as $NaNO_2$, with the nitrooxylation compound as the main product (entry 5). In contrast, low yield was observed when no acid was added (entry 9). Almost no oxygenation product was observed by replacing the nitrite salt with nitrate salt ($AgNO_3$ in entry 7 or $NaNO_3$ in entry 8), or only adding TFA without nitrite salt (entry 10).

Table 3–5. Nitrite and nitrate salts screening

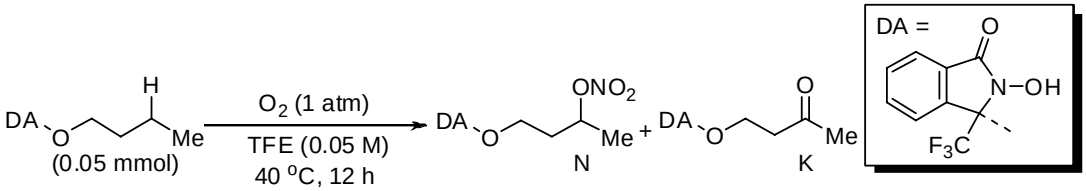

Entry	reactant (equiv)	combine yield (%)[a]	ratio (N/K)
1	Bu_4NNO_2 (10) + TFA (10)[b]	41	0.8
2	$NaNO_2$ (10) + Bu_4NHSO_4 (10)	50	1.0
3	$NaNO_2$ (10) + TFA (50)[b]	45	2.7
4	KNO_2 (10) + TFA (10)[b]	61	1.6
5	$AgNO_2$ (10) + TFA (10)[b]	74	1.6
6	$NaNO_2$ (10) + TFA (10)[b]	72	1.6
7	$AgNO_3$ (10) +TFA (10)[b]	trace	-
8	$NaNO_3$ (10) +TFA (10)[b]	trace	-
9	$NaNO_2$ (10)	29	3.3
10	TFA (10)	trace	-

[a] NMR yield.
[b] TFA was diluted by TFE and then slowly added in 8 h.

3–4–1. Optimization of the reaction conditions

The oxygenation was conducted at 25, 30, 40, 50 and 60 °C. The reaction was sluggish at 25 °C, and became slightly complicated at 50 °C. The nitrate ester/ketone ratio decreased at 60 °C. Therefore, 40 °C proved to be the best reaction temperature.

Table 3–6. Temperature screening

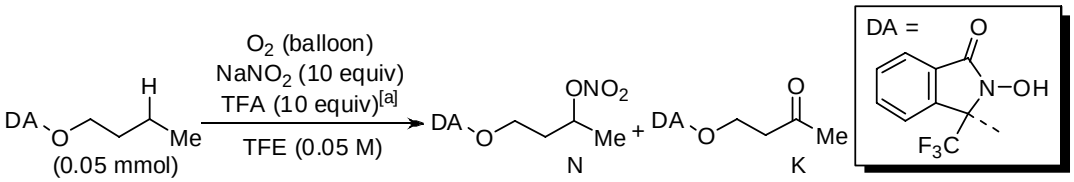

Entry	temp. (°C)	time (h)	combine yield (%)[b]	ratio (N/K)
1	25	24	38	2.3
2	30	12	59	1.4
3	40	12	72	1.6
4	50	12	37	1.6
5	50	4	64	1.2
6	60	2	64	0.9

[a] TFA was diluted by TFE and then slowly added in 8 h.
[b] NMR yield.

The screening of the solvents for methylene oxygenation is shown in **Table 3–7**.

Table 3–7. Solvent screening

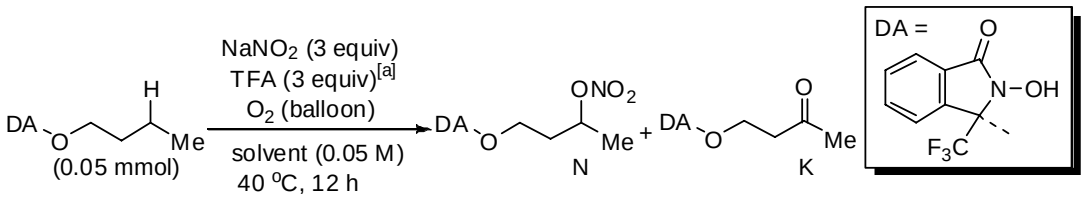

entry	solvent	combine yield (%)[b]	ratio (N/K)
1	TFE	73	1.6
2	DCE	60	1.6
3	CH_3CN	52	1.1
4	HFIP	61	1.6
5	^{t}BuOH	59	1.3
6	$PhCF_3$	55	1.1

[a] TFA was diluted by the solvent and then slowly added in 8 h.
[b] NMR yield.

As shown in the table, in TFE (2,2,2-trifluoroethanol), DCE (1,2-dichloroethane) or

HFIP (1,1,1,3,3,3-hexafluoroisopropanol) solvent, higher nitrate ester/ketone ratio was obtained. TFE afforded the highest yield. Almost no product was obtained while using other solvents, such as PhCl, EtOH, EtOAc, $(CF_3)_2CO$, CCl_4, $CHCl_3$, 1,4-dioxane, acetone, CH_3NO_2, Ph_2O, *t*-BuOMe, DMF, DMSO, *etc*.

Additive effect

Nitrosonium species or NO_x can be fixed and gradually released by supramolecules calix[4]arenes,[59] [2.2]paracyclophane[60] and triptycene[61]. This prompted me to consider about using supramolecules for easier handling or facilitated generation of NO_x gases in solvent media, since the NO_x concentration affected the oxygenation result.

Table 3–8. Supramolecule additive effect

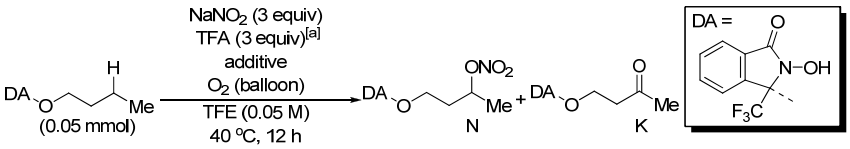

entry	additive	combine yield (%)[b]	ratio (N/K)
1	Triptycene (2 equiv)	37	2.1
2	calix [4] arene (2.equiv)	-	-
3	[2,2] paracyclophane (2 equiv)	-	-

[a] TFA was diluted by the solvent and then slowly added in 8 h.
[b] NMR yield.

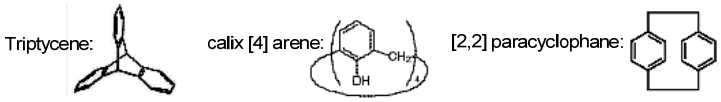

[59] (a) Zyryanov, G. V.; Kang, Y.; Stampp, S. P .; Rudkevich, D. M. *Chem. Commun*. **2002**, 2792. (b) Zyryanov, G. Y.; Rudkevich, D. M. *Org. Lett.* **2003**, *5*, 1253. (c) Zyryanov, G. V.; Kang, Y.; Stampp, S. P .; Rudkevich, D. M. *J. Am. Chem. Soc*. **2003**, *125*, 2997.

[60] Borodkin, G. I.; Elanov, I. R.; Andreev, R. V.; Shakirov, M. M.; Shubin, V. G. *Russ. J. Org. Chem*. **2006**, *42*, 406.

[61] Borodkin, G. I.; Elanov, I. R.; Andreev, R. V.; Shubin, V. G. *Russ. J. Org. Chem*. **2009**, *45*, 1344.

I examined NO^+ or NO_x encapsulation to see if it could control the reaction selectivity between the nitrate ester and ketone (**Table 3–8**). However, the results showed that none of these supramolecules can improve the yield of the nitrate ester. [2.2]Paracyclophane led to complete decomposition of the starting material.

I also used molecular sieves 3A, 4A and 5A to capture the possibly generated water. The nitrate ester product yield was not improved under these conditions (**Table 3–9**, entries 1–3).

Some Lewis acids were also tried, but no promising result was observed (**Table 3–9**, entries 4–8). These Lewis acids accelerated decomposition of the starting material. MnO_2 also showed no effect to improve the yield.

Table 3–9. Molecular sieve and some Lewis acid additive effect

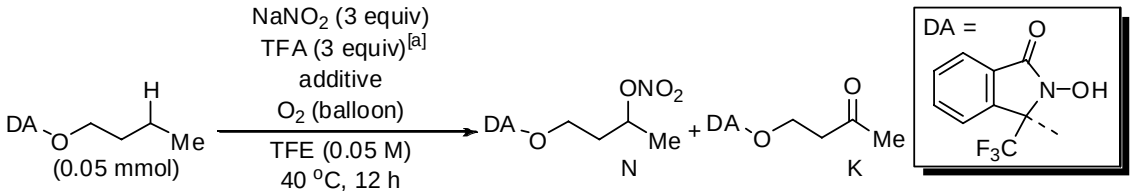

entry	additive	combine yield (%)[b]	ratio (N/K)
1	MS 3A (200 g/mol)	52	2.1
2	MS 4A (200 g/mol)	60	2.2
3	MS 5A (200 g/mol)	55	2.2
4	NiF (0.4 equiv)	68	1.5
5	$Cu(OAc)_2$ (0.3 equiv)	42	2.1
6	$Cu(OTf)_2$ (0.2 equiv)	46	2.2
7	$FeBr_3$ (0.2 equiv)	47	2.4
8	$Zn(OTf)_2$ (0,2 equiv)	61	1.7
9	MnO_2 (2 equiv)	36	3.0

[a] TFA was diluted by the solvent and then slowly added in 8 h.
[b] NMR yield.

Brønsted acid screening

TFA is a strong Brønsted acid. If TFA was mixed with $NaNO_2$ in the reaction mixture in one portion, a high concentration of NO_x species might be generated at once and this might be disadvantageous. Although slow addition can somehow solve this problem, the inconvenient slow addition operation of TFA prompted me to find other alternative Brønsted acids. The screening results were shown in **Table 3–10**.

Table 3–10. Brønsted acid screening

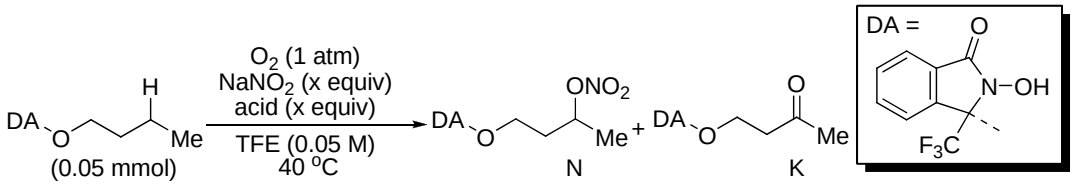

Entry	reactant (x equiv)	combine yield (%)[a]	ratio (N/K)
1	$MeSO_3H$ (10)	41	1.0
2	H_2SO_4 (10)	30	2.5
3	BzOH (10)	43	2.1
4	BzOH (5)	71	1.7
5	BzOH (3)	62	1.8
6	4-F-BzOH (5)	63	1.6
7	3-Cl-BzOH (5)	76	1.7
8	2-Cl-BzOH (5)	70	1.8
9	3-NO_2-BzOH (5)	77	1.6
10	4-MeO-BzOH (5)	78	1.6
11	3,5-diCl-BzOH (5)	69	1.8
12	2,6-diCl-BzOH (5)	78	1.8
13	2-NO_2-BzOH (5)	78	1.8
14	3-NO_2-BzOH (5)	77	1.7
15	$ClCH_2CO_2H$ (5)	61	1.9
16	Cl_2CHCO_2H (5)	48	1.9
17	Cl_3CCO_2H (5)	72	1.6

[a] NMR Yield.

Combining with $NaNO_2$, strong acid such as methanesulfonic acid (entry 1) and sulfuric acid (entry 2) were first tested. Low yields were observed in both cases. In

benzoic acid (BzOH) case (entry 3), there was no significant improvement. However, when the loadings of the acid and nitrite salt were halved (5 equiv), significant yield improvement was observed (entry 4). This means again that high NO_x concentration at the initial stage is harmful for the starting material or product stability. Further reducing the acid and nitrite salt loadings to 3 equivalents lowered the yield, while keeping similar nitrate ester/ketone ratio (entry 6). Substituted benzoic acid performed better than simple BzOH. I found that 5 equivalents of 2,6-diCl-BzOH (entry 12) or 2-NO_2-BzOH (entry 13) combining with 5 equivalents of $NaNO_2$ gave the highest yield (78%) and highest nitrate/ketone ratio (1.8/1). Chlorinated acetic acids (entries 15–16) performed plainly in this process.

The ratio of nitrite salt and acid was also investigated (**Table 3–11**). If $NaNO_2$ was loaded more than acid, in many cases, the reaction was not complete. 5 equivalents of benzoic acid were necessary.

Table 3–11. Reactant ratio

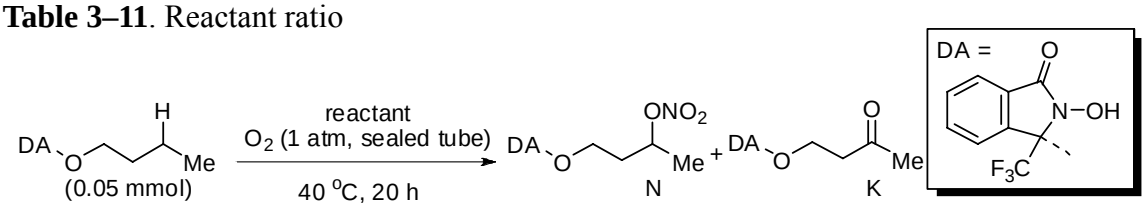

entry	reactant (equiv)	rsm	combine yield (%)[a]	ratio (N/K)
0	2,6-diCl-$PhCO_2H$ (5) + $NaNO_2$ (5)	-	78	1.8
1	2,6-diCl-$PhCO_2H$ (5) + $NaNO_2$ (3)	-	73	1.7
2	2,6-diCl-$PhCO_2H$ (3) + $NaNO_2$ (5)	11	76	1.9
3	2,6-diCl-$PhCO_2H$ (3) + $NaNO_2$ (3)	23	63	1.8
4	2,6-diCl-$PhCO_2H$ (10) + $NaNO_2$ (2)	24	61	1.8
5	2-NO_2-$PhCO_2H$ (3) + $NaNO_2$ (5)	28	56	1.7
6	2-NO_2-$PhCO_2H$ (5) + $NaNO_2$ (10)	28	57	1.8
7	2-NO_2-$PhCO_2H$ (3) + $NaNO_2$ (3)	5	73	1.5

[a] NMR yield.

After investigation of the concentration, 0.05 M of the substrate proved to afford the highest yield in a sealed tube (**Table 3–12**, entry 1). When using balloon under the same conditions, 16% of the starting material remained after 20 h, possibly because NO_x species escaped from the reaction system. Sealed tube was important to maintain enough NO_x in the reaction mixture.

Yield did not improve by portionwise addition of 2,6-dichlorobenzoic acid (entry 5). On the other hand, slow addition of the acid slightly improved the yield, but at the expense of N/K ratio (entry 6).

Table 3–12. More conditions

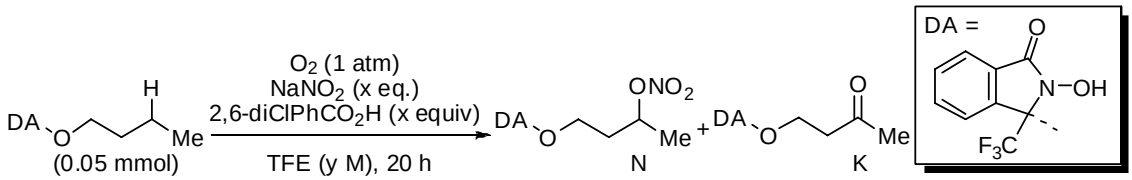

entry	x	y	O_2	rsm	combine yield (%)[c]	ratio (N/K)
1	5	0.05	sealed tube	-	78	1.8
2	5	0.05	balloon	16	68	1.5
3	5	0.1	sealed tube	22	44	1.6
4	5	0.02	sealed tube	-	72	1.6
5[a]	5	0.05	sealed tube	-	71	1.4
6[b]	5	0.03	sealed tube	9	80	1.4

[a] Portionwise add. of 2,6-diClPhCO$_2$H.
[b] Slow add. of acid/TFE solution over 15 h.
[c] NMR yield.

3–4–2. Substrate scope

Although the N/K selectivity was still moderate, I applied the optimal conditions to oxidation-state selective secondary C-H oxygenation (**Table 3–13**):

1-butanol (entry 1) and substituted butanol (entries 2 and 3) afforded nitrooxy adducts with 1.7/1 to 6.5/1 selectivity. Functionalized pentanols (entries 4–7) also worked well, although a bit higher temperature was required (50 ^{o}C or 60 ^{o}C). The diastereomer ratios were 1/1 in all these products.

When the substrate with longer alkyl chain was used, δ-positions were also found to be oxidized (entries 8–10). But still γ-oxidation was the major process. The γ/δ ratio was around 2.5 to 1.

If the γ-position was blocked, the reaction only occurred at the δ-position (entry 11). In this case, C–C cleaved byproduct was also obtained in a small amount.

Table 3–13. Substrate scope

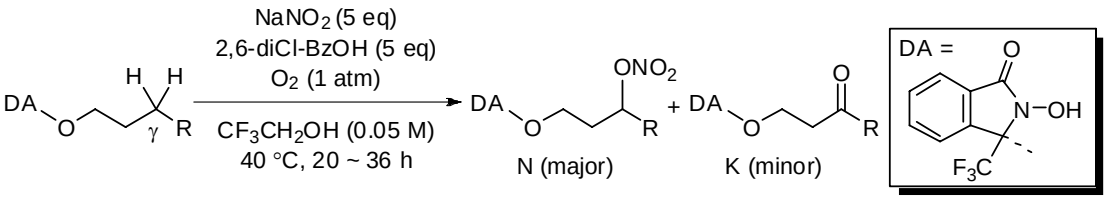

entry	SM	temp. time	product	combined yield (N/K ratio)
1	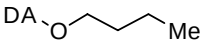	40 °C 20 h	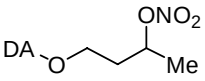	72% (1.7/1)
2	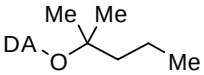	40 °C 20 h	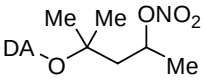	40% (2.6/1)
3	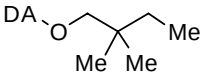	40 °C 20 h	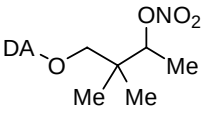	35% (6.5/1)
4	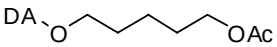	50 °C 24 h	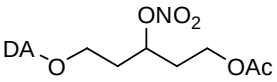	60% (2.2/1)
5	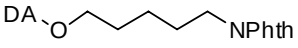	50 °C 24 h	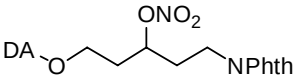	65% (2.0/1)
6	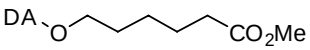	50 °C 24 h	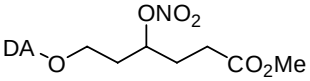	62% (1.8/1)
7	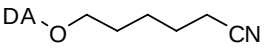	60 °C 30 h	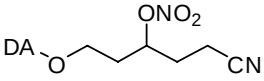	52% (1.4/1)

Table 3–13. Substrate scope (continued)

entry	SM	temp. time	product	combined yield (N/K ratio)
8	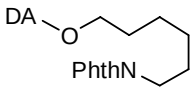	50 °C 22 h	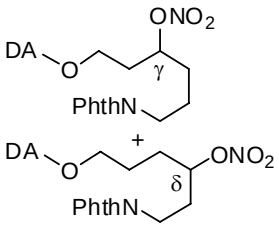	54% (2.4/1) γ / δ = 3.2/1 (N)
9	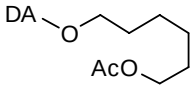	50 °C 20 h	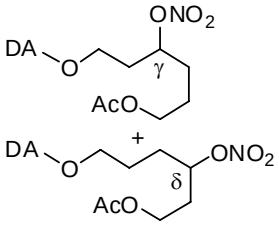	57% (4.0/1) γ / δ = 3.0/1 (N)
10	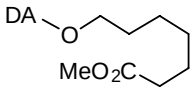	50 °C 22 h	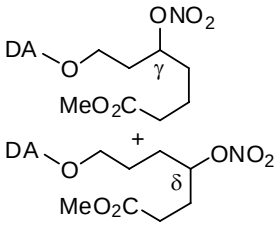	70% (2.2/1) γ / δ = 2.7/1 (N)
11	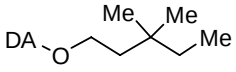	40 °C 36 h	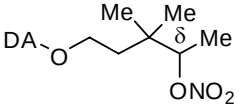 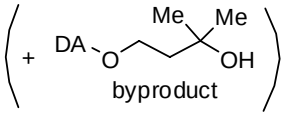	32% (5.9/1) 11%

3–4–3. Control experiments

To further ensure the intramolecularity of the current C(sp^3)–H oxygenation, control experiments were conducted (**Scheme 3–13**). A DA-bound alcohol was converted to the corresponding oxygenated products smoothly at 50 °C. However, when the *N*-hydroxy group was methylated, intermolecular oxygenation promoted by NHPI or catalyst III-c produced a significantly different profile: no oxidation was observed even at 80 °C. This means that intramolecular DA-promoted C-H activation is the key to the success of the developed method.

Scheme 3–13.

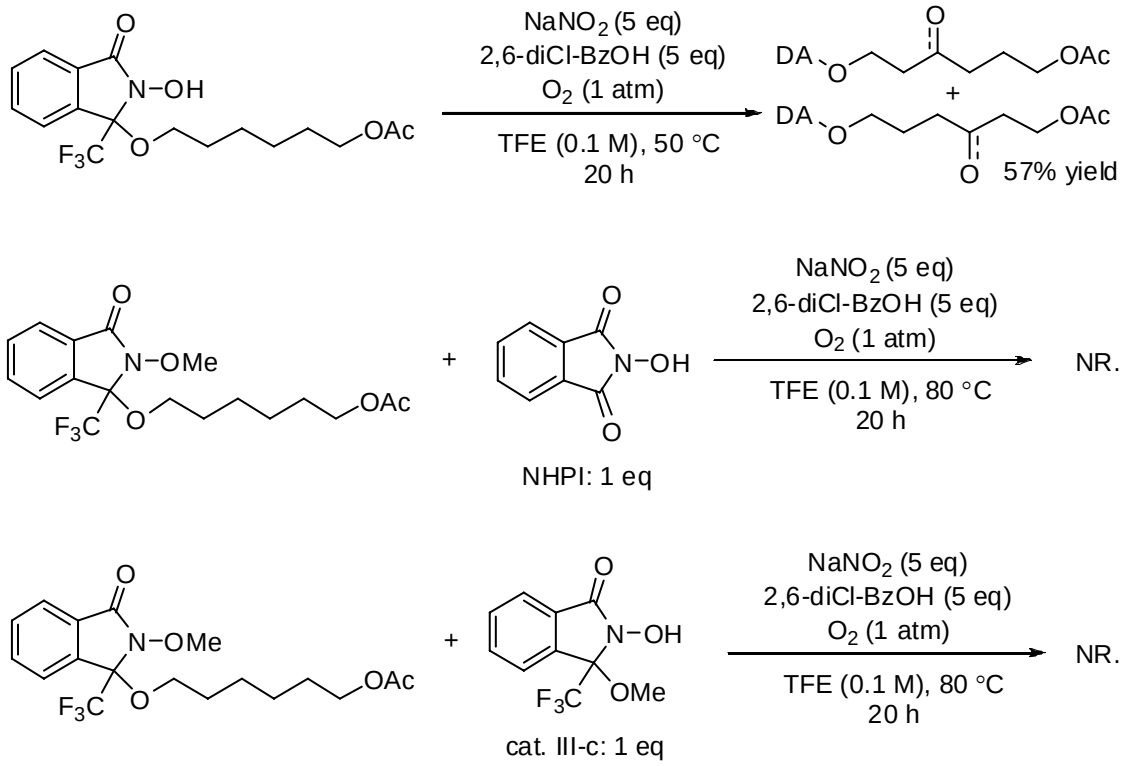

3–4–4. Mechanistic discussion

Even though nitration of aliphatic C–H bonds is a difficult reaction, Ishii *et al*. proved its feasibility by using NHPI catalysis. They conducted the nitration process with nitrogen dioxide (NO_2) in the presence of air (O_2).[50, 62] Because of the higher concentration of NO_2 in the reaction medium compared to that of O_2, the alkyl radicals react predominately with NO_2 rather than O_2, giving nitroalkanes as the major products.

In contrast, under my conditions, the C–O bonds were exclusively formed. The low concentration of the *in situ* generated NO_x species was a main factor for this selectivity. This operation is easier handling compared to the use of poisonous NO_2 gas.

Scheme 3–14. C–O *vs.* C–N

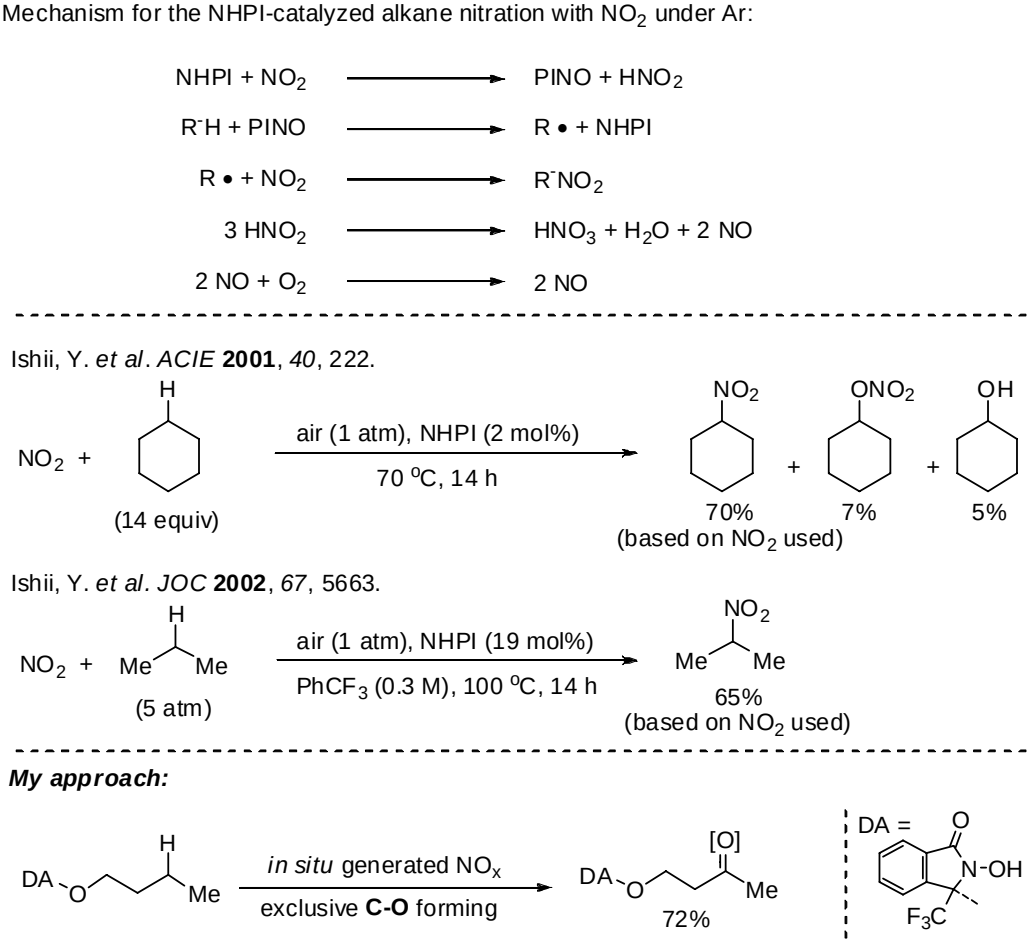

[62] Nishiwaki, Y.; Sakaguchi, S.; Ishii, Y. *J. Org. Chem*. **2002**, *67*, 5663.

A plausible mechanism is proposed here (**Scheme 3–15**). The *in situ* generated nitrosonium ion species[63] is a strong oxidant to promote *N*-oxyl radical generation. Then the γ-H atom is abstracted by the *N*-oxyl radical through an intramolecular way. Oxygen quickly captures the alkyl radical to give a peroxyl radical, which is trapped by NO in the system. Homolytic cleavage and rearrangement process occur in path a, providing nitrooxy adduct.[55] If NO_2 (as shown in path b) or other radical species abstracts the H atom, ketone product will be obtained. These two paths are the competitive processes.

Scheme 3–15. Postulated mechanism

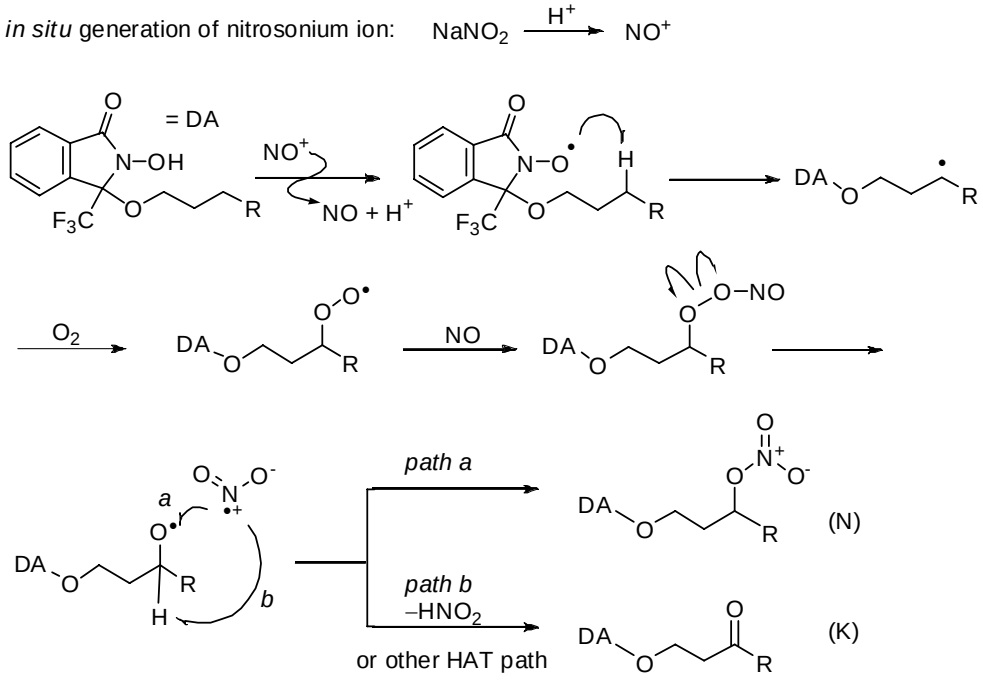

[63] For oxidation of cycloalkanols by sodium nitrite with molecular oxygen in trifluoroacetic acid, see: Matsumura, Y.; Yamamoto, Y.; Moriyama, N.; Furukubo, S.; Iwasaki, F.; Onomura, O. *Tetrahedron Lett*. **2004**, *45*, 8221.

3–4–5. Removal of protecting group and directing activator

After aerobic C-H oxygenation, removal of the nitro group (NO_2) was easily performed in the presence of Pd/C catalyst under hydrogen atmosphere at room temperature.[55c] The directing activator was successfully removed under reductive conditions using $LiAlH_4$, producing oxygenated alcohol 1,3-butanediol in high yield (**Scheme 3–16**).

Scheme 3–16. Removal of PG and DA

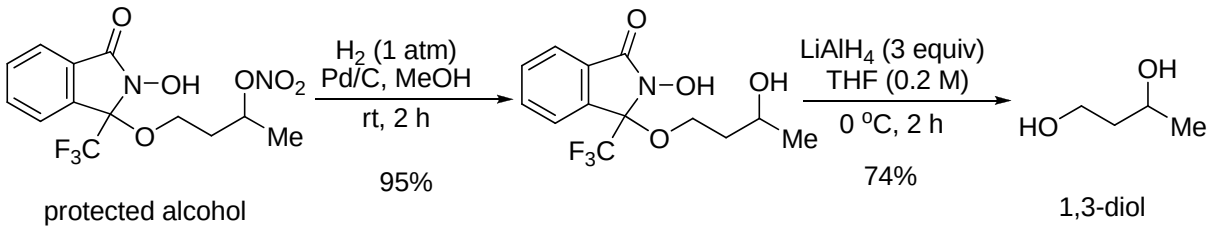

3–4–6. Outlook for catalytic turnover of directing activator

With the success of *N*–hydroxy group mediated C–H bond activation, the design of novel *N*-hydroxy catalyst for the regioselective C–H functionalization will be of great significance.

The designed catalysts have several important features: (1) an *N*–hydroxyl reactive site as a hydrogen atom abstracting moiety, (2) an electron-withdrawing group (e.g. trifluoromethyl group) attached to the α-carbon of the nitrogen atom to improve the hydrogen abstracting ability, and especially (3) a connector of the directing activator, which is very important to reversibly bind with the substrate (**Scheme 17**).

Scheme 3–17. Directed C-H functionalization using the *N*-hydroxy catalyst

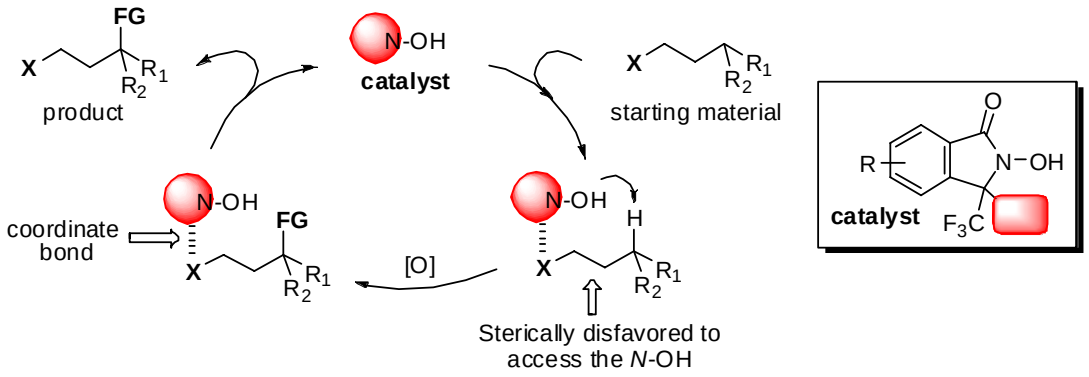

Initial try

Based on the above design, I synthesized a new catalyst candidate bearing a pyridyl moiety[64]. In the presence of metal co-catalysts (such as Co and Fe), however, no oxidation products were produced from an alcohol, a carboxylic acid and an amide substrates. Efforts toward devising catalytic turnover of the directing activator are still ongoing.

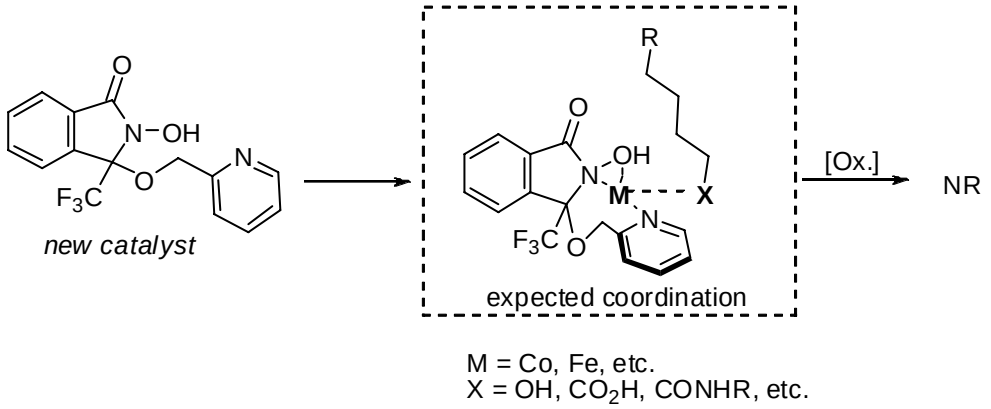

[64] For pyridyl-containing *N*-oxyl radicals, see: Gartshore, C. J.; Lupton, D. W. *Adv. Synth. Catal*. **2010**, *352*, 3321.

Summary

(1) I developed several novel *N*-hydroxy organocatalysts with H atom abstraction ability. Some of them showed appealing merits (in terms of reactivity and solubility) comparing to the well-known NHPI.

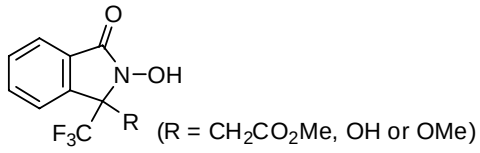

Comparing to the classic NHPI
+ Higher reactivity
+ Significantly improved solubility

(2) By employing a new *N*-oxyl radical directing activator, very challenging acyclic methylene C(sp^3)–H bonds were converted to C=O bonds in a Co(II)/O_2 system, while C–O bonds were preferentially obtained via a NO_x/O_2 system under mild (moderate temperature) conditions. The reaction proceeded regioselectively at the γ (and δ) position(s), and α, β and other positions farther than the δ position were intact. These characteristics were resulted from the intramolecularity of the directing activator strategy.

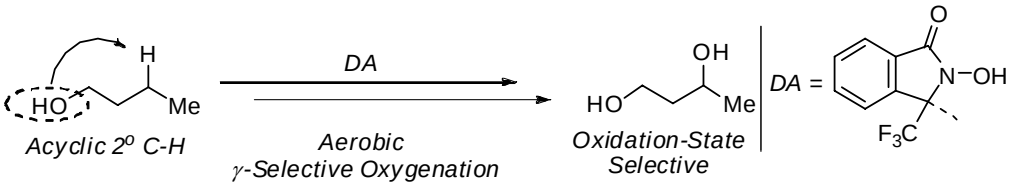

Experimental Section

1. General Method

^{1}H NMR spectra were recorded on JEOL ECX500 (500 MHz for ^{1}H NMR and 125 MHz for ^{13}C NMR), and JEOL ECS400 (400 MHz for ^{1}H NMR, 100 MHz for ^{13}C NMR and 400 MHz for ^{19}F NMR) spectrometer. Proton and carbon chemical shifts are reported relative to the solvent used as an internal reference. Fluorine chemical shifts are reported relative to trifluoroacetic acid (δ –76.55 ppm) as an external reference. Infrared (IR) spectra were recorded on a JASCO FT/IR 410 Fourier transform infrared spectrophotometer. ESI-MS spectra were measured on a JEOL JMS-T100LC AccuTOF spectrometer (for HRMS). Column chromatographies were performed with silica gel Merck 60 (230-400 mesh ASTM). The ratios of regioisomers were determined by HPLC analysis (JASCO HPLC systems; pump: PU-2080; detector: UV-2075, measured at 254 nm; column: CHIRALPAK AD-H or Inertsil® diol column; mobile phase: 2-propanol/^{n}hexane).All reactions other than substrates synthesis were carried out in normal solvents without any purification (purchased from Aldrich or Wako Pure Chemical Industries, Ltd.) unless otherwise noted. Other reagents of which preparation is not described in this manuscript were purchased from Aldrich, Tokyo Chemical Industry Co., Ltd. (TCI), Kanto Chemical Co., Inc., and Wako Pure Chemical Industries, Ltd., and used without further purification.. NMR yields were calculated by ^{1}H NMR of crude products using 1,1,2,2-tetrachloroethane as an internal standard.

2. Synthetic procedure and analytical data of Type I, Type II and Type III catalysts

1-hydroxypyridin-4(1*H*)-one (I-a)

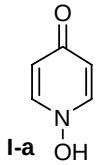

I-a

The synthesis of **I-a** followed a similar procedure in Ref.[15]

pale yellow solid; ^{1}H NMR (500 MHz, DMSO-*d*6) δ 7.91 (d, *J* = 7.6 Hz, 2H), 6.52 (d, *J* = 7.3 Hz, 2H).

1-hydroxy-2-methylquinolin-4(1*H*)-one (I-b)

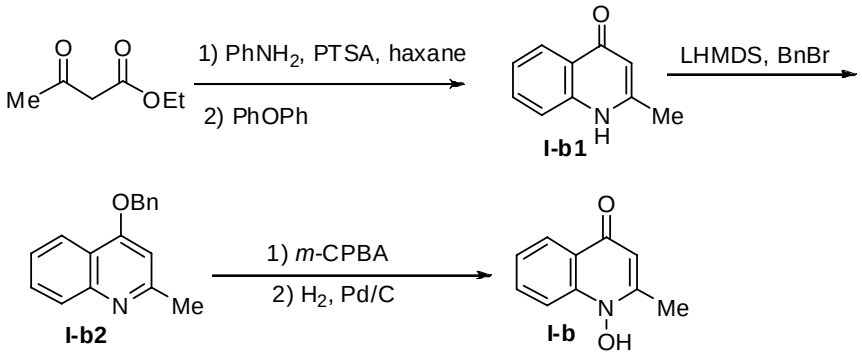

A mixture of ethyl 3-oxobutanoate (2.5 mL, 20 mmol), aniline (1.8 mL, 20 mmol), and PTSA•H_2O (0.04 g, 0.2 mmol) in hexanes (40 mL) was heated at reflux using a Dean–Stark water separator for 5 h. The solution was concentrated under reduced pressure and the residue was added dropwise to refluxing diphenyl ether (10 mL). Refluxing was continued for 40 min and the formed EtOH was removed by distillation. After cooling, the mixture was concentrated in vacuo to provide a dark brown crude **I-b1** (1.4 g, 43%), which was used in the next step without further purification.

To a solution of **I-b1** (0.8 g, 5.0 mmol) in DMSO (10 mL) LHMDS (5.3 mL, 5.3 mmol; 1.0 M in THF) was added dropwise at room temperature, and the resulting solution was stirred for 1 h. Afterwards benzyl bromide (0.6 mL, 5.0 mmol) was added and the mixture was stirred at ambient temperature overnight. The reaction was

quenched by addition of brine (30 mL) and the mixture extracted with ether (3 × 20 mL). The combined organic extracts were washed with brine (2 × 40 mL), dried over Na_2SO_4 and concentrated under reduced pressure. Purification of the residue by column chromatography (hexane/EtOAc, 2:1) provided **I-b2** (0.9 g, 72%) as a yellow solid. ^{1}H NMR (500 MHz, $CDCl_3$) δ 8.21 (dd, *J* = 8.3, 1.0 Hz, 1H), 7.96 (d, *J* = 8.5 Hz, 1H), 7.67 (td, *J* = 6.9, 3.4 Hz, 1H), 7.51 (d, *J* = 7.4 Hz, 2H), 7.44 (t, *J* = 7.5 Hz, 3H), 7.39 (d, *J* = 7.3 Hz, 1H), 6.72 (s, 1H), 5.28 (s, 2H), 2.70 (s, 3H); LRMS (ESI): m/z 182 $[M+Na]^+$.

To a solution of **I-b2** (0.9 g, 3.6 mmol) in DCM (40 mL) at 0 ^{o}C was added a mixture of *m*-CPBA (1.3 g, ca. 4.3 mmol) in DCM (40 mL). The reaction was stirred at room temperature for 1 h and then quenched by saturated $NaHCO_3$ solution. The organic phase was separated, dried over Na_2SO_4 and concentrated under reduced pressure. The crude product was dissolved in MeOH and palladium on activated charcoal (0.1 g, 10%) was added to the mixture. After hydrogenolysis at room temperature for 1.5 h, the mixture was filtered and concentrated. Column chromatography purification (MeOH/DCM, 1:5) afforded a pure pale yellow solid **I-b** (0.25g, 40%). ^{1}H NMR (500 MHz, $CDCl_3$) δ 8.35 (dd, *J* = 8.1, 1.4 Hz, 1H), 7.63 – 7.52 (m, 1H), 7.45 (d, *J* = 8.5 Hz, 1H), 7.33 (dd, *J* = 12.8, 5.2 Hz, 1H), 6.19 (s, 1H), 2.44 (s, 3H); LRMS (ESI): m/z 198 $[M+Na]^+$.

ethyl 1-hydroxy-4-oxo-1,4-dihydroquinoline-3-carboxylate[16]

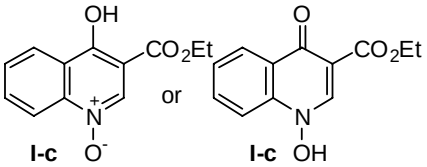

^{1}H NMR (500 MHz, $CDCl_3$) δ 8.78 (s, 1H), 8.55 (s, 1H), 8.35 (d, *J* = 8.1 Hz, 1H), 7.83 (s, 1H), 7.64 (s, 1H), 4.45 (q, *J* = 7.1 Hz, 2H), 1.42 (t, *J* = 7.2 Hz, 3H); LRMS (ESI): m/z 256 $[M+Na]^+$.

3-hydroxyquinazolin-4(3*H*)-one (II-a)[17]

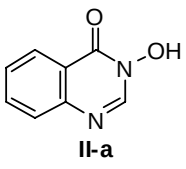

^{1}H NMR (500 MHz, $CDCl_3$) δ 8.43 (s, 1H), 8.28 (d, *J* = 7.9 Hz, 1H), 7.79 (dd, *J* = 4.7, 1.3 Hz, 2H), 7.58 – 7.50 (m, 1H); LRMS (ESI): m/z 185 $[M+Na]^+$.

2-(furan-2-yl)-3-hydroxyquinazolin-4(3*H*)-one (II-b) [18]

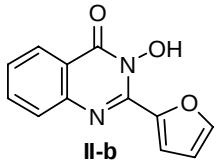

II-b

^{1}H NMR (DMSO-*d*6) δ 6.53 – 8.70 (m, 7H), 11.7 (s, 1H); LRMS (ESI): m/z 251 $[M+Na]^+$.

methyl 3-hydroxy-4-oxo-3,4-dihydroquinazoline-2-carboxylate (II-c)

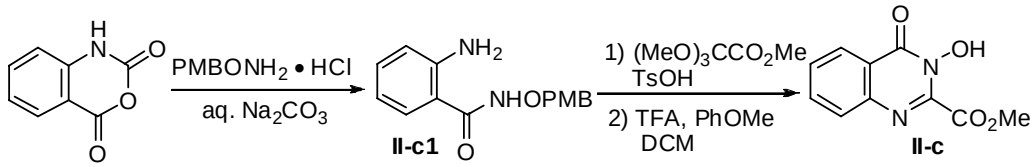

II-c1 **II-c**

O-(4-Methoxybenzyl)hydroxylamine hydrochloride (3.8 g, 20.2 mmol) was suspended in aq. Na_2CO_3 (90 mL, 11.0 mmol) and the resulting mixture was stirred for 30 min before isatoic anhydride (3.0 g, 18.4 mmol) was added in portions. After stirring vigorously for 1 d, the formed solid was filtered and dried to afford crude **II-c1** (4.7 g, 93%).

A mixture of **II-c1** (4.7 g, 17.1 mmol), methyl 2,2,2-trimethoxyacetate (3.6 g, 22.1 mmol) and *p*-toluenesulfonic acid monohydrate (0.07 g, 2% w/w) in MeCN (90 mL) was refluxed under argon for 5 h. The solution was then cooled and concentrated to give a crude mixture, which was subject to column separation (hexane/EtOAc, 3:1) to afford PMB-**II-c** (5.4 g, 92%).

To a solution of PMB-**II-c** (0.68 g, 2.0 mmol), PhOMe (1.3 mL, 12 mmol) in DCM (3.6 mL) under argon was added TFA (1.8 mL, 12 mmol) slowly. The mixture was stirred at room temperature for 4 h and concentrated. After column chromatography purification (hexane/EtOAc, 1:1), a pale yellow solid **II-c** (0.38g, 86%) was obtained. ^{1}H NMR (400 MHz, $CDCl_3$) δ 9.81 (br s, 1H), 8.31 (s, 1H), 7.98 – 7.81 (m, 2H), 7.61 (s,

1H), 4.08 (s, 3H); LRMS (ESI): m/z 243 $[M+Na]^+$.

For synthesis of **IIIa**,**IIIb** and **IIIc**, see preparation of **S2** and **S5** in the following part.

2,3-dihydroxy-3-(trifluoromethyl)isoindolin-1-one (III-a)

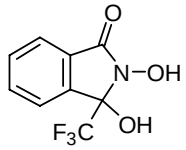

^{1}H NMR (500 MHz, CD_3OD) δ 7.79 (d, *J* = 7.4 Hz, 1H), 7.76 – 7.60 (m, 3H); LRMS (ESI): m/z 256 $[M+Na]^+$.

2-hydroxy-3-methoxy-3-(trifluoromethyl)isoindolin-1-one (III-b)

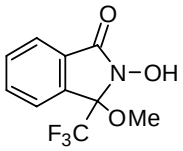

^{1}H NMR (500 MHz, $CDCl_3$) δ 9.45 (s, 1H), 7.83 (d, *J* = 7.2 Hz, 1H), 7.78 – 7.47 (m, 3H), 3.16 (s, 3H); ^{13}C NMR (125 MHz, $CDCl_3$) δ 165.92, 134.58, 133.40, 131.69, 130.06, 124.16, 124.05, 121.88 (q, *J* = 286.2 Hz), 91.40 (q, *J* = 33.1 Hz), 51.58; LRMS (ESI): m/z 270 $[M+Na]^+$.

methyl 2-(2-hydroxy-3-oxo-1-(trifluoromethyl)isoindolin-1-yl)acetate (III-c)

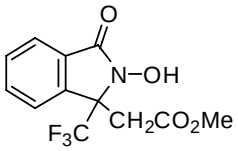

^{1}H NMR (500 MHz, $CDCl_3$) δ 9.84 (br s, 1H), 7.84 (d, *J* = 7.4 Hz, 1H), 7.67 – 7.46 (m, 3H), 3.61 (d, *J* = 15.9 Hz, 1H), 3.38 (d, *J* = 17.7 Hz, 3H), 3.20 (d, *J* = 15.9 Hz, 1H); ^{13}C NMR (125 MHz, $CDCl_3$) δ 167.67, 167.35, 137.11, 132.87, 130.40, 130.17, 123.99, 122.77, 52.07, 32.13; LRMS (ESI): m/z 312 $[M+Na]^+$.

3. Representative procedures in Chapter 3

(A) Representative procedure for oxidation state-selective methylene oxygenation:

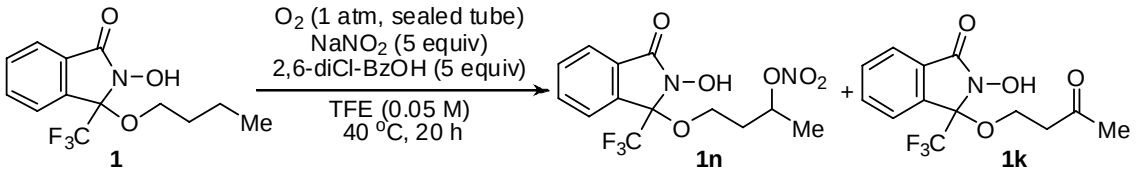

To a dry test tube (ca. 18 mL volume) with a stir bar, **1** (28.9 mg, 0.1 mmol), $NaNO_2$ (34.5 mg, 0.5 mmol) and 2,6-dichlorobenzoic acid (95.5 mg, 0.5 mmol) were added. The tube was capped with a three-way stopcock, and the inside atmosphere was replaced to oxygen (1 atm). Then 2,2,2-trifluoroethanol (2 mL) was added via a syringe. The tube was immediately sealed tightly and the resulting mixture was stirred on a heated metal block (40 ^{o}C). During this process, white solid gradually appeared and the reaction mixture turned light yellow. After agitated for 20 h, the mixture was cooled to room temperature and then concentrated under reduced pressure. The residue was purified by silica gel column chromatography (hexane/EtOAc/HCO_2H = 80/40/1) to give the oxidation products **1n** (white solid, 15.9 mg) and **1k** (colorless oil, 8.1 mg).

(B) Representative procedure for methylene oxygenation:

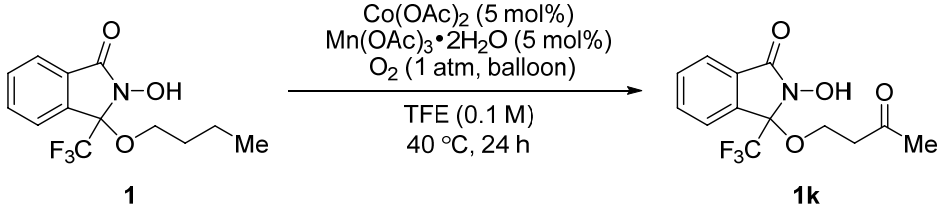

To a test tube were added $Co(OAc)_2$ (0.89 mg, 0.005 mmol), $Mn(OAc)_3 \cdot 2H_2O$(1.34 mg, 0.005 mmol), **1** (28.9 mg, 0.1 mmol), and TFE (1 mL, 0.1 M). The mixture was stirred at 40 °C after replacing air inside the tube with O_2 (1 atm, balloon). After **1** was consumed, which was checked on TLC, TFE was removed by evaporation and then EtOAc was added. The EtOAc solution was filtered through silica gel to remove the metals and concentrated to afford a crude mixture. Purification by silica gel column chromatography (EtOAc/hexane = 1/1) gave **1k** as a colorless oil (18.6 mg, 62%).

(C) Hydrogenolysis of nitrate

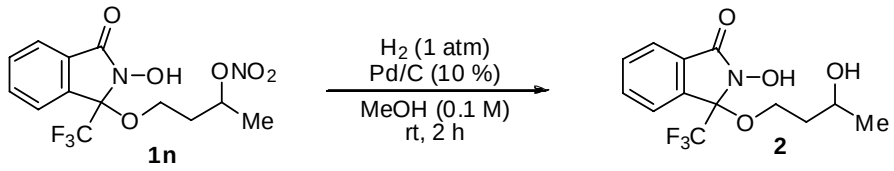

To a solution of nitrate **1n** (17.5 mg, 0.05mmol) in methanol (0.5 mL), Pd/C (1.8 mg, 10%) was added and the solution stirred under hydrogen atmosphere at room temperature. After **1n** was consumed (about 2 h), he reaction mixture was filtered and evaporated in vacuo to give the desired product as a white solid (14.5 mg, 95 %).

(D) Cleavage of the directing activator

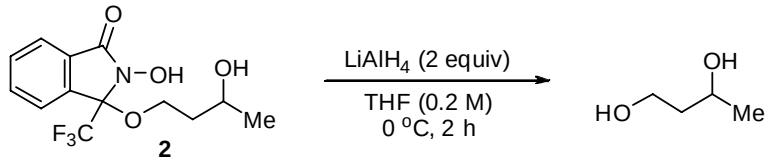

To a round-bottom flask dried by heat gun under reduced pressure were added **2** (30.5 mg, 0.1 mmol, 1 equiv) and dry THF (0.5 mL, 0.2 M), and the mixture was cooled at 0 °C. $LiAlH_4$ (7.6 mg, 2 equiv) was added to the reaction mixture carefully. After two hours water (10 μL), 2 M NaOH (20 μL), and water (10 μL) were added successively to the reaction mixture, with vigorous stirring being kept. Insoluble materials were removed by celite filtration and the filtrate was dried under reduced pressure to obtain the crude mixture. Purification by silica gel column chromatography (hexane/EtOAc = 1/2) afforded butane-1,3-diol as slightly yellow oil (6.7 mg, 74%).

(E) Typical synthetic procedure for directing-activator-anchored alcohols

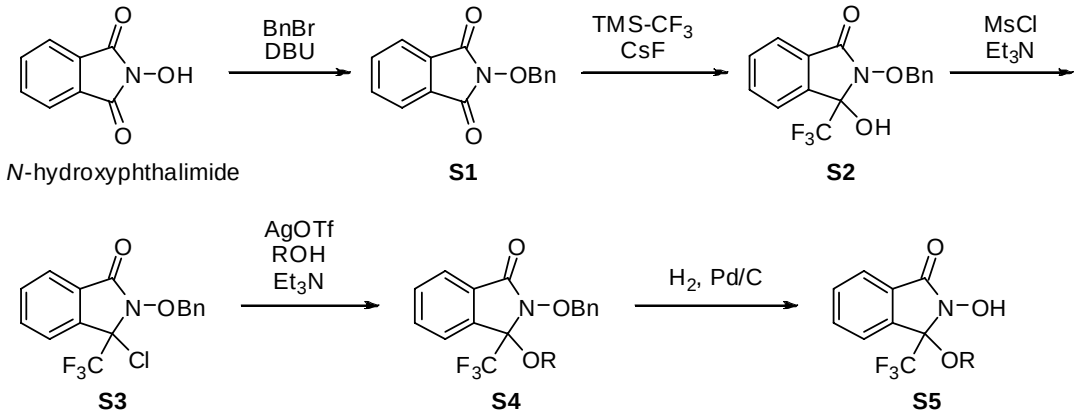

***O*-benzyl-*N*-hydroxyphthalimide (S1)**

To a stirred mixture of *N*-hydroxyphthalimide (8.16 g, 50 mmol, 1 equiv) and benzyl bromide (6.6 mL, 55 mmol, 1.1 equiv) in DMF (50 mL, 1 M) was added DBU (9.0 mL, 60 mmol, 1.2 equiv) over 30 minutes at ambient temperature. After completion of the addition, 100 mL of aq. HCl (1 N) was added. The white precipitate was filtered off and the residue was washed with DCM. Drying the solution over Na_2SO_4 and evaporating the solvent afforded **S1** as white solid (11.5 g, 91% yield).

^{1}H NMR (500 MHz, $CDCl_3$) δ 7.80 (dd, 2H, *J* = 2.9 Hz, 5.2 Hz), 7.72 (dd, 2H, *J* = 2.9 Hz, 5.2 Hz), 7.53 (dd, 2H, *J* = 4.0 Hz, 7.5 Hz), 7.36-7.40 (m, 3H), 5.21 (s, 2H); ^{13}C NMR (126 MHz, $CDCl_3$) δ 163.4, 134.4, 133.6, 129.8, 129.3, 128.8, 128.5, 123.4, 79.8; IR (KBr, cm^{-1}) 3076, 3034, 2954, 2887, 1789, 1731, 1464; LRMS (ESI): m/z 276 $[M+Na]^+$; HRMS (ESI): m/z calcd for $C_{15}H_{11}NO_3Na$ $[M+Na]^+$ 276.0631, Found 276.0630.

***N*-benzyloxy-3-hydroxy-3-trifluoromethyl-isoindolinone (S2)**

To a stirred mixture of **S1** (11.5 g, 45.4 mmol, 1 equiv) and $TMSCF_3$ (8.1 mL, 54.5 mmol, 1.2 equiv) in DMF (45 mL, 1 M) was added CsF (8.3 g, 54.5 mmol, 1.2 equiv) at 0 °C and stirred for one hour. Water was added and the mixture was extracted with ethyl acetate. The organic layer was washed with 1 N aq. HCl, water, and saturated NaCl solution and dried over Na_2SO_4. Evaporating the solvent afforded **S2** as light yellow solid (16 g, 99% yield). **S2** was used in the next step without further purification.

^{1}H NMR (500 MHz, acetone-d_6) δ 7.78-7.85 (m, 3H), 7.72-7.76 (m, 1H), 7.59 (d,

2H, J = 7.5 Hz), 7.37-7.45 (m, 3H), 5.34 (d, 1H, J = 9.8 Hz), 5.22 (d, 1H, J = 9.8 Hz), 3.05 (s, 1H); ^{13}C NMR (126 MHz, acetone-d_6) δ 164.9, 139.1, 136.0, 134.5, 132.5, 130.2, 130.0, 129.5, 129.1, 125.0, 124.2, 123.9 (q, J = 286.7 Hz), 88.0 (q, J = 32.4 Hz), 80.5; ^{19}F NMR (369 MHz, acetone-d_6) δ -79.5; IR (KBr, cm^{-1}) 3223, 3031, 1719, 1618, 1470, 1378, 1261, 1195; LRMS (ESI): m/z 346 $[M+Na]^+$; HRMS (ESI): m/z calcd for $C_{16}H_{12}F_3NO_3Na$ $[M+Na]^+$ 346.0662, Found 346.0674.

_N_-benzyloxy-3-chloro-3-trifluoromethyl-isoindolinone (S3)

To a stirred mixture of **S2** (16 g, 45 mmol, 1 equiv) and triethylamine (10 mL, 72 mmol, 1.6 equiv) in DCM (45 mL, 1 M) was added MsCl (5.2 mL, 67.5 mmol, 1.5 equiv) at 0 °C, and stirred for three hours. Water was added. The separated organic layer was washed with water and saturated NaCl solution, and dried over Na_2SO_4. Evaporating the solvent afforded the crude mixture of **S3**. Purification by silica gel column chromatography (hexane/EtOAc = 3/1) afforded **S3** as light yellow liquid (14 g, 91% yield). **S3** is stored as 1 M solution in heptane.

^{1}H NMR (400 MHz, $CDCl_3$) δ 7.90 (d, 1H, J = 7.2 Hz), 7.71-7.76 (m, 2H), 7.63-770 (m, 1H), 7.55-7.61 (m, 2H), 7.37-7.46 (m, 3H), 5.41 (d, 1H, J = 9.4 Hz), 5.25 (d, 1H, J = 9.4 Hz); ^{13}C NMR (126 MHz, $CDCl_3$) δ 164.5, 137.9, 134.2, 133.9, 131.8, 129.6, 129.1, 128.5, 127.3, 124.4, 124.1, 121.7 (q, J = 284.3 Hz), 79.7, 79.5 (q, J = 36.4 Hz); ^{19}F NMR (369 MHz, $CDCl_3$) -75.8; IR (neat, cm^{-1}) 1755, 1469, 1258, 1197; LRMS (ESI): m/z 364 $[M+Na]^+$; HRMS (ESI): m/z calcd for $C_{16}H_{11}ClF_3NO_2Na$ $[M+Na]^+$ 364.0323, Found 364.0325.

_N_-benzyloxy-3-butoxy-3-trifluoromethyl-isoindolinone (S4, R = _n_-Bu)

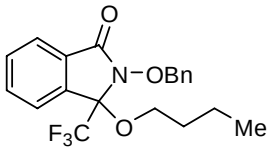

To a shaded mixture of AgOTf (6.9 g, 26.7 mmol, 1.5 eq), 1-butanol (2.0 mL, 21.4 mmol, 1.2 eq) and triethylamine (3.2 mL, 23.1 mmol, 1.3 eq) in toluene (17.8 mL, 0.5 M altogether) was added **S3** solution (17.8 mL, 17.8 mmol, 1 eq) at ambient temperature. The reaction mixture was stirred overnight and saturated NaCl solution

was added. After celite filtration to remove the silver salts, the organic layer was washed with water and saturated NaCl solution, and dried over Na_2SO_4. Evaporating the solvent afforded the crude oily liquid. Purification by silica gel column chromatography (hexane/EtOAc = 10/1) afforded **S4** (R = *n*-Bu) as slightly yellow liquid (5.7 g, 84%).

^{1}H NMR (500 MHz, $CDCl_3$) δ 7.90 (d, 1H, *J* = 7.7 Hz), 7.69 (dd, 1H, *J* = 6.9 Hz, 7.8 Hz), 7.60-7.66 (m, 2 H), 7.57 (d, 2H, *J* = 6.9 Hz), 7.35-7.43 (m, 3H), 5.32 (d, 1H, *J* = 9.8 Hz), 5.16 (d, 1H, *J* = 9.8 Hz), 3.28 (dt, 1H, *J* = 8.6 Hz, 6.3 Hz), 2.95 (dt, 1H, *J* = 8.6 Hz, 6.3 Hz), 1.44-1.59 (m, 2H), 1.23-1.39 (m, 2H), 0.83 (t, 3H, *J* = 7.2 Hz); ^{13}C NMR (125 MHz, $CDCl_3$) δ 165.6, 135.3, 134.6, 133.4, 131.6, 130.0, 129.3, 128.8, 128.4, 124.2, 124.1, 122.2 (q, *J* = 286.7 Hz), 91.0 (q, *J* = 32.4 Hz), 79.1, 63.8, 31.0, 18.9, 13.6; ^{19}F NMR (369 MHz, $CDCl_3$) δ -78.1; IR (neat, cm^{-1}) 2960, 1746, 1468, 1294, 1195; LRMS (ESI): m/z 402 $[M+Na]^+$; HRMS (ESI): m/z calcd for $C_{20}H_{20}F_3NO_3Na$ $[M+Na]^+$ 402.1288, Found 402.1284.

3-butoxy-*N*-hydroxy-3-trifluoromethyl-isoindolinone (1)

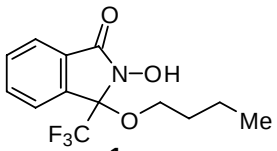

1

A stirred mixture of **S4** (R = *n*-Bu) (2.6 g, 6.8 mmol, 1 eq), Pd/C (10 wt%, 362 mg, 0.34 mmol, 0.05 eq) in ethanol (14 mL, 0.5 M) was exposed to H_2 (balloon pressure) at ambient temperature. The reaction mixture was stirred for two hours and then H_2 was removed. Celite filtration and evaporation of the filtrate afforded the crude oily liquid. Purification by silica gel column chromatography (hexane/EtOAc = 4/1) afforded **1** as slightly orange liquid. The liquid was gradually solidified into white solid (1.8 g, 92%).

^{1}H NMR (500 MHz, $CDCl_3$) δ 9.88 (s, 1H), 7.79 (d, 1H, *J* = 7.8 Hz), 7.66 (dd, 1H, *J* = 7.4 Hz, 6.9 Hz), 7.61 (d, 1H, *J* = 7.4 Hz), 7.60 (dd, 1H, *J* = 6.9 Hz, 7.8 Hz), 3.43 (dt, 1H, *J* = 8.6 Hz, 6.6 Hz), 2.98 (dt, 1H, *J* = 8.6 Hz, 6.6 Hz), 1.54-1.68 (m, 2H), 1.29-1.46 (m, 2H), 0.88 (t, 3H, *J* = 7.2 Hz); ^{13}C NMR (125 MHz, $CDCl_3$) δ 165.9, 135.3, 133.2, 131.5, 130.0, 124.0, 123.8, 121.9 (q, *J* = 286.7 Hz), 91.0 (q, *J* = 32.4 Hz), 64.1, 31.1, 19.0, 13.7; ^{19}F NMR (369 MHz, $CDCl_3$) δ -78.5; IR (KBr, cm^{-1}) 3435, 3136, 2964, 1878, 1719, 1472, 1305, 1201; LRMS (ESI): m/z 312 $[M+Na]^+$; HRMS (ESI): m/z calcd for

$C_{13}H_{14}F_3NO_3Na$ $[M+Na]^+$ 312.0818, Found 312.0831.

4. Analytical data in Chapter 3

N-hydroxy-3-((2-methylpentan-2-yl)oxy)-3-trifluoromethyl-isoindolinone

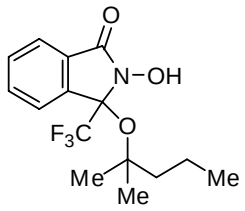

reddish solid; ^{1}H NMR (500 MHz, $CDCl_3$) δ 9.95 (s, 1H), 7.78 (d, 1H, *J* = 7.3 Hz), 7.66 (d, 1H, *J* = 7.3 Hz), 7.61 (dd, 1H, *J* = 7.3 Hz, 7.3 Hz), 7.57 (dd, 1H, *J* = 7.3 Hz, 7.3 Hz), 1.40-1.55 (m, 4H), 1.15 (s, 3H), 0.96 (s, 3H), 0.90 (t, 3H, *J* = 6.6 Hz); ^{13}C NMR (126 MHz, $CDCl_3$) δ 165.4, 137.6, 132.5, 131.2, 129.8, 125.2, 123.7, 122.1 (q, *J* = 288.2 Hz), 89.9 (q, *J* = 32.3 Hz),82.6, 46.2, 27.2, 26.2, 17.1, 14.4; ^{19}F NMR (369 MHz, $CDCl_3$) δ -79.5, -79.7; IR (KBr, cm^{-1}) 3159, 2962, 1718, 1473, 1391, 1373, 1192; LRMS (ESI): m/z $[M+Na]^+$; HRMS (ESI): m/z calcd for $C_{15}H_{18}F_3NO_3Na$ $[M+Na]^+$ 340.1131, Found 340.1117.

3-(2,2-dimethylbutoxy)-*N*-hydroxy-3-trifluoromethyl-isoindolinone

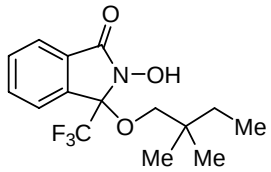

white solid; ^{1}H NMR (500 MHz, $CDCl_3$) δ 9.89 (s, 1H), 7.79 (d, 1H, *J* = 7.4 Hz), 7.66 (dd, 1H, *J* = 7.4 Hz, 7.4 Hz), 7.56-7.62 (m, 2H), 3.16 (d, 1H, *J* = 8.0 Hz), 2.61 (d, 1H, *J* = 8.0 Hz), 1.29-1.40 (m, 2H), 0.91 (s, 3H), 0.88 (s, 3H), 0.81 (t, 3H, *J* = 7.4 Hz); ^{13}C NMR (126 MHz, $CDCl_3$) δ 165.8, 135.3, 133.2, 131.4, 130.0, 124.0, 123.8, 122.0 (q, *J* = 287.1 Hz), 90.9 (q, *J* = 32.8 Hz), 71.8, 34.1, 31.2, 23.8, 23.7, 8.1; ^{19}F NMR (369 MHz, $CDCl_3$) δ -78.6; IR (KBr, cm^{-1}) 3168, 2964, 2883, 1721, 1525, 1473, 1382, 1311, 1203; LRMS (ESI): m/z $[M+Na]^+$; HRMS (ESI): m/z calcd for $C_{15}H_{18}F_3NO_3Na$ $[M+Na]^+$ 340.1131, Found 340.1117.

5-((*N*-hydroxy-3-oxo-1-(trifluoromethyl)isoindolin-1-yl)oxy)pentyl acetate

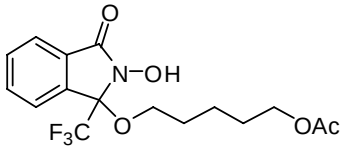

light yellow liquid; ^{1}H NMR (500 MHz, $CDCl_3$) δ 9.76 (s, 1H), 7.80 (d, 1H, *J* = 7.5 Hz), 7.66 (ddd, 1H, *J* = 1.2 Hz, 7.5 Hz, 7.5 Hz), 7.60 (dd, 2H, *J* = 7.5 Hz, 7.5 Hz), 4.06 (t, 2H, *J* = 6.9 Hz), 3.40 (dt, 1H, *J* = 9.2 Hz, 6.3 Hz), 2.98 (dt, 1H, *J* = 9.2 Hz, 6.3 Hz),2.02 (s, 3H), 1.57-1.67 (m, 4H), 1.34-1.50 (m, 2H); ^{13}C NMR (126 MHz, $CDCl_3$) δ 171.5, 165.7, 135.1, 133.2, 131.5, 130.0, 124.0, 123.9, 121.9 (q, *J* = 285.5 Hz), 90.9 (q, *J* = 33.6 Hz), 64.3, 63.9, 28.5, 28.1, 22.2, 20.9; ^{19}F NMR (369 MHz, $CDCl_3$) δ -78.5; IR (neat, cm^{-1}) 3175, 2955, 1736, 1470, 1241, 1198; LRMS (ESI): m/z 384 $[M+Na]^+$; HRMS (ESI): m/z calcd for $C_{16}H_{18}F_3NO_5Na$ $[M+Na]^+$ 384.1029, Found 384.1039.

2-(5-((2-hydroxy-3-oxo-1-(trifluoromethyl)isoindolin-1-yl)oxy)pentyl)isoindoline-1, 3-dione

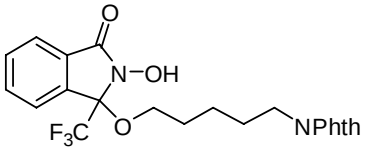

white solid; ^{1}H NMR (400 MHz, acetone-d_6) δ 7.66-7.84 (m, 8H), 3.61 (t, 2H, *J* = 7.2 Hz), 3.41 (dt, 1H, *J* = 11.5 Hz, 4.4 Hz), 3.00 (dt, 1H, *J* = 11.5 Hz, 4.4 Hz), 1.55-1.71 (m, 4H), 1.28-1.48 (m, 2H); ^{13}C NMR (100 MHz, $CDCl_3$) δ 168.7, 164.6, 135.7, 134.9, 134.1, 132.9, 132.6, 131.5, 125.1, 124.2, 123.6, 123.3 (q, *J* = 286.6 Hz), 91.4 (q, *J* = 31.9 Hz), 64.2, 38.1, 29.2, 28.7, 23.8; ^{19}F NMR (369 MHz, $CDCl_3$) δ -78.7; IR (KBr, cm^{-1}) 3524, 3368, 2940, 2889, 2712, 1731, 1699, 1200; LRMS (ESI): m/z $[M+Na]^+$; HRMS (ESI): m/z calcd for $C_{22}H_{19}F_3N_2O_5Na$ $[M+Na]^+$ 471.1138, Found 471.1119.

methyl 6-((2-hydroxy-3-oxo-1-(trifluoromethyl)isoindolin-1-yl)oxy)hexanoate

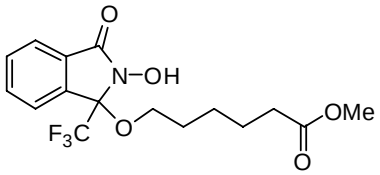

red liquid; ^{1}H NMR (500 MHz, $CDCl_3$) δ 9.71 (s, 1H), 7.81 (d, 1H, *J* = 7.4 Hz), 7.63-7.68 (m, 1H), 7.56-7.62 (m, 2H), 3.64 (s, 3H), 3.39 (dt, 1H, *J* = 5.8 Hz, 7.7 Hz), 2.98 (dt, 1H, *J* = 5.8 Hz, 7.7 Hz), 2.29 (t, 2H, *J* = 7.4 Hz), 1.55-1.66 (m, 4H), 1.30-1.46 (m, 2H); ^{13}C NMR (126 MHz, $CDCl_3$) δ 174.4, 165.6, 135.0, 133.2, 131.5, 130.0, 124.0, 123.9, 121.9 (q, *J* = 286.7 Hz), 90.9 (q, *J* = 32.8 Hz), 63.8, 51.6, 33.8, 28.5, 25.2, 24.3; ^{19}F NMR (369 MHz, $CDCl_3$) δ -78.4; IR (neat, cm^{-1}) 3177,2951, 1719, 1469, 1303, 1199; LRMS (ESI): m/z 384 $[M+Na]^+$; HRMS (ESI): m/z calcd for $C_{16}H_{18}F_3NO_5Na$ $[M+Na]^+$ 384.1029, Found 384.1029.

2-hydroxy-3-(3-oxobutoxy)-3-(trifluoromethyl)isoindolin-1-one

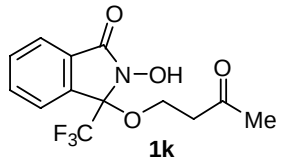

1k

colorless oil; ^{1}H NMR (500 MHz, $CDCl_3$) δ 8.83 (s, 1H), 7.87 (d, 1H, *J* = 7.5 Hz), 7.58-7.68 (m, 3H), 3.57 (dt, 1H, *J* = 3.5 Hz, 9.8 Hz), 3.21-3.26 (m, 1H), 2.93 (ddd, 1H, *J* = 3.5 Hz, 9.2 Hz, 18.9 Hz), 2.63 (dt, 1H, *J* = 18.9 Hz, 3.5 Hz), 2.23 (s, 3H); ^{13}C NMR (126 MHz, $CDCl_3$) δ 208.3, 163.8, 133.9, 133.0, 131.7, 130.5, 124.2, 124.1, 121.7 (q, *J* = 286.7 Hz), 90.5 (q, *J* = 32.4 Hz), 57.7, 42.1, 30.4; ^{19}F NMR (369 MHz, $CDCl_3$) δ -78.2; IR (neat, cm^{-1}) 3213, 2952, 1719, 1469, 1363, 1304, 1197; LRMS (ESI): m/z 326 $[M+Na]^+$; HRMS (ESI): m/z calcd for $C_{13}H_{12}F_3NO_4Na$ $[M+Na]^+$ 326.0611, Found 326.0620.

3-(2,2-dimethyl-3-oxobutoxy)-2-hydroxy-3-(trifluoromethyl)isoindolin-1-one

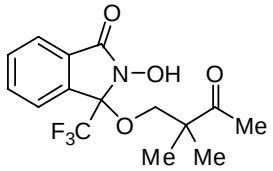

white solid; ^{1}H NMR (400 MHz, $CDCl_3$) δ 9.17 (s, 1H), 7. (d, 1H, *J* = 7.2 Hz), 7.54-7.70 (m, 3H), 3.49 (d, 1H, *J* = 8.7 Hz), 2.87 (d, 1H, *J* = 8.7 Hz), 2.23 (s, 3H), 1.23 (s, 3H), 1.11 (s, 3H); ^{13}C NMR (126 MHz, $CDCl_3$) δ 213.4, 164.6, 134.2, 133.2, 131.7, 130.2, 124.1, 121.7 (q, *J* = 286.1 Hz), 90.5 (q, *J* = 34.1 Hz), 69.0, 47.9, 25.8, 22.0, 21.7; ^{19}F NMR (369 MHz, $CDCl_3$) δ -78.4; IR (KBr, cm^{-1}) 3138, 2941, 1709, 1471, 1304, 1199; LRMS (ESI): m/z 354 $[M+Na]^+$; HRMS (ESI): m/z calcd for $C_{15}H_{16}F_3NO_4Na$ $[M+Na]^+$354.0924, Found 354.0924.

a mixture of
2-hydroxy-3-(2-methyl-4-oxopentan-2-yloxy)-3-(trifluoromethyl)isoindolin-1-one
(3)

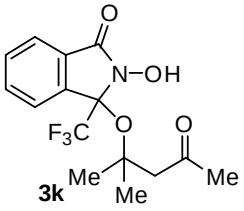

3k

and

4-hydroxy-2,2,4-trimethyl-11b-(trifluoromethyl)-3,4-dihydro-2*H*-[1,4,2]dioxazepino[3,2-*a*]isoindol-7(11b*H*)-one (3'; diastereomixture)

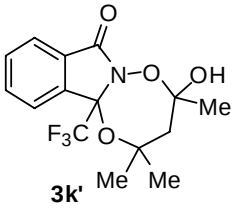

3k'

white solid; ^{1}H NMR (500 MHz, acetone-d_6; underlined chemical shifts for **3k**) δ 9.47 (s, 1H), 7.68-7.86 (m, 4H + 4H), 5.68-5.71 (m, 1H), 2.81 (d, 1H, J = 14.9 Hz), 2.72 (d, 1H, J = 14.9 Hz), 2.23 (d, 1H, J = 14.9 Hz), 2.21 (s, 3H), 2.10 (d, 1H, J = 14.9 Hz), 1.60 (s, 3H), 1.31 (s, 3H), 1.18 (s, 3H), 1.12 (s, 3H), 1.11 (s, 3H); ^{13}C NMR (126 MHz, acetone-d_6; underlined chemical shifts for **3k**; wavylined shifts for **3k** or **3k'**; dashed-lined shifts for both **3k** and **3k'**; two shifts in brackets derived from "the same" carbon of the diastereomers) δ 207.4, 164.0, 163.5, 139.8, 137.8, 134.1, 133.6, 132.6, 132.0, 131.5, 130.4, 126.6, 124.7, 124.2, 124.1,123.6 (q, J = 288.5 Hz), [107.8, 107.7], 90.3 (q, J = 31.7 Hz),56.1, 52.8, 33.9, 32.1, 28.2, [27.6, 27.5], 26.1, 25.6; ^{19}F NMR (369 MHz, $CDCl_3$; underlined chemical shifts for **2b**) δ -79.1, -79.7; IR (KBr, cm^{-1}) 3460, 2985, 1730, 1469, 1250, 1191; LRMS (ESI): m/z 354 $[M+Na]^+$; HRMS (ESI): m/z calcd for $C_{15}H_{16}F_3NO_4Na$ $[M+Na]^+$354.0924, Found 354.0924.

5-((*N*-hydroxy-3-oxo-1-(trifluoromethyl)isoindolin-1-yl)oxy)-3-oxopentyl acetate

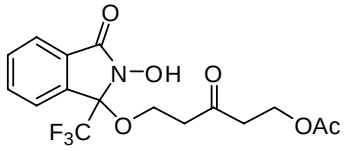

light yellow liquid; ^{1}H NMR (500 MHz, $CDCl_3$) δ 7.88 (d, 1H, J = 7.4 Hz), 7.58-7.69 (m, 3H), 4.34 (t, 2H, J = 6.0 Hz), 3.59 (dt, 1H, J= 3.4 Hz, 9.5 Hz), 3.26-3.30 (m, 1H),

2.93 (ddd, 1H, *J* = 18.3 Hz, 3.4 Hz, 1.8 Hz), 2.83 (t, 2H, *J* = 6.0 Hz), 2.70 (ddd, 1H, *J* = 18.3 Hz, 3.4 Hz, 1.8 Hz), 2.02 (s, 3H); ^{13}C NMR (125 MHz, $CDCl_3$) δ 207.4, 170.9, 163.9, 133.9, 133.0, 131.8, 130.4, 124.2, 124.1, 121.7 (q, *J* = 286.7 Hz), 90.5 (q, *J* = 33.6 Hz), 58.8, 57.7, 41.9, 41.6, 20.7; ^{19}F NMR (369 MHz, $CDCl_3$) δ -78.2; IR (neat, cm^{-1}) ν: 3302, 2955, 1738, 1469, 1370, 1191; LRMS (ESI): m/z 398 $[M+Na]^+$; HRMS (ESI): m/z calcd for $C_{16}H_{16}F_3NO_6Na$ $[M+Na]^+$ 398.0822, Found 398.0808.

2-(5-((2-hydroxy-3-oxo-1-(trifluoromethyl)isoindolin-1-yl)oxy)-3-oxopentyl)isoindoline-1,3-dione

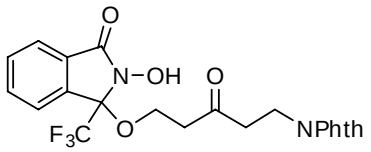

light yellow liquid; ^{1}H NMR (500 MHz, $CDCl_3$) δ 8.32 (s, 1H), 7.89 (dd, 1H, *J* = 6.3 Hz, 1.1 Hz), 7.84 (dd, 2H, *J* = 3.1 Hz, 5.6 Hz), 7.72 (dd, 2H, *J* = 3.1 Hz, 5.6 Hz), 7.58-7.69 (m, 3H), 3.98 (t, 2H, *J* = 7.2 Hz), 3.57 (dt, 1H, *J* = 2.9 Hz, 9.7 Hz), 3.23-3.28 (m, 1H), 2.91-3.02 (m, 3H), 2.67-275 (m, 1H); ^{13}C NMR (125 MHz, $CDCl_3$) δ 207.7, 168.1, 163.8, 134.1, 133.9, 133.0, 131.8, 131.7, 130.4, 124.2, 124.1, 123.4, 121.7 (q, *J* = 286.6 Hz), 90.5 (q, *J* = 33.6 Hz), 57.7, 41.3, 41.2, 32.7; ^{19}F NMR (369 MHz, $CDCl_3$) δ -78.1; IR (neat, cm^{-1}) 3222, 2950, 1714, 1469, 1397, 1374, 1191; LRMS (ESI): m/z 485 $[M+Na]^+$.

methyl 6-((2-hydroxy-3-oxo-1-(trifluoromethyl)isoindolin-1-yl)oxy)-4-oxohexanoate

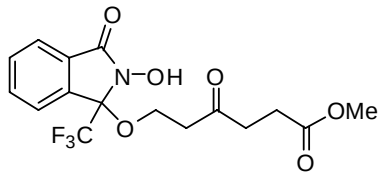

light yellow liquid; ^{1}H NMR (500 MHz, $CDCl_3$) δ 8.60 (s, 1H), 7.88 (d, 1H, *J* = 8.0 Hz), 7.57-7.68 (m, 3H), 3.67 (s, 3H), 3.57 (dt, 1H, *J* = 2.5 Hz, 9.6 Hz), 3.24-3.29 (m, 1H), 2.97 (ddd, 1H, *J* = 18.3 Hz, 10.0 Hz, 3.7 Hz), 2.62-2.87 (m, 4H), 2.55-2.62 (m, 1H); ^{13}C NMR (125 MHz, $CDCl_3$) δ 208.8, 173.1, 163.7, 133.8, 132.9, 131.7, 130.5, 124.2, 124.1, 121.2 (q, *J* = 286.6 Hz), 90.5 (q, *J* = 33.6 Hz), 57.8, 52.0, 41.4, 37.5, 27.6; ^{19}F NMR

(369 MHz, $CDCl_3$) δ -78.1; IR (neat, cm^{-1}) 3222, 2954, 1718, 1197; LRMS (ESI): m/z 398 $[M+Na]^+$; HRMS (ESI): m/z calcd for $C_{16}H_{16}F_3NO_6Na$ $[M+Na]^+$398.0822, Found 398.0804.

6-(2-hydroxy-3-oxo-1-(trifluoromethyl)isoindolin-1-yloxy)-4-oxohexyl acetate

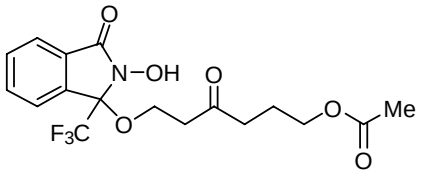

^{1}H NMR (500 MHz, $CDCl_3$) δ 8.40 (br s, 1H), 7.90 (d, *J* = 7.2 Hz, 1H), 7.80 – 7.61 (m, 3H), 4.07 (t, *J* = 6.2 Hz, 2H), 3.66 – 3.51 (m, 1H), 3.29 – 3.20 (m, 1H), 3.01 – 2.89 (m, 1H), 2.68 – 2.56 (m, 3H), 2.04 (s, 3H), 2.00 – 1.86 (m, 2H); LRMS (ESI): m/z 412 $[M+Na]^+$.

2-(6-(2-hydroxy-3-oxo-1-(trifluoromethyl)isoindolin-1-yloxy)-4-oxohexyl)isoindoline-1,3-dione

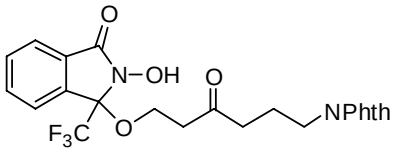

^{1}H NMR (500 MHz, $CDCl_3$) δ 8.43 (br s, 1H), 7.97 – 7.79 (m, 3H), 7.79 – 7.55 (m, 5H), 3.76 – 3.61 (m, 2H), 3.31 – 3.71 (m, 1H), 3.01 – 2.86 (m, 1H), 2.60 – 2.50 (m, 2H), 2.12 – 1.86 (m, 2H), 1.78 – 1.54 (m, 2H); LRMS (ESI): m/z 499 $[M+Na]^+$.

methyl 7-(2-hydroxy-3-oxo-1-(trifluoromethyl)isoindolin-1-yloxy)-5-oxoheptanoate

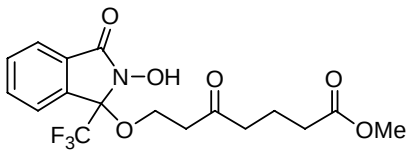

^{1}H NMR (400 MHz, $CDCl_3$) δ 8.49 (br s, 1H), 7.91 (d, *J* = 7.4 Hz, 1H), 7.75 – 7.62 (m, 3H), 3.70 – 3.61 (m, 3H), 3.60 – 3.49 (m, 1H), 3.26 – 3.12 (m, 1H), 3.01 – 2.87 (m, 1H), 2.64 – 2.50 (m, 3H), 2.38 – 2.24 (m, 2H), 1.97 – 1.86 (m, 2H); LRMS (ESI): m/z 412 $[M+Na]^+$.

Analytically pure nitrooxylation samples of each diastereomer (dr 1:1) were obtained after preparative HPLC separation.

4-(2-hydroxy-3-oxo-1-(trifluoromethyl)isoindolin-1-yloxy)butan-2-yl nitrate

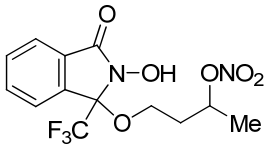

HPLC: Inertsil® diol column, eluent: hex/IPA = 60/1, flow rate: 9.5 ml/min, retention time 117 min and 130 min.

[for less polar diastereomer] white solid; ^{1}H NMR (500 MHz, $CDCl_3$) δ 9.37 (brs, 1H), 7.81 (d, *J* = 7.1 Hz, 1H), 7.69 – 7.61 (m, 2H), 7.53 (d, *J* = 7.4 Hz, 1H), 5.44 – 5.28 (m, 1H), 3.59 – 3.41 (m, 1H), 3.17 – 3.01 (m, 1H), 2.12 – 1.99 (m, 1H), 1.98 – 1.83 (m, 1H), 1.43 (d, *J* = 6.2 Hz, 3H); ^{13}C NMR (125 MHz, CDCl3) δ 165.84, 134.68, 133.72, 131.87, 129.70, 124.11, 123.67, 121.74 (q, *J* = 284.95 Hz), 90.76 (q, *J* = 33.3), 77.74, 59.69, 33.35, 18.74; ^{19}F NMR (400 MHz, $CDCl_3$) δ –78.90; IR (neat, cm^{-1}) 2926, 1716, 1623, 1507, 1279, 1199, 864; HRMS (ESI): m/z calcd for $C_{13}H_{13}F_3N_2O_6Na$ $[M+Na]^+$ 373.0618, Found 373.0600.

[for more polar diastereomer] white solid; ^{1}H NMR (500 MHz, $CDCl_3$) δ 9.37 (br s, 1H), 7.81 (d, *J* = 7.1 Hz, 1H), 7.70 – 7.60 (m, 2H), 7.53 (d, *J* = 7.4 Hz, 1H), 5.44 – 5.28 (m, 1H), 3.59 – 3.41 (m, 1H), 3.17 –3.01 (m, 1H), 2.14 –1.96 (m, 1H), 1.96 –1.78 (m, 1H), 1.43 (d, *J* = 6.2 Hz, 3H); ^{13}C NMR (125 MHz, $CDCl_3$) δ 165.55, 134.64, 133.52, 131.88, 129.75, 124.29, 123.96, 78.20, 60.18, 33.48, 18.90; ^{19}F NMR (400 MHz, $CDCl_3$) δ –78.90; IR (neat, cm^{-1}) 2987, 1716,1624, 1507, 1266, 1200, 897; HRMS (ESI): m/z calcd for $C_{13}H_{13}F_3N_2O_6Na$ $[M+Na]^+$ 373.0618, Found 373.0600.

4-(2-hydroxy-3-oxo-1-(trifluoromethyl)isoindolin-1-yloxy)-3,3-dimethylbutan-2-yl nitrate

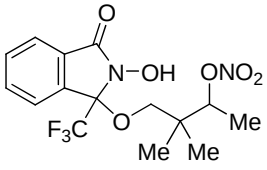

HPLC: Inertsil® diol column, eluent: hex/IPA = 60/1, flow rate: 9.5 ml/min, retention time 64 min and 78 min.

[for less polar diastereomer] white solid; ^{1}H NMR (400 MHz, $CDCl_3$) δ 9.47 (br s, 1H), 7.79 (d, *J* = 7.1 Hz, 1H), 7.71 – 7.59 (m, 2H), 7.47 (d, *J* = 7.4 Hz, 1H), 5.31 (q, *J* = 6.4 Hz, 1H), 3.15 (d, *J* = 8.4 Hz, 1H), 2.86 (d, *J* = 8.4 Hz, 1H), 1.37 (d, *J* = 6.6 Hz, 3H), 1.09 (s, 3H), 0.91 (s, 3H); ^{13}C NMR (125 MHz, $CDCl_3$) δ 165.84, 134.61, 133.77, 131.77, 129.63, 124.02, 123.67, 121.78 (q, *J* = 283.8), 90.54 (q, *J* = 33.4), 82.79, 69.03, 38.01, 21.62, 19.53, 13.38; ^{19}F NMR (400 MHz, $CDCl_3$) δ –79.05; IR (neat, cm^{-1}) 2973, 1716, 1624, 1277, 1200, 877, 737; HRMS (ESI): m/z calcd for $C_{15}H_{17}F_3N_2O_6Na$ $[M+Na]^+$ 401.0931, Found 401.0916.

[for more polar diastereomer] white solid; ^{1}H NMR (400 MHz, $CDCl_3$) 8.97 (br s, 1H), 7.84 (d, *J* = 7.1 Hz, 1H), 7.72 – 7.54 (m, 3H), 5.22 (dd, *J* = 12.8, 6.5 Hz, 1H), 3.35 – 3.23 (m, 1H), 2.76 – 2.63 (m, 1H), 1.31 (t, *J* = 6.4 Hz, 3H), 0.99 (t, *J* = 5.0 Hz, 6H); ^{13}C NMR (100 MHz, $CDCl_3$) δ 165.57, 134.66, 133.46, 131.79, 129.84, 124.21, 123.85, 121.81 (q, *J* = 290.9), 90.52 (q, *J* = 33.4), 83.13, 69.32, 38.04, 21.42, 20.00, 13.71; ^{19}F NMR (400 MHz, $CDCl_3$) δ –78.96; IR (neat, cm^{-1}) 2925, 1716, 1625, 1278, 1200, 877, 737; HRMS (ESI): m/z calcd for $C_{15}H_{17}F_3N_2O_6Na$ $[M+Na]^+$ 401.0931, Found 401.0952.

5-(2-hydroxy-3-oxo-1-(trifluoromethyl)isoindolin-1-yloxy)-3,3-dimethylpentan-2-yl nitrate

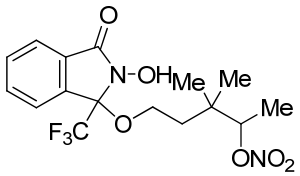

diastereo mixture (dr1:1); white solid; ^{1}H NMR (400 MHz, $CDCl_3$, D_2O was added.) δ 7.84 (d, *J* = 7.4 Hz, 1H), 7.76 – 7.60 (m, 3H), 5.04 (m, 1H), 3.50 – 3.48 (m, 1H), 3.16 – 2.96 (m, 1H), 1.83 – 1.57 (m, 2H), 1.31 (t, *J* = 8.0, 3H), 0.99 (0.94) (d, *J* = 8.0, 6H); ^{13}C NMR (125 MHz, $CDCl_3$) δ 165.51, 134.82, 133.49, 133.45, 131.75, 129.95, 124.10, 123.94, 86.55, 86.42, 60.83, 60.69, 37.51, 37.42, 36.53, 36.45, 23.42, 23.24, 13.57; ^{19}F NMR (400 MHz, $CDCl_3$) δ –78.99; IR (neat, cm^{-1}) 1719, 1639, 1490, 1277, 1008, 823, 750; HRMS (ESI): m/z calcd for $C_{16}H_{19}F_3N_2O_6Na$ $[M+Na]^+$ 415.1087, Found 415.1107.

2-hydroxy-3-(3-hydroxy-3-methylbutoxy)-3-(trifluoromethyl)isoindolin-1-one

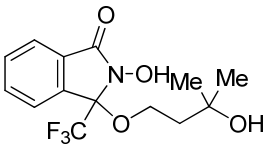

colorless oil; ^{1}H NMR (500 MHz, $CDCl_3$) δ 7.86 (d, *J* = 7.1 Hz, 1H), 7.64 (m, 3H), 3.57 –3.47 (m, 1H), 3.36 – 3.24 (m, 1H), 2.02 – 1.91 (m, 1H), 1.73 – 1.58 (m, 1H), 1.42 (s, 3H), 1.27 (s, 3H); ^{13}C NMR (125 MHz, $CDCl_3$) δ 164.51, 134.33, 132.96, 131.62, 130.49, 124.18, 124.07, 121.86 (q, *J* = 285.0 Hz), 90.87 (q, *J* = 33.8 Hz),70.87, 60.72, 40.83, 30.28, 30.12; ^{19}F NMR (400 MHz, $CDCl_3$) δ –78.53; IR (neat, cm^{-1}) 1716, 1635, 1507, 1457, 1199, 1081, 764; HRMS (ESI): m/z calcd for $C_{14}H_{16}F_3NO_4Na$ $[M+Na]^+$ 342.0924, Found 342.0945.

4-(2-hydroxy-3-oxo-1-(trifluoromethyl)isoindolin-1-yloxy)-4-methylpentan-2-yl nitrate

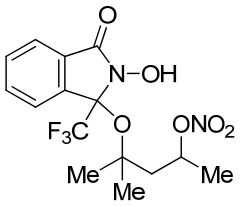

HPLC: Inertsil® diol column, eluent: hex/IPA = 60/1, flow rate: 9.5 ml/min, retention time 74 min and 79 min.

[for less polar diastereomer] white solid; ^{1}H NMR (400 MHz, $CDCl_3$) δ 8.82 (s, 1H), 7.82 (d, *J* = 7.2, 1H), 7.71 – 7.59 (m, 3H), 5.68 – 5.53 (m, 1H), 2.03 (dd, *J* = 15.3, 3.2 Hz, 1H), 1.82 (dd, *J* = 15.3, 7.5 Hz, 1H), 1.47 (d, *J* = 6.3 Hz, 3H), 1.10 (s, 3H), 1.06 (s, 3H); ^{13}C NMR (100 MHz, $CDCl_3$) δ 165.14, 137.38, 133.10, 131.58, 129.35, 125.04, 124.07, 80.55, 78.34, 47.50, 27.88, 26.90, 20.29; ^{19}F NMR (400 MHz, $CDCl_3$) δ –79.95; IR (neat, cm^{-1}) 3054, 2986, 1716, 1623, 1265, 896, 741, 705; HRMS (ESI): m/z calcd for $C_{15}H_{17}F_3N_2O_6Na$ $[M+Na]^+$ 401.0931, Found 401.0944.

[for more polar diastereomer] white solid; ^{1}H NMR (400 MHz, $CDCl_3$) δ 7.84 (d, *J* = 6.8 Hz, 1H), 7.69 – 7.61 (m, 3H), 5.64– 5.56 (m, 1H), 1.92 (dd, *J* = 15.1, 4.3 Hz, 1H), 1.82 (dd, *J* = 15.1, 6.6 Hz, 1H), 1.47 (d, *J* = 6.3 Hz, 3H), 1.23 (s, 3H), 1.00 (s, 3H); ^{13}C

NMR (125 MHz, $CDCl_3$) δ 164.95, 136.76, 132.76, 131.64, 129.78, 125.39, 124.14, 80.90, 78.27, 48.51, 29.47, 24.42, 20.22; ^{19}F NMR (400 MHz, $CDCl_3$) δ –80.23; IR (neat, cm^{-1}) 2925, 2852, 1716, 1623, 1267, 1196, 874, 741; HRMS (ESI): m/z calcd for $C_{15}H_{17}F_3N_2O_6Na$ $[M+Na]^+$ 401.0931, Found 401.0944.

1-cyano-5-(2-hydroxy-3-oxo-1-(trifluoromethyl)isoindolin-1-yloxy)pentan-3-yl nitrate

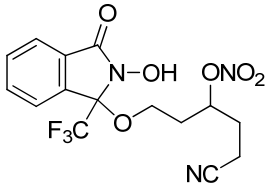

HPLC: Inertsil® diol column, eluent: hex/IPA = 5/1, flow rate: 9.5 ml/min, retention time 43 min and 45 min.

[for less polar diastereomer] colorless oil; ^1H NMR (500 MHz, $CDCl_3$) δ 7.85 (d, *J* = 7.3 Hz, 1H), 7.72 – 7.63 (m, 2H), 7.59 (d, *J* = 7.3 Hz, 1H), 5.45 – 5.35 (m, 1H), 3.56 – 3.44 (m, 1H), 3.21 – 3.10 (m, 1H), 2.54 (t, *J* = 7.1 Hz, 2H), 2.30 – 2.20 (m, 1H), 2.18 – 2.05 (m, 2H), 2.04 – 1.98 (m, 1H); ^{13}C NMR (125 MHz, $CDCl_3$) δ 165.79, 134.32, 133.82, 132.02, 129.62, 124.29, 123.83, 118.37, 79.09, 59.51, 31.57, 28.28, 13.39; ^{19}F NMR (400 MHz, $CDCl_3$) δ –78.93; IR (neat, cm^{-1}) 3053, 2986, 1716, 1623, 1265, 1201, 896, 739; HRMS (ESI): m/z calcd for $C_{15}H_{14}F_3N_3O_6Na$ $[M+Na]^+$ 412.0727, Found 412.0727.

[for more polar diastereomer] colorless oil; ^1H NMR (400 MHz, $CDCl_3$) δ 9.01 (br s, 1H), 7.86 (d, *J* = 7.3 Hz, 1H), 7.73 – 7.62 (m, 3H), 5.38 – 5.30 (m, 1H), 3.55 – 3.36 (m, 1H), 3.22 – 3.17 (m, 1H), 2.54 (t, *J* = 7.7 Hz, 2H), 2.35 – 2.20 (m, 1H), 2.17 – 2.10 (m, 1H), 2.10 – 1.97 (m, 2H); ^{13}C NMR (100 MHz, $CDCl_3$) δ 165.75, 134.27, 133.69, 132.04, 129.65, 124.39, 124.03, 121.66 (q, *J* = 290.2 Hz), 118.45, 90.65 (q, *J* = 33.4 Hz), 79.78, 60.07, 31.58, 28.67, 13.31; ^{19}F NMR (400 MHz, $CDCl_3$) δ –78.93;IR (neat, cm^{-1}) 3055, 2925, 1716, 1624, 1265, 1201, 896, 742; HRMS (ESI): m/z calcd for $C_{15}H_{14}F_3N_3O_6Na$ $[M+Na]^+$ 412.0727, Found 412.0727.

methyl 6-(2-hydroxy-3-oxo-1-(trifluoromethyl)isoindolin-1-yloxy)-4-(nitrooxy)hexanoate

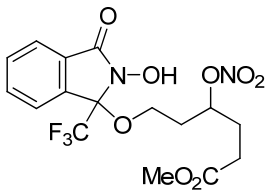

HPLC: Inertsil® diol column, eluent: hex/IPA = 20/1, flow rate: 9.5 ml/min, retention time 87 min and 95 min.

[for less polar diastereomer] colorless oil; ^{1}H NMR (400 MHz, $CDCl_3$) δ 8.45 (br s, 1H), 7.88 (d, *J* = 7.6 Hz, 1H), 7.72 – 7.62 (m, 2H), 7.58 (d, *J* = 6.8 Hz, 1H), 5.38 – 5.32 (m, 1H), 3.73 (s, 3H), 3.47 – 3.41 (m, 1H), 3.26 – 3.12 (m, 1H), 2.57 – 2.35 (m, 2H), 2.20 – 2.09 (m, 1H), 2.09 – 1.97 (m, 1H), 1.95 – 1.82 (m, 2H); ^{13}C NMR (100 MHz, $CDCl_3$) δ 173.74, 165.21, 134.36, 133.55, 131.88, 129.99, 124.32, 124.09, 79.98, 59.51, 52.31, 32.10, 29.19, 27.18; ^{19}F NMR (400 MHz, $CDCl_3$) δ –78.53; IR (neat, cm^{-1}) 3055, 1716, 1624, 1265, 1020, 740, 706; HRMS (ESI): m/z calcd for $C_{16}H_{17}F_3N_2O_8Na$ $[M+Na]^+$ 445.0829, Found 445.0831.

[for more polar diastereomer] colorless oil; ^{1}H NMR (400 MHz, $CDCl_3$) δ 7.90 (d, *J* = 6.8 Hz, 1H), 7.72 – 7.61 (m, 3H), 5.24 – 5.13 (m, 1H), 3.73 (s, 3H), 3.46 –3.40 (m, 1H), 3.28 –3.23 (m, 1H), 2.51 – 2.48 (m, 2H), 2.39 –2.32 (m, 1H), 2.04 – 1.93 (m, 3H); ^{13}C NMR (125 MHz, $CDCl_3$) δ 173.81, 165.28, 134.25, 133.42, 131.88, 130.03, 124.38, 124.21, 81.37, 60.38, 52.23, 31.98, 29.26, 27.65; ^{19}F NMR (400 MHz, $CDCl_3$) δ –78.50; IR (neat, cm^{-1}) 3055, 1716, 1624, 1265, 1200, 896, 740, 705; HRMS (ESI): m/z calcd for $C_{16}H_{17}F_3N_2O_8Na$ $[M+Na]^+$ 445.0829, Found 445.0831.

methyl 7-(2-hydroxy-3-oxo-1-(trifluoromethyl)isoindolin-1-yloxy)-5-(nitrooxy)heptanoate

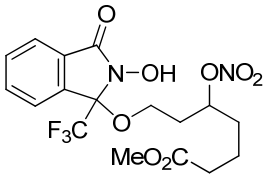

HPLC: AD-H column, eluent: hex/IPA = 20/1, flow rate: 9.5 ml/min, retention time 55 min and 65 min and 115 min.

[for less polar diastereomer] colorless oil; ^{1}H NMR (500 MHz, $CDCl_3$) δ 7.86 (d, *J* = 7.4 Hz, 1H), 7.71 – 7.62 (m, 2H), 7.56 (d, *J* = 7.3 Hz, 1H), 5.33 –5.30 (m, 1H), 3.71 (s,

3H), 3.50 – 3.42 (m, 1H), 3.17 – 3.06 (m, 1H), 2.44 – 2.33 (m, 2H), 2.05 – 1.95 (m, 2H), 1.17 – 1.69 (m, 4H); ^{13}C NMR (125 MHz, $CDCl_3$) δ 174.11, 165.29, 134.53, 133.60, 131.86, 129.90, 124.20, 123.88, 80.73, 59.53, 51.97, 33.13, 31.40, 31.38, 19.95; ^{19}F NMR (400 MHz, $CDCl_3$) δ –78.74; IR (neat, cm^{-1}) 2926, 1716, 1625, 1472, 1276, 1198, 1082, 877, 731; HRMS (ESI): m/z calcd for $C_{17}H_{19}F_3N_2O_8Na$ $[M+Na]^+$ 459.0986, Found 445.0983.

[for more polar diastereomer] colorless oil; ^{1}H NMR (500 MHz, $CDCl_3$) δ 8.62 (s, 1H), 7.86 (d, *J* = 7.4 Hz, 1H), 7.72 – 7.59 (m, 3H), 5.25 – 5.16 (m, 1H), 3.69 (s, 3H), 3.48 – 3.38 (m, 1H), 3.18 – 3.09 (m, 1H), 2.42 – 2.26 (m, 2H), 2.12 – 2.00 (m, 1H), 2.00 – 1.92 (m, 1H), 1.91 – 1.80 (m, 1H), 1.79 – 1.70 (m, 3H); ^{13}C NMR (125 MHz, $CDCl_3$) δ173.80, 165.43, 134.54, 133.49, 131.87, 129.86, 124.30, 124.05, 81.50, 60.32, 51.80, 33.30, 32.04, 31.66, 20.05; ^{19}F NMR (400 MHz, $CDCl_3$) δ –78.87; IR (neat, cm^{-1}) 2987, 1716, 1625, 1474, 1265, 1200, 896, 739, 705; HRMS (ESI): m/z calcd for $C_{17}H_{19}F_3N_2O_8Na$ $[M+Na]^+$ 459.0986, Found 445.0988.

methyl 7-(2-hydroxy-3-oxo-1-(trifluoromethyl)isoindolin-1-yloxy)-4-(nitrooxy)heptanoate

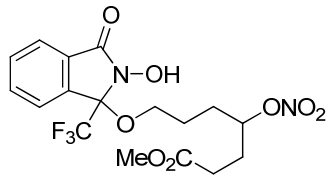

HPLC: AD-H column, eluent: hex/IPA = 20/1, flow rate: 9.5 ml/min, retention time 65 min, 68 min and 97 min.

[for less polar diastereomer] colorless oil; colorless oil; ^{1}H NMR (500 MHz, $CDCl_3$) δ 7.86 (d, *J* = 7.3, 1H), 7.71 – 7.60 (m, 3H), 5.24 – 5.04 (m, 1H), 3.72 (3.71) (s, 3H), 3.40 – 3.29 (m, 1H), 3.13 – 3.03 (m, 1H), 2.49 – 2.35 (m, 2H), 2.15 – 2.05 (m, 1H), 2.03 – 1.91 (m, 1H), 1.85 – 1.79 (m, 1H), 1.77 – 1.67 (m, 3H); ^{13}C NMR (125 MHz, $CDCl_3$) δ 173.45, 173.20, 165.55, 165.45, 134.83, 133.49, 133.43, 131.76, 129.87, 129.83, 124.16, 124.04, 83.08, 82.71, 63.71, 62.93, 52.12, 51.99, 29.48, 29.40, 29.20, 28.79, 27.56, 24.47; ^{19}F NMR (400 MHz, $CDCl_3$) δ –78.77, –78.87; IR (neat, cm^{-1}) 3054, 2926, 1716, 1635, 1473, 1264, 1200, 1023, 746; HRMS (ESI): m/z calcd for $C_{17}H_{19}F_3N_2O_8Na$ $[M+Na]^+$ 459.0986, Found 445.0983.

[for more polar diastereomer] colorless oil; ^{1}H NMR (500 MHz, $CDCl_3$) δ 7.86 (d, *J* =

7.6 Hz, 1H), 7.70 – 7.62 (m, 3H), 5.24 – 5.15 (m, 1H), 3.70 (s, 3H), 3.35 – 3.31 (m, 1H), 3.12 – 3.04 (m, 1H), 2.44 (t, *J* = 7.2 Hz, 2H), 2.13 – 2.04 (m, 1H), 2.00 –1.94 (m, 1H), 1.84 – 1.80 (m, 2H), 1.75 – 1.70 (m, 2H); ^{13}C NMR (125 MHz, $CDCl_3$) δ 173.26, 165.41, 134.81, 133.49, 131.78, 129.84, 124.18, 124.03, 83.06, 63.71, 52.02, 29.39, 29.21, 27.54, 24.45; ^{19}F NMR (400 MHz, $CDCl_3$) δ –78.89; IR (neat, cm^{-1}) 2926, 1716, 1624, 1276, 1200, 1007, 749; HRMS (ESI): m/z calcd for $C_{17}H_{19}F_3N_2O_8Na$ $[M+Na]^+$ 459.0986, Found445.0979.

1-(1,3-dioxoisoindolin-2-yl)-5-(2-hydroxy-3-oxo-1-(trifluoromethyl)isoindolin-1-yloxy)pentan-3-yl nitrate

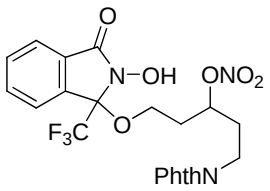

HPLC: Inertsil® diol column, eluent: hex/IPA = 10/1, flow rate: 9.5 ml/min, retention time 107 min/116 min.

[for less polar diastereomer] colorless oil; ^{1}H NMR (400 MHz, $CDCl_3$) δ 7.89 – 7.81 (m, 3H), 7.76 – 7.73 (m, 2H), 7.67 – 7.48 (m, 3H), 5.35 – 5.22 (m, 1H), 3.90 – 3.77 (m, 2H), 3.52 – 3.33 (m, 1H), 3.19 – 3.03 (m, 1H), 2.27 – 2.14 (m, 1H), 2.12 –2.06 (m, 3H); ^{13}C NMR (125 MHz, $CDCl_3$) δ 168.40, 165.48, 134.46, 134.25, 133.61, 131.89, 131.79, 129.86, 124.25, 123.96, 123.51, 122.84, 90.81 (d, *J* = 33.3 Hz), 78.80, 59.60, 34.01, 31.64, 30.86; ^{19}F NMR (400 MHz, $CDCl_3$) δ –78.71; IR (neat, cm^{-1}) 2919, 1716, 1635, 1276, 1189, 1125, 723; HRMS (ESI): m/z calcd for $C_{22}H_{18}F_3N_3O_8Na$ $[M+Na]^+$ 532.0938, Found 532.0929.

[for more polar diastereomer] white solid; ^{1}H NMR (500 MHz, $CDCl_3$) δ 8.66 (br s, 1H), 7.88 – 7.83 (m, 3H), 7.76 – 7.71 (m, 2H), 7.67 – 7.60 (m, 2H), 7.55 (d, *J* = 7.1 Hz, 1H), 5.35 – 5.25 (m, 1H), 3.94 – 3.75 (m, 2H), 3.50 – 3.46 (m, 1H), 3.19 – 3.10 (m, 1H), 2.23 – 3.17 (m, 1H), 2.15 – 2.02 (m, 3H); ^{13}C NMR (100 MHz, $CDCl_3$) δ 168.43, 165.35, 134.33, 134.17, 133.52, 131.91, 131.87, 129.78, 124.33, 124.10, 123.41, 80.11, 60.48, 34.02, 31.93, 31.57; ^{19}F NMR (400 MHz, $CDCl_3$) δ –78.68; IR (neat, cm^{-1}) 2927, 1716, 1635, 1265, 1202, 909, 738; HRMS (ESI): m/z calcd for $C_{22}H_{18}F_3N_3O_8Na$ $[M+Na]^+$ 532.0938, Found 532.0954.

6-(1,3-dioxoisoindolin-2-yl)-1-(2-hydroxy-3-oxo-1-(trifluoromethyl)isoindolin-1-yloxy)hexan-3-yl nitrate

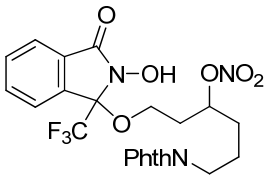

HPLC: Inertsil® diol column, eluent: hex/IPA = 5/1, flow rate: 9.5 ml/min, retention time 41 min and 45 min.

[for less polar diastereomer] colorless oil; ^{1}H NMR (500 MHz, $CDCL_3$) δ 9.09 (br s, 1H), 7.92 – 7.86 (m, 2H), 7.83 (d, *J* = 7.4 Hz, 1H), 7.76 –7.70 (m, 2H), 7.64 (dt, *J* = 25.2, 7.4 Hz, 2H), 7.54 (d, *J* = 7.4 Hz, 1H), 5.45 – 5.32 (m, 1H), 3.74 (t, *J* = 6.4 Hz, 2H), 3.46 (dt, *J* = 9.6, 5.0 Hz, 1H), 3.09 (td, *J* = 8.9, 3.7 Hz, 1H), 2.07 – 2.01 (m, 1H), 1.95 – 1.88 (m, 1H), 1.86 – 1.71 (m, 4H); ^{13}C NMR (125 MHz, $CDCl_3$) δ 168.57, 165.52, 134.54, 134.17, 133.61, 131.85, 131.84, 129.84, 124.15, 123.84, 123.43, 90.81 (q, *J* = 33.1 Hz), 80.31, 59.58, 37.24, 31.97, 29.98, 24.09; ^{19}F NMR (400 MHz, $CDCl_3$) δ –78.74; IR (neat, cm^{-1}) 2927, 1716, 1625, 1267, 1191, 866, 738; HRMS (ESI): m/z calcd for $C_{23}H_{20}F_3N_3O_8Na$ $[M+Na]^+$ 546.1095, Found 546.1107.

[for more polar diastereomer] colorless oil; ^{1}H NMR (500 MHz, $CDCl_3$) δ 8.94 (br s, 1H), 7.91 – 7.81 (m, 3H), 7.75 – 7.67 (m, 3H), 7.61 (dd, *J* = 15.9, 7.6 Hz, 2H), 5.32 – 5.21 (m, 1H), 3.79 – 3.66 (m, 2H), 3.64 – 3.42 (m, 1H), 3.19 – 3.08 (m, 1H), 2.07 – 1.91 (m, 2H), 1.91 – 1.69 (m, 4H); ^{13}C NMR (125 MHz, $CDCl_3$) δ 168.51, 165.49, 134.50, 134.09, 133.48, 131.90, 131.84, 129.86, 124.25, 124.02, 123.37, 90.72 (d, *J* = 32.4 Hz), 81.25, 60.33, 37.29, 31.92, 30.16, 24.14; ^{19}F NMR (400 MHz, $CDCl_3$) δ –78.80; IR (neat, cm^{-1}) 2923, 1713, 1628, 1277, 1190, 877, 721; HRMS (ESI): m/z calcd for $C_{23}H_{20}F_3N_3O_8Na$ $[M+Na]^+$ 546.1095, Found 546.1072.

6-(1,3-dioxoisoindolin-2-yl)-1-(2-hydroxy-3-oxo-1-(trifluoromethyl)isoindolin-1-yloxy)hexan-3-yl nitrate

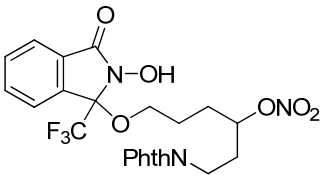

HPLC: Inertsil® diol column, eluent: hex/IPA = 5/1, flow rate: 9.5 ml/min, retention time 41 min 48 min.

[diastereo mixture (dr1:1)] colorless oil; ^{1}H NMR (500 MHz, $CDCl_3$) δ 7.89 – 7.84 (m, 3H), 7.77 – 7.71 (m, 2H), 7.70 – 7.58 (m, 3H), 5.21 – 5.02 (m, 1H), 3.92 – 3.73 (m, 2H), 3.41 – 3.37 (m, 1H), 3.12 – 2.99 (m, 1H), 2.13 – 2..02 (m, 2H), 2.02 – 1.92 (m, 1H), 1.92 – 1.71 (m, 3H); ^{13}C NMR (125 MHz, $CDCl_3$) δ 168.51, 168.45, 165.36, 134.80, 134.30, 134.23, 133.37, 131.81, 131.76, 131.72, 130.01, 124.10, 123.56, 123.50, 90.88 (q, *J* = 33.0 Hz), 81.57, 81.17, 63.85, 62.97, 34.10, 34.05, 31.45, 31.33, 29.43, 28.75, 24.34; ^{19}F NMR (400 MHz, $CDCl_3$) δ –78.68, –78.77; IR (neat, cm^{-1}) 2924, 1716, 1624, 1266, 1190, 875, 738, 705; HRMS (ESI): m/z calcd for $C_{23}H_{20}F_3N_3O_8Na$ $[M+Na]^+$ 546.1095, Found 546.1075.

5-(2-hydroxy-3-oxo-1-(trifluoromethyl)isoindolin-1-yloxy)-3-(nitrooxy)pentyl acetate

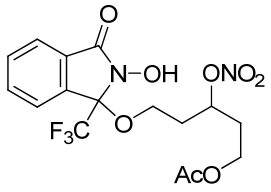

HPLC: Inertsil® diol column, eluent: hex/IPA = 20/1, flow rate: 9.5 ml/min, retention time 93 min and 98 min.

[for less polar diastereomer] colorless oil; ^{1}H NMR (500 MHz, $CDCl_3$) δ 9.47 (br s, 1H), 7.83 (d, *J* = 7.2 Hz, 1H), 7.70 – 7.62 (m, 2H), 7.56 (d, *J* = 7.4 Hz, 1H), 5.54–5.37 (m, 1H), 4.31 – 4.11 (m, 2H), 3.60 – 3.42 (m, 1H), 3.19 – 3.06 (m, 1H), 2.20 – 2.03 (m, 6H), 2.02 – 1.93 (m, 1H); ^{13}C NMR (125 MHz, $CDCl_3$) δ 171.13, 165.78, 134.51, 133.70, 131.90, 129.73, 124.17, 123.79, 121.72 (q, *J* = 286.4 Hz), 90.76 (q, *J* = 33.4 Hz), 78.40, 60.20, 59.54, 31.89, 31.68, 20.79; ^{19}F NMR (400 MHz, $CDCl_3$) δ –78.90; IR (neat, cm^{-1}) 2986, 1734, 1716, 1635, 1276, 1200, 766, 710; HRMS (ESI): m/z calcd for $C_{16}H_{17}F_3N_2O_8Na$ $[M+Na]^+$ 445.0829, Found 445.0845.

[for more polar diastereomer] colorless oil; ^{1}H NMR (500 MHz, $CDCl_3$) δ 7.85 (d, *J* = 7.4 Hz, 1H), 7.72 – 7.59 (m, 3H), 5.42 – 5.38 (m, 1H), 4.25 – 4.16 (m, 2H), 3.54 – 3.43 (m, 1H), 3.21 – 3.11 (m, 1H), 2.21 – 2.14 (m, 1H), 2.11 – 1.96 (m, 6H); ^{13}C NMR (125

MHz, $CDCl_3$) δ 171.13, 165.77, 134.47, 133.53, 131.90, 129.77, 124.28, 124.01, 121.73 (q, *J* = 286.6 Hz), 90.72 (q, *J* = 33.4 Hz), 79.15, 60.21, 60.17, 32.00, 20.79; ^{19}F NMR (400 MHz, $CDCl_3$) δ –78.90; IR (neat, cm^{-1}) 2897, 1734, 1717, 1634, 1265, 1200, 740, 704; HRMS (ESI): m/z calcd for $C_{16}H_{17}F_3N_2O_8Na$ $[M+Na]^+$ 445.0829, Found 445.0831.

6-(2-hydroxy-3-oxo-1-(trifluoromethyl)isoindolin-1-yloxy)-4-(nitrooxy)hexyl acetate

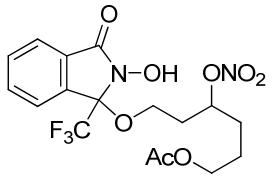

HPLC: Inertsil® diol column, eluent: hex/IPA = 5/1, flow rate: 9.5 ml/min, retention time 14 min; AD-H column, eluent: hex/IPA = 10/1, flow rate: 9.5 ml/min, retention time 54 min.

[for less polar diastereomer] colorless oil; ^1H NMR (500 MHz, $CDCl_3$) δ 7.82 (d, *J* = 7.3 Hz, 1H), 7.65 (dt, *J* = 26.8, 7.5 Hz, 2H), 7.55 (d, *J* = 7.4 Hz, 1H), 5.43 – 5.31 (m, 1H), 4.15 – 4.01 (m, 2H), 3.55 – 3.44 (m, 1H), 3.16 – 3.05 (m, 1H), 2.14 – 2.02 (m, 4H), 1.96 – 1.88 (m, 1H), 1.88 – 1.82 (m, 1H), 1.82 – 1.71 (m, 3H); ^{13}C NMR (125 MHz, $CDCl_3$) δ 171.35, 165.76, 134.56, 133.69, 131.87, 129.74, 124.13, 123.77, 121.74 (q, *J* = 285.9 Hz), 90.76 (q, *J* = 33.5 Hz), 80.63, 63.73, 59.67, 31.81, 29.40, 24.07, 20.87; ^{19}F NMR (400 MHz, $CDCl_3$) δ –78.90; IR (neat, cm^{-1}) 2959, 1733, 1716, 1635, 1270, 1191, 872, 732; HRMS (ESI): m/z calcd for $C_{17}H_{19}F_3N_2O_8Na$ $[M+Na]^+$ 459.0986, Found 459.0977.

[for more polar diastereomer] colorless oil; ^1H NMR (500 MHz, $CDCl_3$) δ 8.97 (s, 1H), 7.85 (d, *J* = 7.4 Hz, 1H), 7.71– 7.60 (m, 3H), 5.32 – 5.25 (m, 1H), 4.14 – 4.00 (m, 2H), 3.53 – 3.41 (m, 1H), 3.19 – 3.11 (m, 1H), 2.06 (s, 3H), 2.04 – 1.93 (m, 2H), 1.93 – 1.86 (m, 1H), 1.84 – 1.71 (m, 3H); ^{13}C NMR (125 MHz, $CDCl_3$) δ 171.34, 165.65, 134.51, 133.52, 131.90, 129.79, 124.28, 124.00, 121.77 (q, *J* = 286.5 Hz), 90.70 (q, *J* = 33.5 Hz), 81.53, 63.75, 60.37, 31.89, 29.63, 24.15, 20.87; ^{19}F NMR (400 MHz, $CDCl_3$) δ –78.90; IR (neat, cm^{-1}) 2986, 1732, 1716, 1631, 1265, 1201, 876, 703; HRMS (ESI): m/z calcd for $C_{17}H_{19}F_3N_2O_8Na$ $[M+Na]^+$ 459.0986, Found 459.0992.

6-(2-hydroxy-3-oxo-1-(trifluoromethyl)isoindolin-1-yloxy)-3-(nitrooxy)hexyl acetate

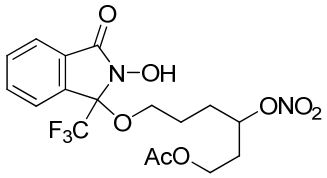

HPLC: Inertsil® diol column, eluent: hex/IPA = 5/1, flow rate: 9.5 ml/min, retention time 18 min; AD-H column, eluent: hex/IPA = 10/1, flow rate: 9.5 ml/min, retention time 35 min.

[for less polar diastereomer] colorless oil; ^{1}H NMR (500 MHz, $CDCl_3$) δ 7.85 (d, *J* = 7.6 Hz, 1H), 7.71 –7.60 (m, 3H), 5.24 – 5.17 (m, 1H), 4.27 – 4.14 (m, 2H), 3.42 –3.32 (m, 1H), 3.12 – 3.03 (m, 1H), 2.08 (s, 3H), 2.07 – 1.99 (m, 2H), 1.96 – 1.86 (m, 1H), 1.86 – 1.67 (m, 3H); ^{13}C NMR (125 MHz, $CDCl_3$) δ 171.27, 165.44, 134.83, 133.49, 131.79, 129.83, 124.17, 124.01, 81.01, 63.14, 60.31, 31.84, 29.04, 24.42, 20.84; ^{19}F NMR (400 MHz, $CDCl_3$) δ –78.84; IR (neat, cm^{-1}) 2923, 2851, 1716, 1624, 1266, 1189, 746; HRMS (ESI): m/z calcd for $C_{17}H_{19}F_3N_2O_8Na$ $[M+Na]^+$ 459.0986, Found 459.0992.

[for more polar diastereomer] colorless oil; ^{1}H NMR (500 MHz, $CDCl_3$) δ 7.84 (d, *J* = 7.4 Hz, 1H), 7.72 7.58 (m, 3H), 5.30 – 5.21 (m, 1H), 4.18 (t, *J* = 6.1 Hz, 2H), 3.41 – 3.31 (m, 1H), 3.13 – 3.04 (m, 1H), 2.07 (s, 3H), 2.05 – 1.99 (m, 2H), 1.89 – 1.81 (m, 2H), 1.76 – 1.70 (m, 2H); ^{13}C NMR (125 MHz, $CDCl_3$) δ 171.18, 165.53, 134.79, 133.45, 131.78, 129.85, 124.11, 123.98, 81.41, 63.77, 60.28, 31.79, 29.52, 24.43, 20.82; ^{19}F NMR (400 MHz, $CDCl_3$) δ –78.90; IR (neat, cm^{-1}) 3054, 1716, 1624, 1265, 1200, 896, 744, 642; HRMS (ESI): m/z calcd for $C_{17}H_{19}F_3N_2O_8Na$ $[M+Na]^+$ 459.0986, Found 459.0975.

2-hydroxy-3-(3-hydroxybutoxy)-3-(trifluoromethyl)isoindolin-1-one

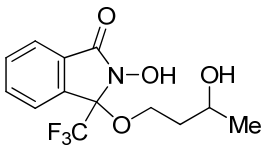

HPLC: Inertsil® diol column, eluent: hex/IPA = 10/1, flow rate: 9.5 ml/min, retention time 37 min/56 min.

[for less polar diastereomer] white solid; ^{1}H NMR (500 MHz, $CDCl_3$) δ 7.87 (d, *J* = 7.8 Hz, 1H), 7.70 – 7.58 (m, 3H), 4.10 – 3.94 (m, 1H), 3.46 – 3.29 (m, 2H), 1.91 – 1.65 (m, 2H), 1.31 (d, *J* = 6.3 Hz, 3H); ^{13}C NMR (125 MHz, $CDCl_3$) δ 164.53, 134.41, 132.98, 131.64, 130.49, 124.14, 124.08, 121.87 (q, *J*= 286.4 Hz), 90.83 (q, *J* = 33.3 Hz), 67.41, 62.36, 36.85, 23.97; ^{19}F NMR (400 MHz, $CDCl_3$) δ –78.59; IR (neat, cm^{-1}) 3175, 2934, 1719, 1470, 1190, 1081, 963, 730; HRMS (ESI): m/z calcd for $C_{13}H_{14}F_3NO_4Na$ $[M+Na]^+$ 328.0767, Found 328.0782.

[for more polar diastereomer] white solid; ^{1}H NMR (500 MHz, $CDCl_3$) δ 7.84 (d, *J* = 8.0 Hz, 1H), 7.68 – 7.58 (m, 3H), 4.39 – 4.28 (m, 1H), 3.52 – 3.42 (m, 1H), 3.30 – 3.22 (m, 1H), 2.03 – 1.91 (m, 1H), 1.51 – 1.41 (m, 1H), 1.35 (d, *J* = 6.2 Hz, 3H); ^{13}C NMR (125 MHz, $CDCl_3$) δ 164.05, 134.49, 132.80, 131.48, 130.56, 123.99, 121.92 (q, *J* = 286.8 Hz), 90.69 (q, *J* = 33.1 Hz), 63.89, 59.28, 36.88, 23.26; ^{19}F NMR (400 MHz, $CDCl_3$) δ –78.59; IR (neat, cm^{-1}) 3173, 2934, 1719, 1470, 1190, 1081, 963, 730; HRMS (ESI): m/z calcd for $C_{13}H_{14}F_3NO_4Na[M+Na]^+$ 328.0767, Found 328.0782.

butane-1,3-diol

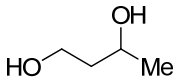

light yellow oil; ^{1}H NMR (500 MHz, $CDCl_3$) δ 4.11 – 4.00 (m, 1H), 3.93 – 3.77 (m, 2H), 2.47 (br s, 2H), 1.71 – 1.65 (m, 2H), 1.22 (d, *J* = 6.1 Hz, 3H); identical to a commercial material.

Acknowledgement

The work described in this thesis would not have been possible without the help, the cooperation and support of many people, to whom I am deeply indebted.

First and foremost, I would like to express my sincere gratitude to my supervisor Professor Dr. Motomu Kanai for his supreme guidance for my research activities at the University of Tokyo. His enthusiasm and his intelligence toward organic chemistry impress me so much that all these will definitely influence me in the future. As an ambitious and famous organic chemist, he kindly provided me such a precious opportunity to work in his group, which is a great honor for me forever.

Second, I deeply appreciate assistant Professor Dr. Kounosuke Oisaki for his excellent daily supervision and kind care during these three years of my Ph. D course study. He has a tremendous energy and excitement for new chemistry, and it's always inspiring to be around him. It's beyond words to describe how many important skills and knowledge I have learned from him through all of our discussions. His nice personality and great characters would also impress me forever.

Third, I gratefully acknowledge other staffs in current organic synthetic lab: associate Profesor Dr. Shigeki Matsunaga, assistant Professor Dr. Yohei Shimizu, Dr. Youhei Sohma, Dr. Yoichiro Kuninobu and Dr. Kenzo Yamatsugu for their fruitful suggestions and kind help in many affairs. Mrs. Sayuri Moroo, the secretary in our lab, is acknowledged for her help in daily routines at lab.

I would like to thank Lecture Mrs. Mikiko Kikuchi, supervisor of the International Students Advising Room in the Department of Pharmaceutical Sciences, for her enthusiastic help and kind care during my stay in Japan.

I would like to thank my co-worker Mr. Jun Ozawa and Mr. Masayuki Tashiro for giving me lots of assistance to finish my research project smoothly. Without their help, I could not accomplish my research project.

I would like to collectively thank all the members in Organic Synthetic Lab for making our laboratory a great working place. There are also a number of people whom I would like to acknowledge individually: Dr. Shi-Liang Shi, Dr. Ying-Jie Xu, Dr. Yao Du, Dr. Lu-Qing Lin, Dr. Yasuaki Kimura, Dr. Qing Xiao, Dr. Prasanna Kumara Chikkade, Dr. Kyalo Stephen Kanyiva, Dr. Shunsuke Sueki, for constructive talks referred to experiment; Mr. Yufei Wang, Mr. Bo Sun, Mr. Xiaofeng Wei, Dr. Haiyan Zhu, Dr. Daisuke Sasaki, Mr. Jiaan Liu, Mr. Zijia Wang, Mr. Yutaka Saga, Mr. Shogo Hashizume, Mr. Harunobu Mitsunuma, Mr. Toshiaki Sonobe, Mr. Kenta Saito, Mr. Keiichi Kaneko, Miss Kumiko Yamamoto, Mr. Masahiro Kojima, Mr. Youhei Seki, Mr. Kiyomichi Shinoda and Mr. Takahiro Shirai for helps in both life and research.

My special acknowledgement goes to Professor Dr. Youjun Xu at Shenyang Pharmaceutical University, who kindly recommended me to Professor Kanai after I got my Master Degree in China, for his persistent encouragement and support.

I would also like to thank the University of Tokyo Fellowship for generous financial supports.

Finally, I would like to express my sincere gratitude to my family for their endless supports and encouragements throughout my oversee study and life.